

Part 1.

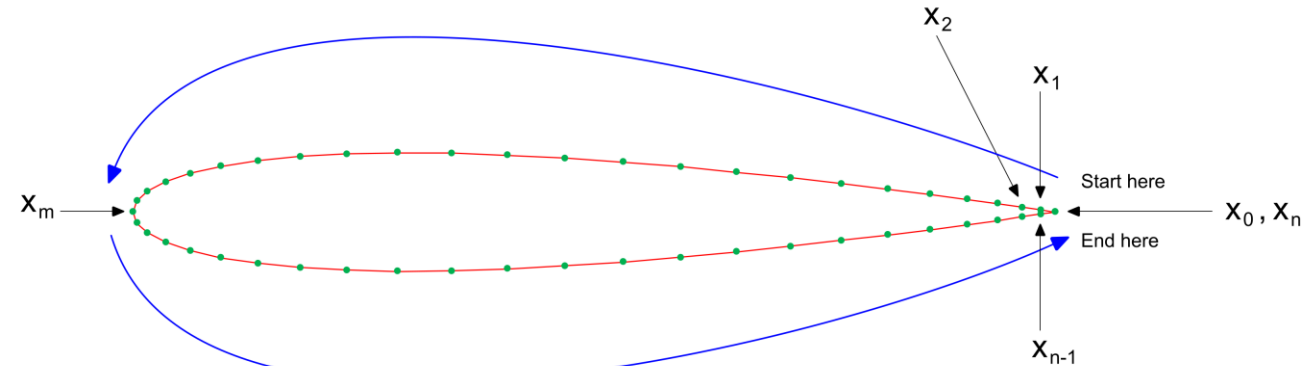
Anatomy of airfoils and their performance

Anatomy of the airfoil

Anatomy of the airfoil

- There are many airfoil types, each one having different geometrical and aerodynamic characteristics.
- The shape of the airfoils is expressed using (x, y) coordinates, that is,

X coordinates	Y coordinates
x_0	y_0
x_1	y_1
x_2	y_2
...	...
x_n	y_n



$$\mathbf{X} \rightarrow (x, y)$$

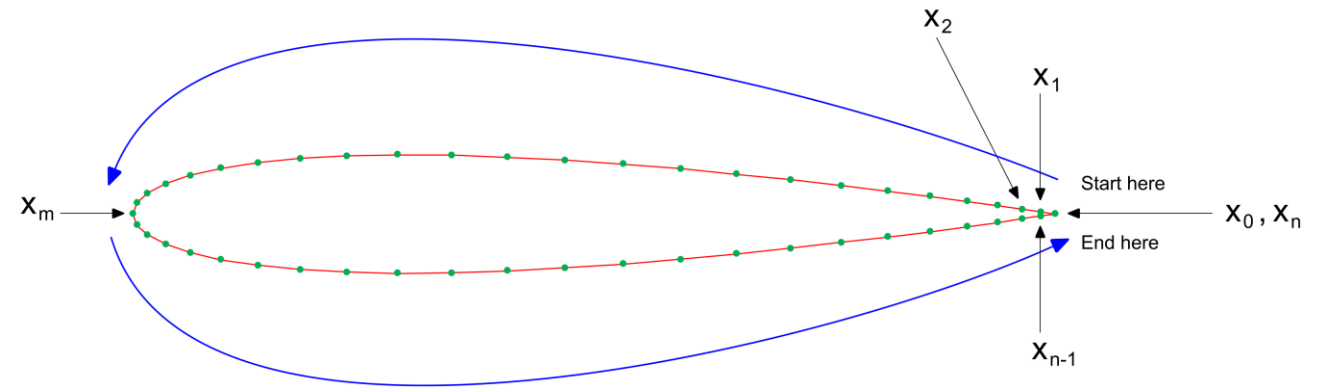
$$m < n$$

- This is not a rule, but usually the airfoil coordinates are given starting from the trailing edge moving to the leading edge, going back to the trailing edge.
- It is also a good practice to start with the upper side and then move to the lower side.
- To read airfoil coordinates in many applications (e.g., XFOIL, XFLR5, etc.), you must follow this format.

Anatomy of the airfoil

- The shape of some airfoils can be expressed using analytical relations, for example:
 - NACA 4 series, NACA 5 series, NACA 6 series, Joukowsky airfoils, Van de Vooren airfoils.
- In many other cases these analytical relations do not exist.
- Disregarding of the airfoil used, at the end of the day we need the (x, y) coordinates of each vertex that made up the airfoil contour.

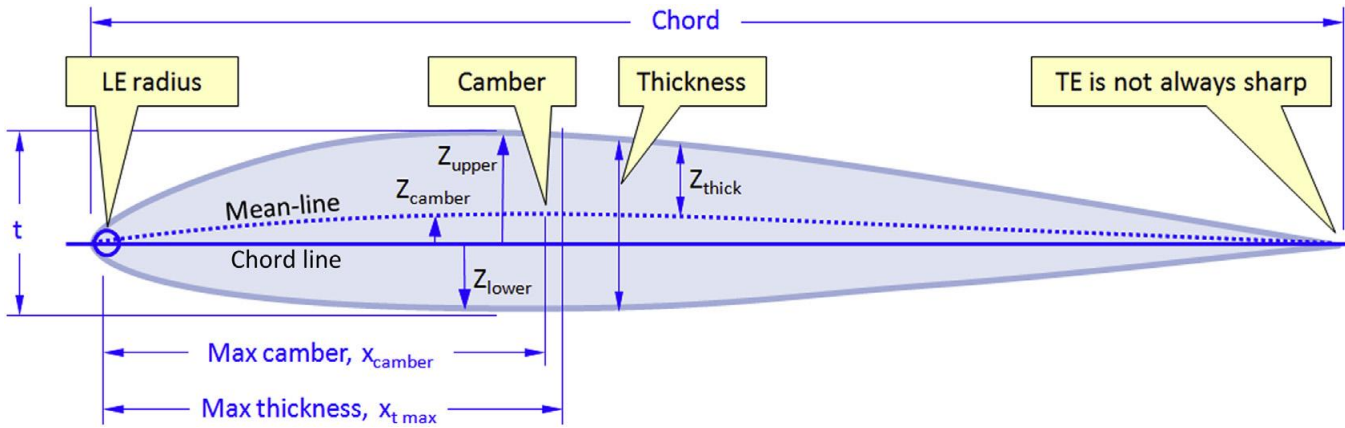
X coordinates	Y coordinates
x_0	y_0
x_1	y_1
x_2	y_2
...	...
x_n	y_n



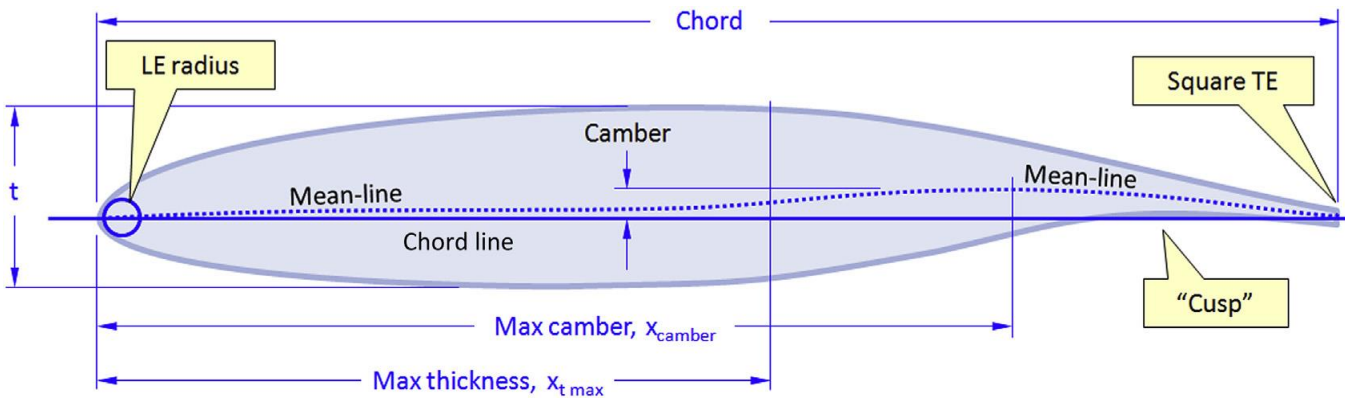
$$\mathbf{X} \rightarrow (x, y)$$

$$m < n$$

Anatomy of the airfoil



Conventional airfoil



Modern natural laminar-flow airfoil

- Geometrical parameters of airfoils:
 - Chord line.
 - Maximum thickness.
 - Position of maximum thickness.
 - Maximum camber.
 - Position of maximum camber.
 - Mean camber line.
 - Leading edge radius.
 - Trailing edge geometry.

Anatomy of the airfoil

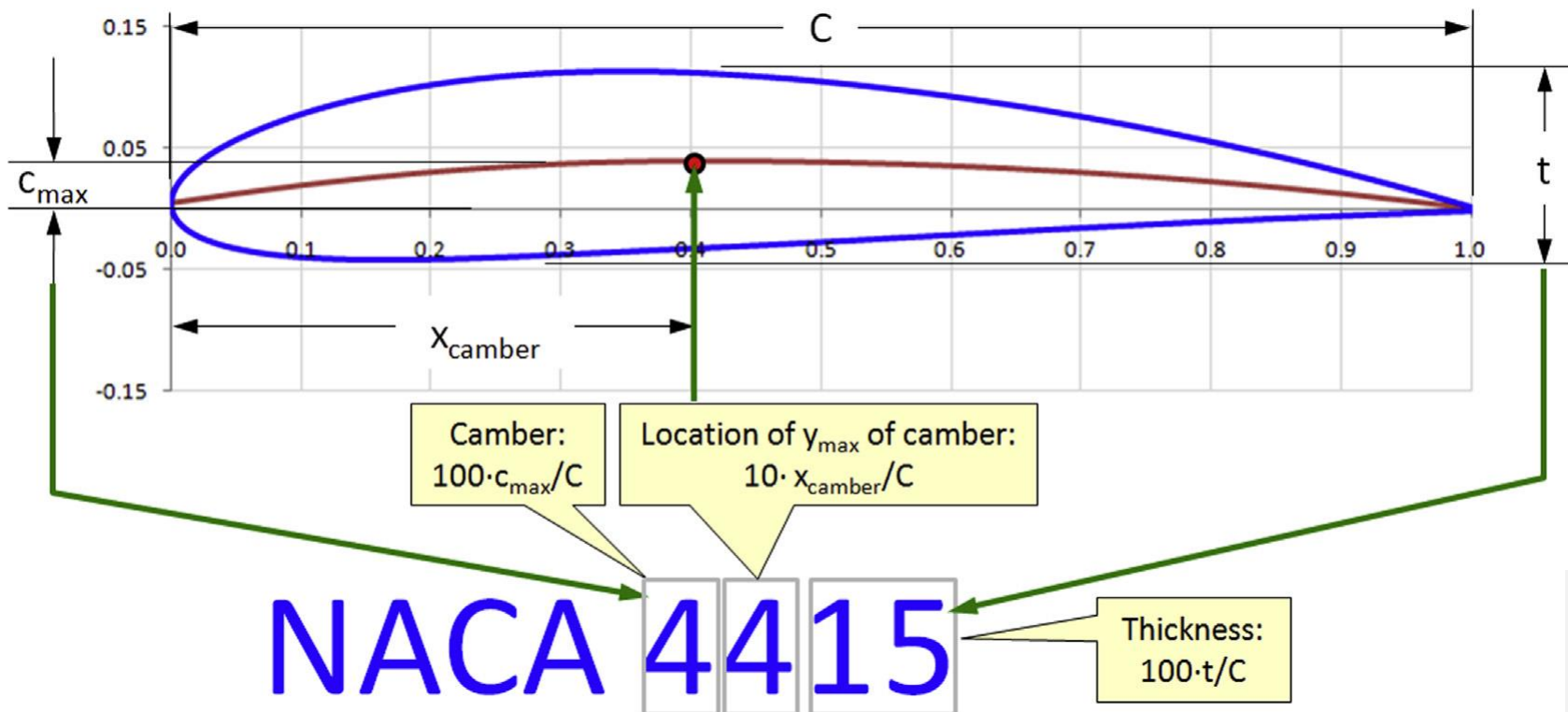
- Few airfoil types:
 - NACA Airfoils – Four digits, five digits, 6-series, 7-series.
 - GA(W)-1 (probably first airfoil designed using CFD).
 - RAE.
 - RAF.
 - Selig.
 - Rutan.
 - Wortmann FX.
 - Clark.
 - Delft University.
 - Eiffel.
 - Gottingen.
 - Eppler.
 - Drela.
 - Boeing.
 - Onera.
 - McDonnell Douglas.
 - NASA.
 - Grumman.
 - DLR.
 - Sikorsky.
- Every airfoil type have different geometrical and aerodynamic characteristics.
- They are designed for very specific missions or applications.

Anatomy of the airfoil

- For an extensive list of airfoil coordinates, visit the UIUC airfoil coordinates database:
 - https://m-selig.ae.illinois.edu/ads/coord_database.html
- For an incomplete guide of airfoil usage:
 - <https://m-selig.ae.illinois.edu/ads/aircraft.html>
 - <https://m-selig.ae.illinois.edu/props/propDB.html>
- Online databases of airfoil coordinates and aerodynamic performance:
 - <http://www.airfoiltools.com/>
 - <http://webfoil.engin.umich.edu/>
- Additional sites that might be useful:
 - <https://aerolab.usu.edu/tools/aerodynamics>
 - <https://aerodynamics.lr.tudelft.nl/cgi-bin/afCDb>
 - <https://github.com/dciliberti/experimentalAirfoilDatabase>
 - <https://www.pdas.com/naca456pdas.html>
 - <https://ntrs.nasa.gov/>

Anatomy of the airfoil

- Probably the most popular airfoils are the NACA series.
- Let us study some of the geometrical features and numbering system of these airfoils.
 - NACA four digits airfoils (because it has four digits on its nomenclature).



NOTE:

This airfoil can be generated from an analytical expression.

<https://www.pdas.com/naca456pdas.html>

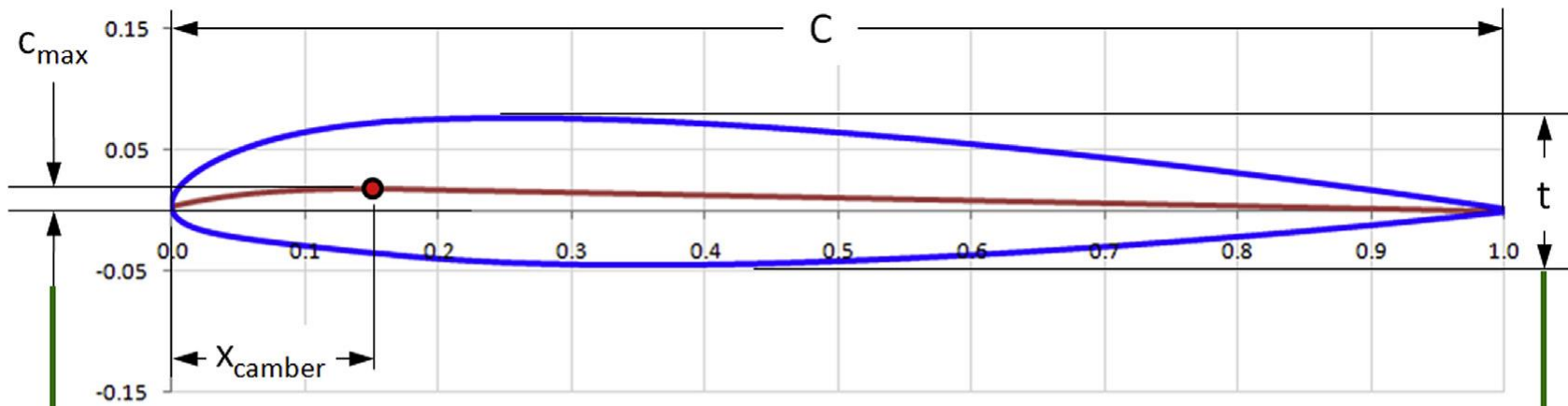
https://en.wikipedia.org/wiki/NACA_airfoil

<https://ntrs.nasa.gov/citations/19930090976>

Note: maximum thickness is located at 30% of the chord

Anatomy of the airfoil

- Probably the most popular airfoils are the NACA series.
- Let us study some of the geometrical features and numbering system of these airfoils.
 - NACA five digits airfoils (because it has five digits on its nomenclature).



Camber:
 $100 \cdot c_{max} / C$

Position of maximum camber:
 $20 \cdot x_{camber} / C$

"0" means a standard 5-digit airfoil
"1" means a reflexed camber

Thickness:
 $100 \cdot t / C$

NACA 23012

NOTE:

This airfoil can be generated from an analytical expression.

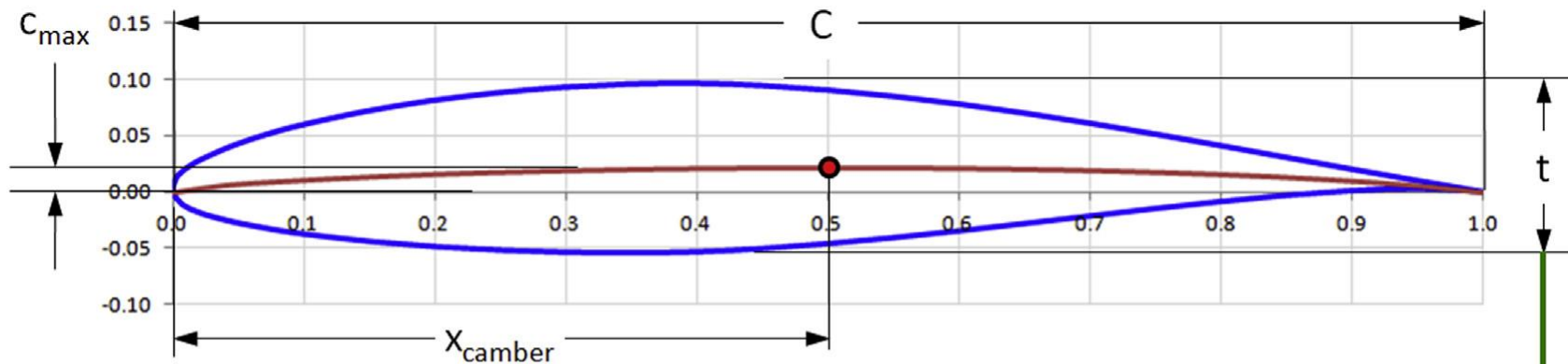
<https://www.pdas.com/naca456pdas.html>

https://en.wikipedia.org/wiki/NACA_airfoil

<https://ntrs.nasa.gov/citations/19930090976>

Anatomy of the airfoil

- Probably the most popular airfoils are the NACA series.
- Let us study some of the geometrical features and numbering system of these airfoils.
 - NACA 6-Series airfoils (because the series starts with the digit 6).



6-Series Position of maximum camber: $10 \cdot x_{\text{camber}}/C$ Range of favorable lift coefficient Design lift coefficient

NACA 65₃-415

Thickness: $100 \cdot t/C$

NOTE:

This airfoil can be generated from an analytical expression.

<https://www.pdas.com/naca456pdas.html>

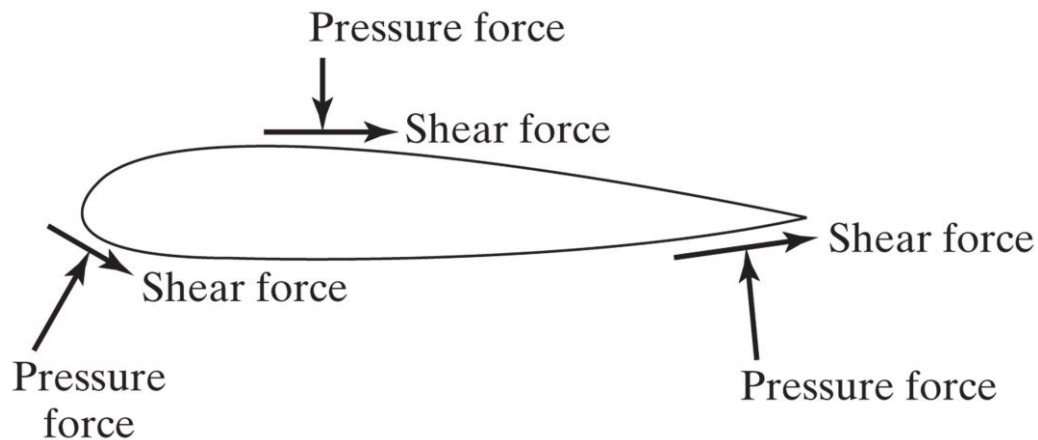
https://en.wikipedia.org/wiki/NACA_airfoil

<https://ntrs.nasa.gov/citations/19930090976>

Forces on a body

Forces on a body

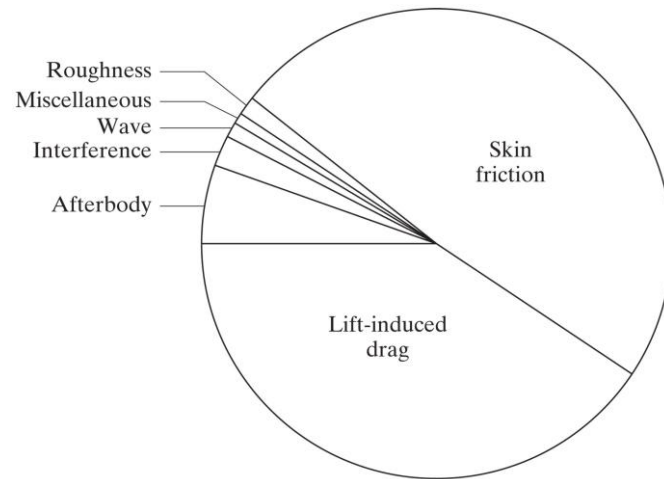
- Aerodynamic forces acting on a body.
 - The aerodynamic forces acting on a body are due to the action of pressure and shear stresses on the surface of the body.
 - The aerodynamic forces can be decomposed into two main contributions, namely,
 - Pressure contribution and viscous contribution (shear stresses).
 - The balance between both contributions can change according to the application or working conditions.
 - Sometimes the pressure contribution is larger than the viscous contribution, and sometimes the viscous contribution can be larger than the pressure contribution



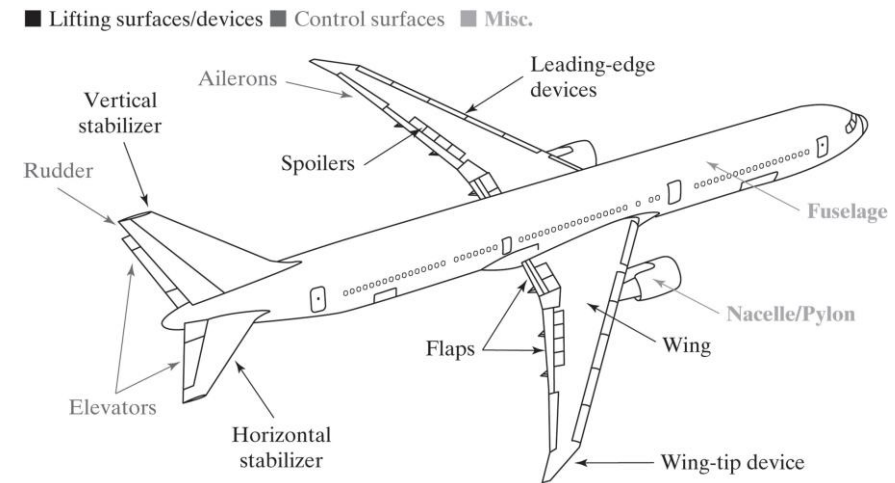
$$\mathbf{F} = \int_{\partial S} \left(\overset{\substack{\text{Pressure contribution} \\ \downarrow}}{-p\mathbf{I}} + \overset{\substack{\uparrow \\ \text{Viscous contribution}}}{\boldsymbol{\tau}} \right) \cdot \mathbf{n} dS$$

Forces on a body

- Aerodynamic forces acting on a body.
 - In the literature, you will find more elaborated force breakdown, in particular for the drag force.
 - These more elaborated forces decomposition are subcategories of the pressure and viscous forces.
 - Sometimes is not very straight forward how to measure these derived forces decomposition.
 - In aeronautical applications, the most general drag breakdown is as follows:
 - Skin friction, pressure drag, wave drag, and induced drag (in wings).
 - You can also will find more complex drag definitions associated to the components of the aircraft:
 - Trim drag, nacelle drag, cooling drag, interference drag, excrescences drag, parasite drag, form drag, base drag, and so on.



Contributions of different drag sources for a typical transport aircraft.



Major components of a modern commercial airliner. Each component contributes differently to the force breakdown

Forces on a body

- Forces and moments acting on an airfoil or a wing.
 - In aerodynamic analysis, it is a common practice to use non-dimensional coefficients when quantifying the aerodynamic forces and aerodynamic moments.
 - By using aerodynamic coefficients, the aerodynamic forces \mathbf{F} and aerodynamic moments \mathbf{M} , can be computed as follows,

The diagram illustrates the calculation of aerodynamic force F and moment M using non-dimensional coefficients. It consists of two equations with arrows pointing to each variable to identify its physical meaning.

Force Equation:

$$F = \frac{1}{2} \times \rho \times V^2 \times S_{ref} \times c_F$$

Labels for Force Equation:

- Lift (L) or Drag (D) points to F .
- Density points to ρ .
- Freestream velocity points to V^2 .
- Reference surface for forces/moments computation points to S_{ref} .
- Force coefficient points to c_F .

Moment Equation:

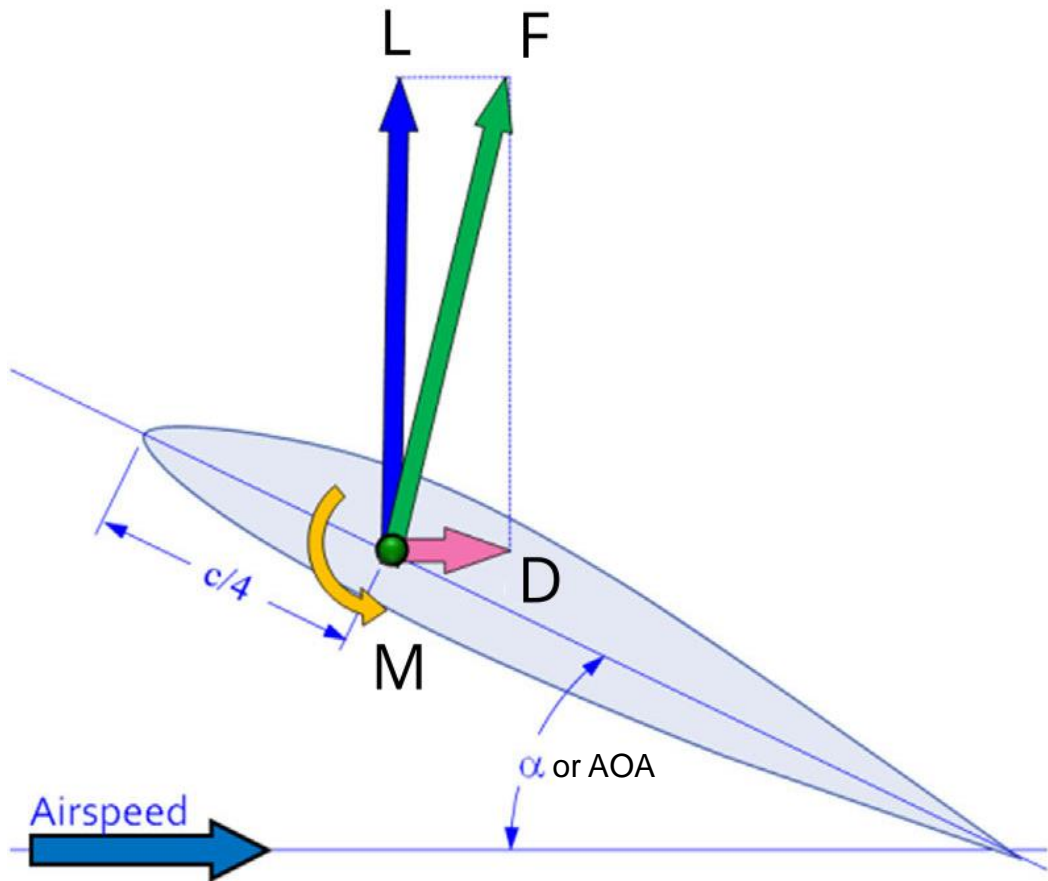
$$M = \frac{1}{2} \times \rho \times V^2 \times S_{ref} \times L_{ref} \times c_M$$

Labels for Moment Equation:

- Moment (M) points to M .
- Density points to ρ .
- Freestream velocity points to V^2 .
- Reference surface for forces/moments computation points to S_{ref} .
- Reference length for moment computation points to L_{ref} .
- Moment coefficient points to c_M .

Forces on a body

- Forces and moments acting on an airfoil or a wing.
 - Notice that in 2D (airfoils), the forces and moments are computed per unit depth.
 - Therefore, S_{ref} refers to the airfoil chord, that is, c_{ref} .
 - Or to be more correct, $c_{ref} \times \text{unit depth}$



$$L = \frac{1}{2} \times \rho \times V^2 \times S_{ref} \times c_l$$

Lift coefficient

$$D = \frac{1}{2} \times \rho \times V^2 \times S_{ref} \times c_d$$

Drag coefficient

$$M = \frac{1}{2} \times \rho \times V^2 \times S_{ref} \times L_{ref} \times c_m$$

Moment coefficient

Forces on a body

- Forces and moments acting on an airfoil (2D).

$$L = \frac{1}{2} \times \rho \times V^2 \times c \times c_l$$

where c_l is the airfoil lift coefficient, c the airfoil chord, V is the free-stream velocity and ρ is the air density

$$D = \frac{1}{2} \times \rho \times V^2 \times c \times c_d$$

where c_d is the airfoil drag coefficient, c the airfoil chord, V is the free-stream velocity and ρ is the air density

$$M = \frac{1}{2} \times \rho \times V^2 \times c \times c_{ref} \times c_m$$

where c_m is the airfoil pitching moment coefficient (usually computed at $c/4$), c the airfoil chord, c_{ref} is the reference arm, V is the free-stream velocity and ρ is the air density

- Notice that the forces and moments are computed per unit depth.

Forces on a body

- Forces and moments acting on a wing (3D).

$$L = \frac{1}{2} \times \rho \times V^2 \times S_{ref} \times C_L$$

where C_L is the wing lift coefficient, S_{ref} is the wing reference area, V is the free-stream velocity and ρ is the air density.

$$D = \frac{1}{2} \times \rho \times V^2 \times S_{ref} \times C_D$$

where C_D is the wing drag coefficient, S_{ref} is the wing reference area, V is the free-stream velocity and ρ is the air density.

$$M = \frac{1}{2} \times \rho \times V^2 \times S_{ref} \times c_{ref} \times C_M$$

where C_M is the wing pitching moment coefficient (usually computed at $c/4$ of the MAC), c_{ref} is the reference arm, S_{ref} is the wing reference area, V is the free-stream velocity and ρ is the air density.

Forces on a body

- A final reminder about notation:

- The following notation refers to wing coefficients:

C_L C_D C_M  All in uppercase letters

- The following notation refers to wing section coefficients:

C_l C_d C_m  The subscripts are in lowercase letters

- The following notation refers to airfoil coefficients:

c_l c_d c_m  All in lowercase letters

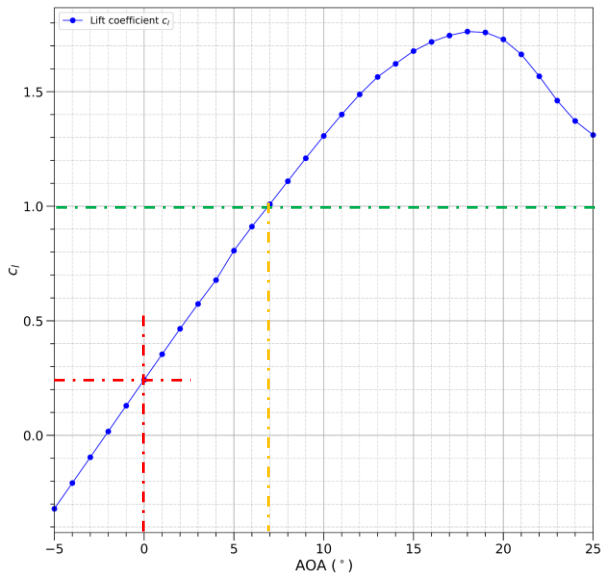
Airfoil performance plots

Airfoil performance plots

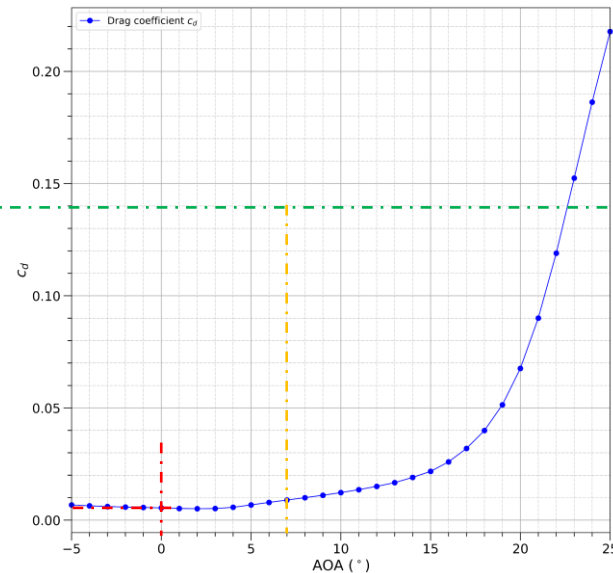
- The performance of airfoils can be described using four plots:
 - Lift coefficient (C_L) vs. AOA.
 - Drag coefficient (C_D) vs. AOA.
 - Pitching moment coefficient about $c/4$ ($C_{M-c/4}$) vs. AOA.
 - Polar plot – Lift coefficient vs. Drag coefficient (or the opposite).

Note:
AOA \rightarrow angle of attack (incidence angle)

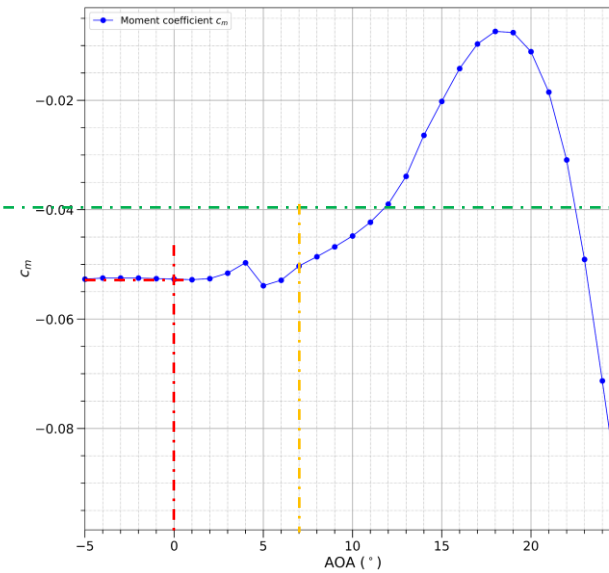
Lift coefficient (C_L) vs. AOA



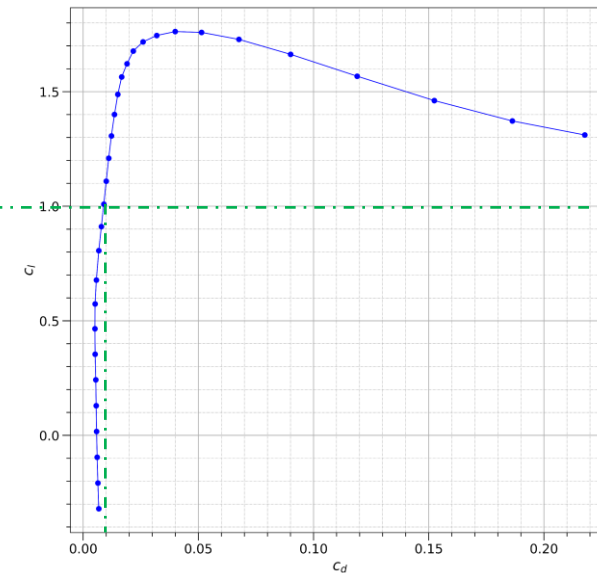
Drag coefficient (C_D) vs. AOA



Pitching moment coefficient about $c/4$ ($C_{M-c/4}$) vs. AOA



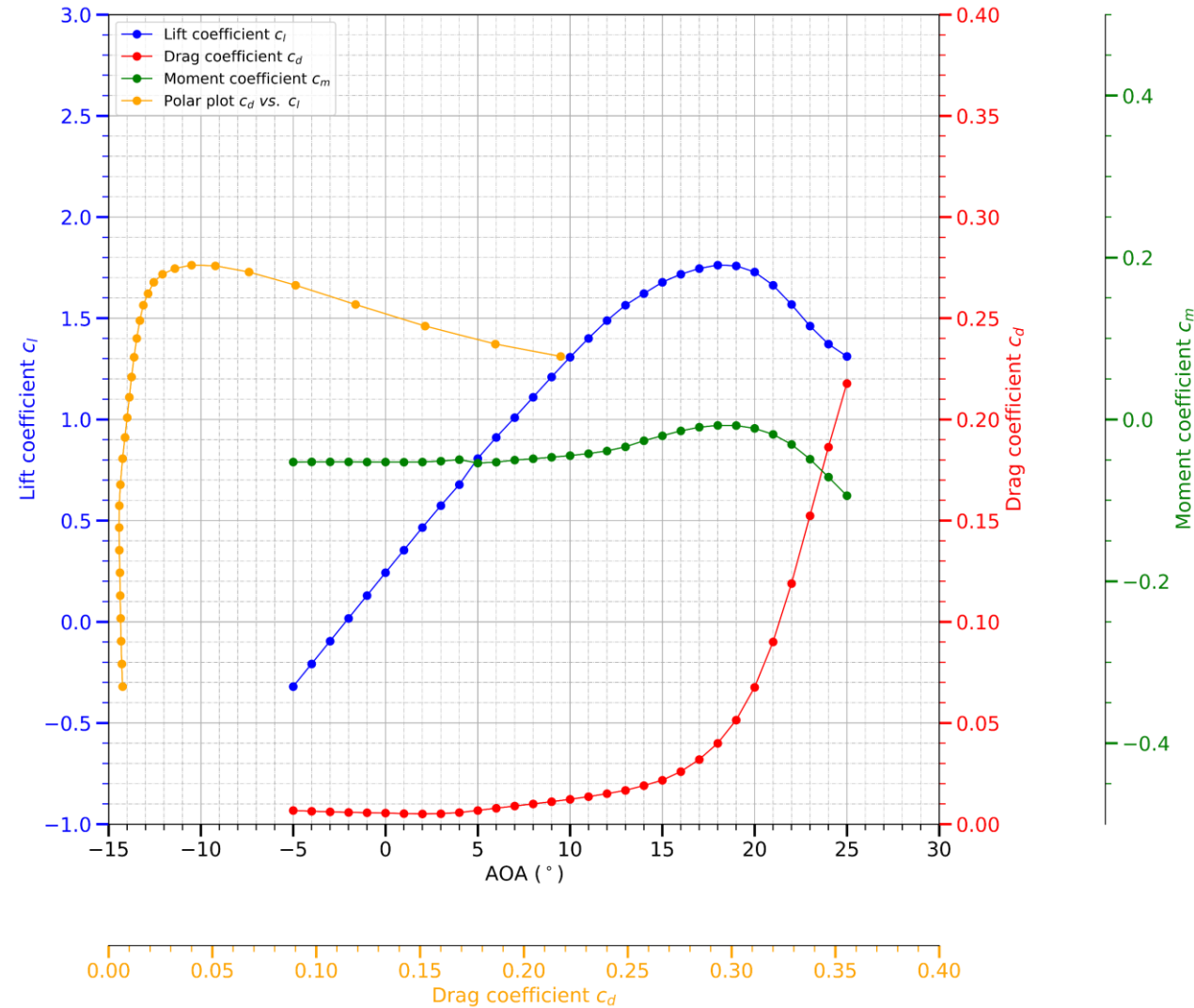
Polar plot - C_L vs. C_D



These results corresponds to a NACA 2412 airfoil, $Re = 3\,000\,000$.
The results were obtained using XFOIL.

Airfoil performance plots

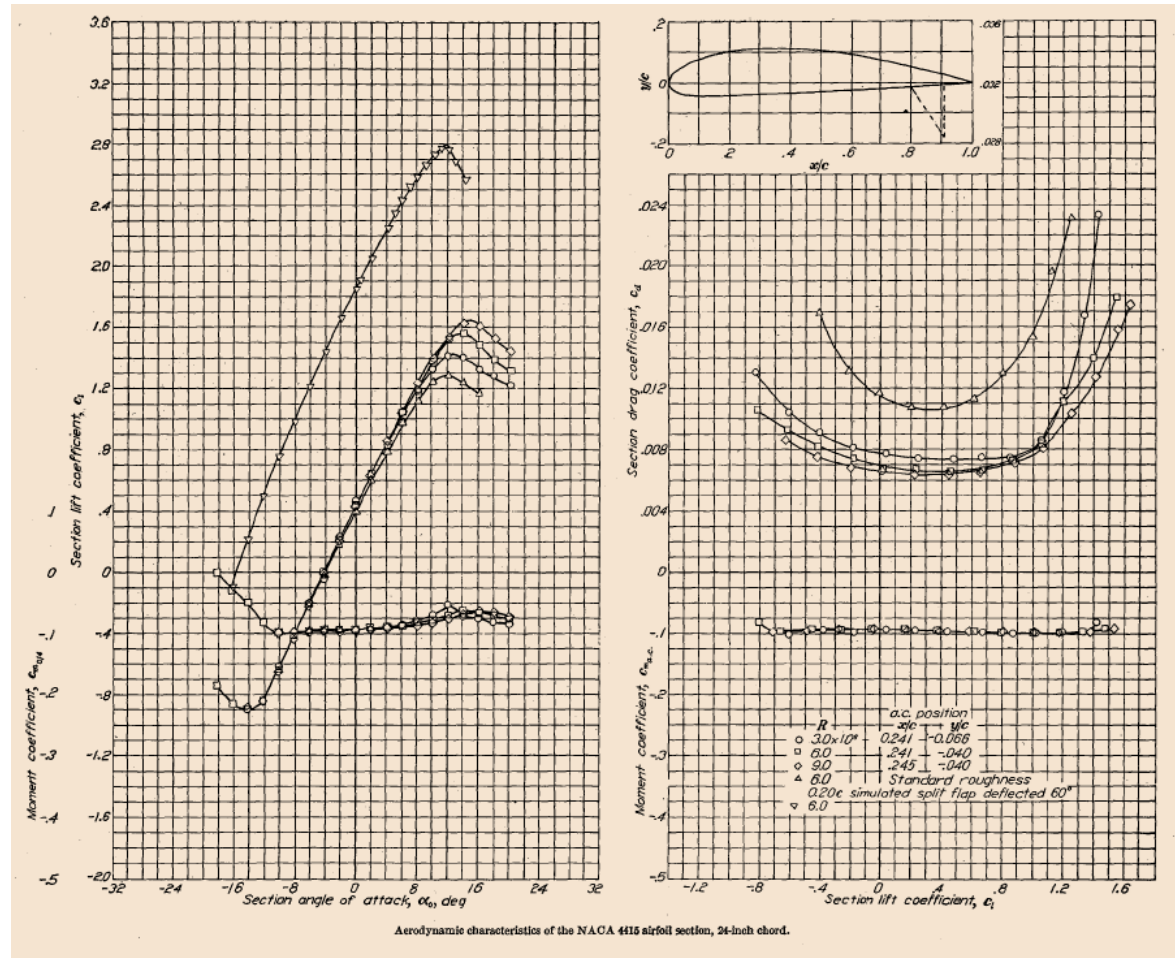
- And to simplify things, we can put all the previous plots in one single graph.



These results corresponds to a NACA 2412 airfoil, $Re = 3\,000\,000$.
The results were obtained using XFOIL.

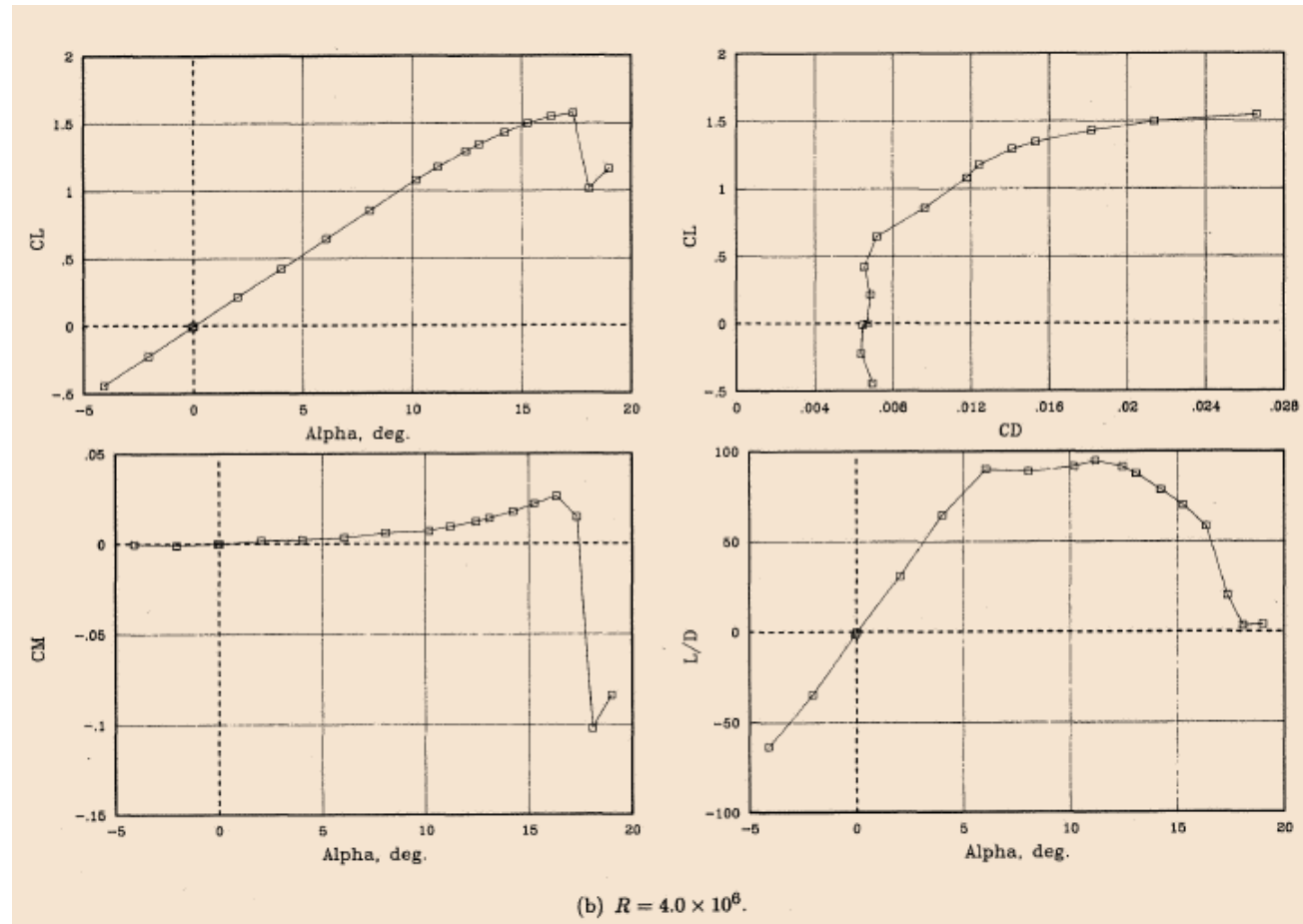
Airfoil performance plots

- In the literature, you will find these plots in different layouts and formats.
- Independently of the layout used, they always convey the same information.



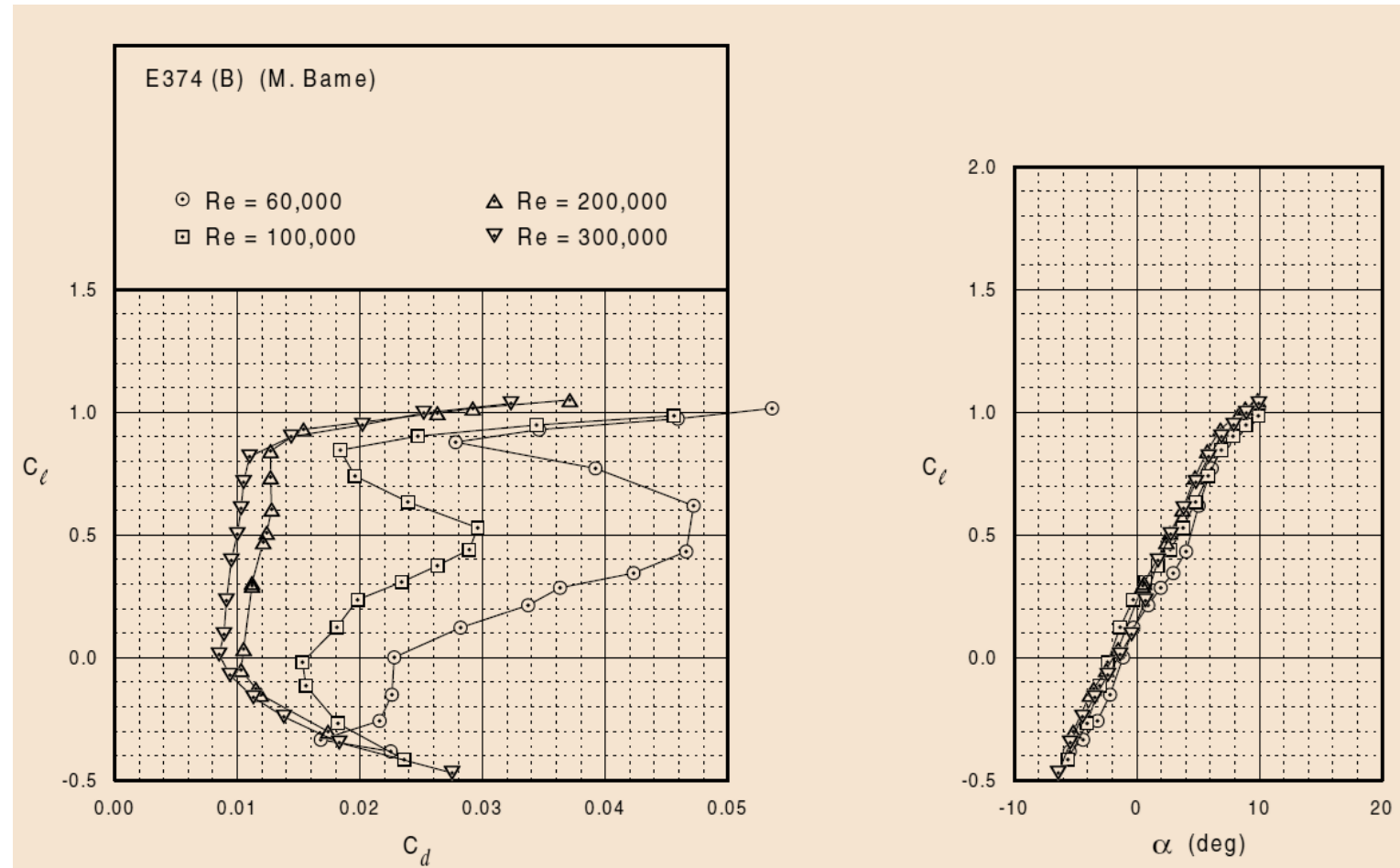
Airfoil performance plots

- In the literature, you will find these plots in different layouts and formats.
- Independently of the layout used, they always convey the same information.



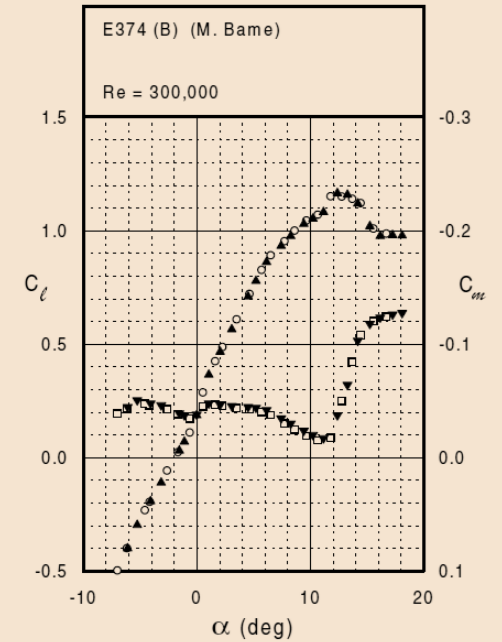
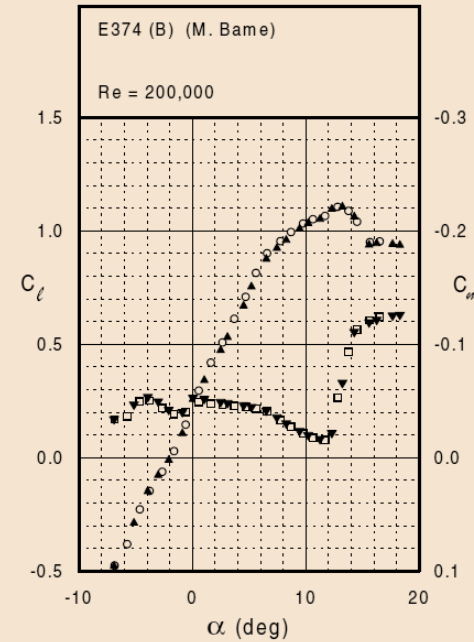
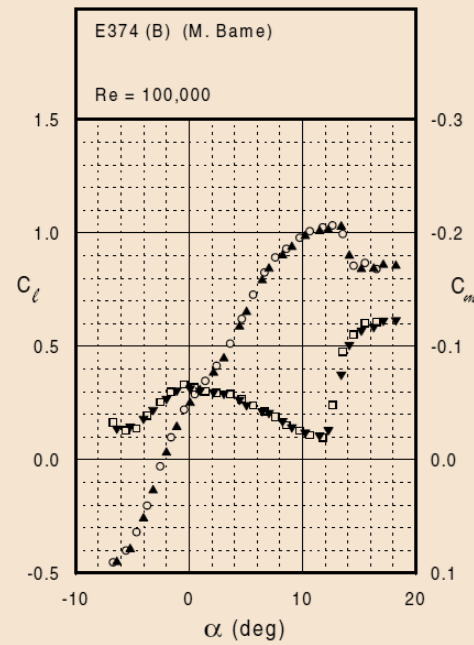
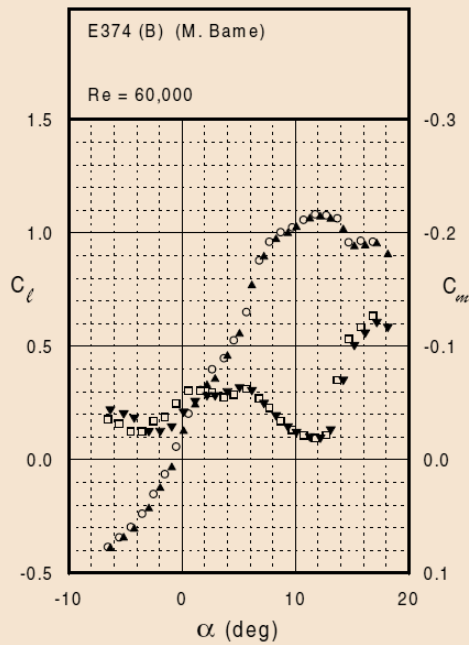
Airfoil performance plots

- In the literature, you will find these plots in different layouts and formats.
- Independently of the layout used, they always convey the same information.



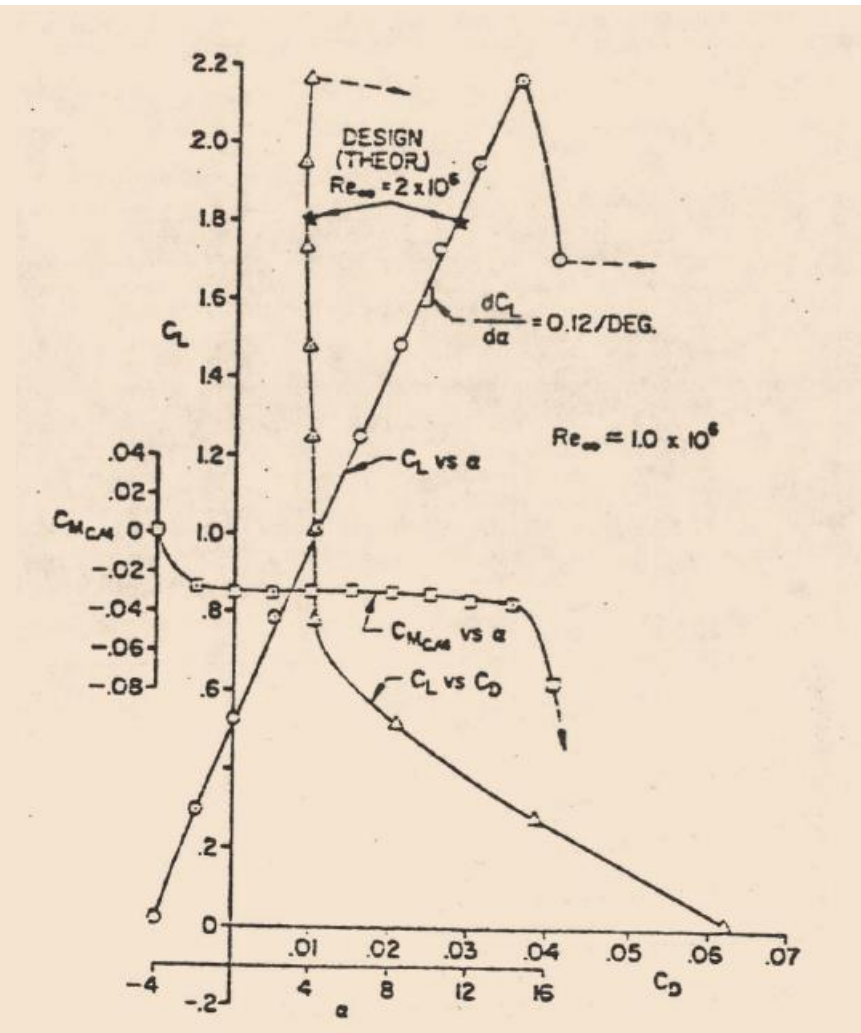
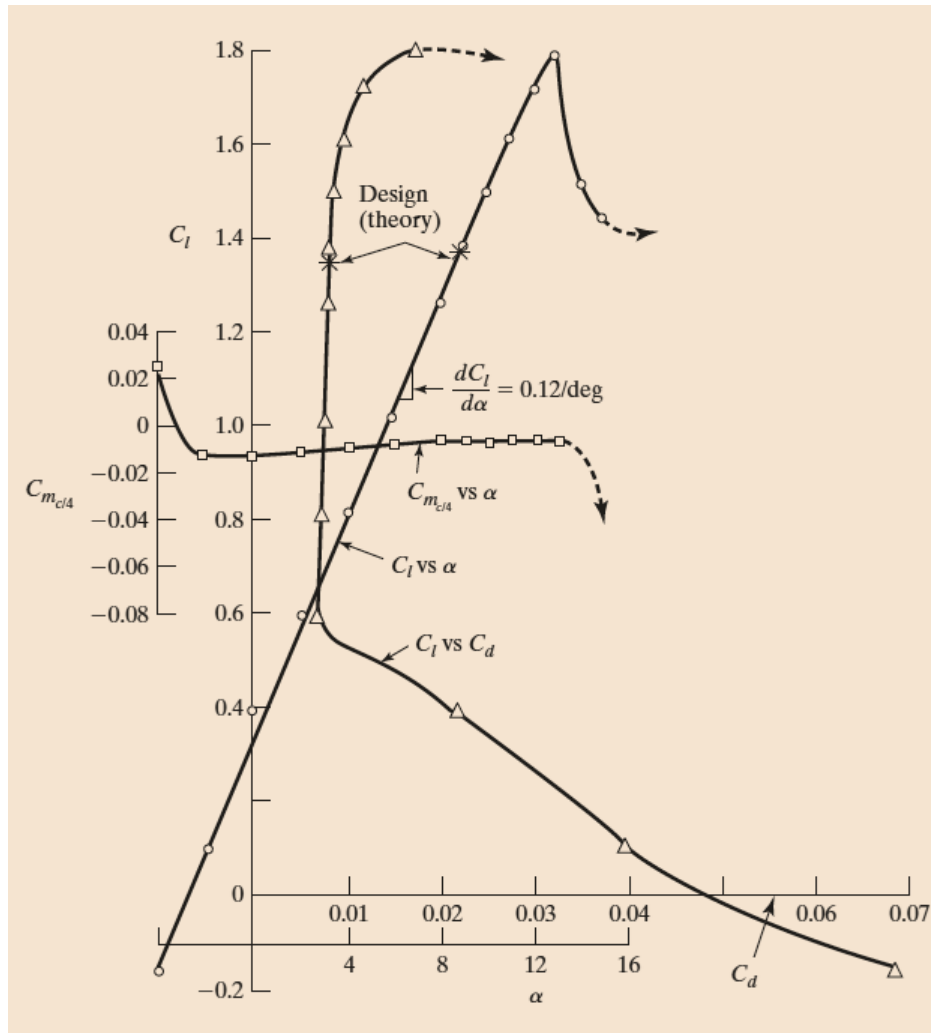
Airfoil performance plots

- In the literature, you will find these plots in different layouts and formats.
- Independently of the layout used, they always convey the same information.



Airfoil performance plots

- In the literature, you will find these plots in different layouts and formats.
- Independently of the layout used, they always convey the same information.

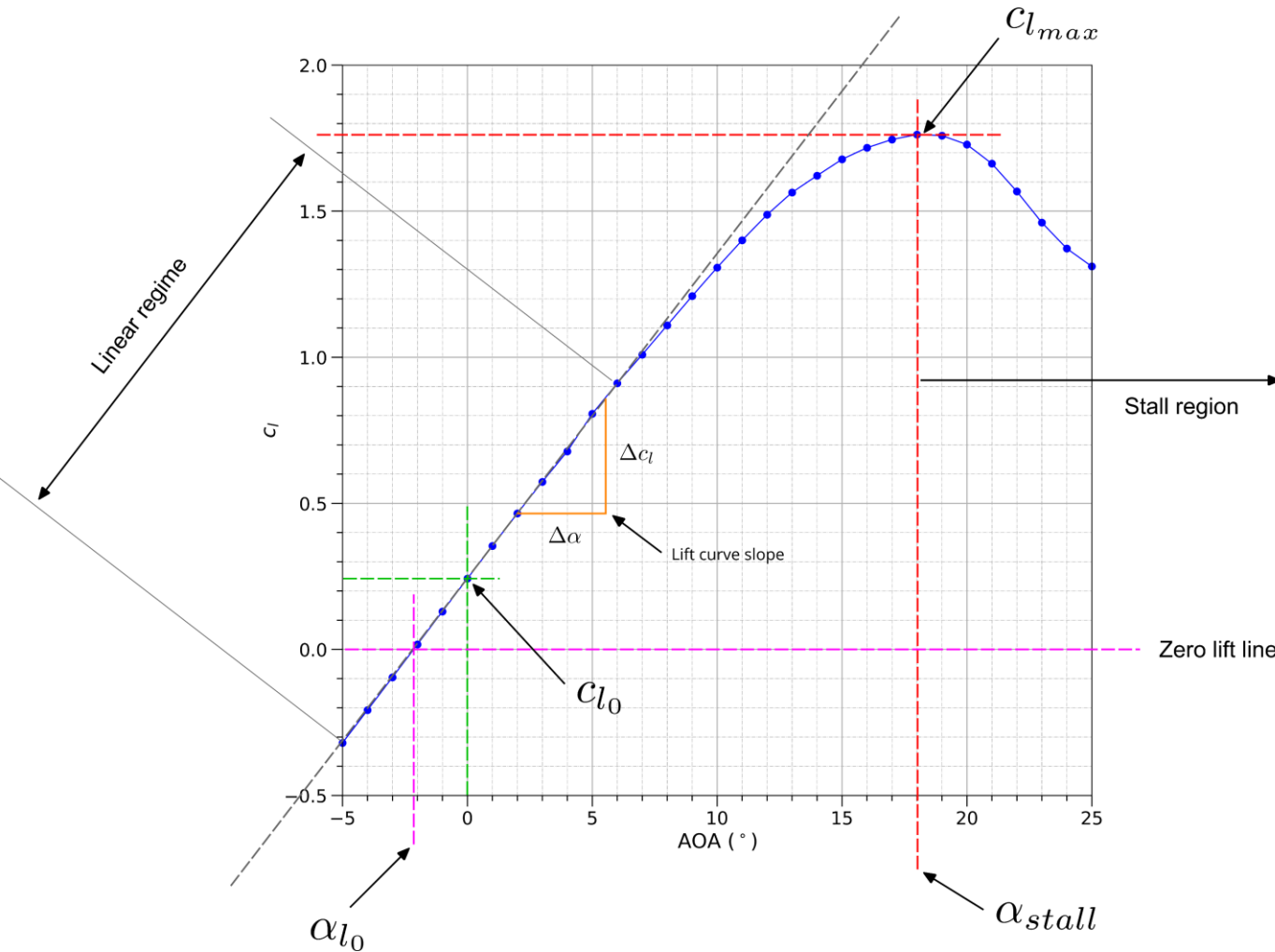


Dissecting airfoil performance plots

Airfoil characteristics

Dissecting airfoil performance plots – Airfoil characteristics

- Typical lift coefficient vs. AOA plot.



$C_{l_{max}}$

→ Maximum lift coefficient

C_{l_0}

→ Lift coefficient at zero AOA

α_{l_0}

→ AOA at zero lift

α_{stall}

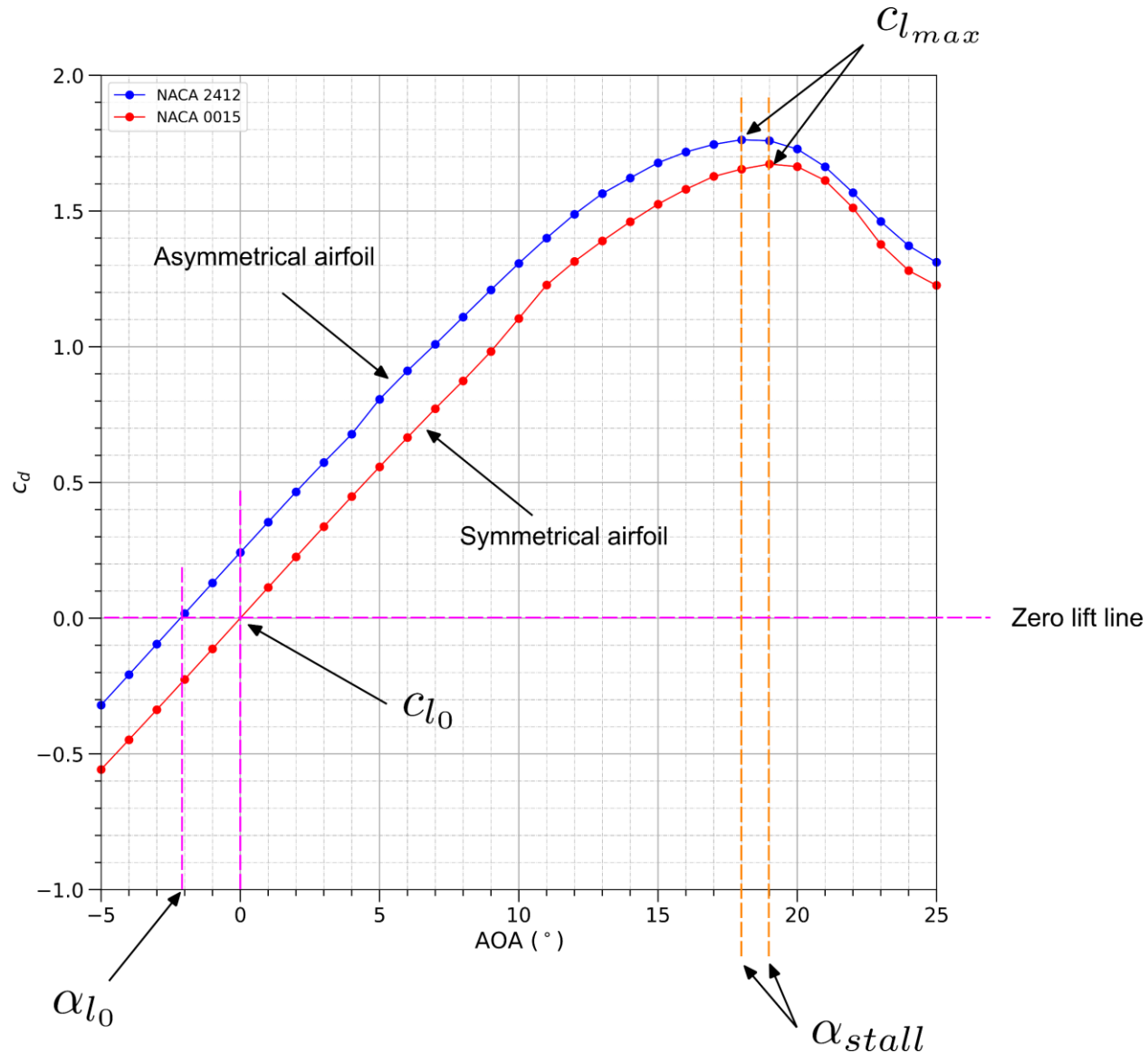
→ Stall AOA

α or AOA

→ angle-of-attack (in degrees)

Dissecting airfoil performance plots – Airfoil characteristics

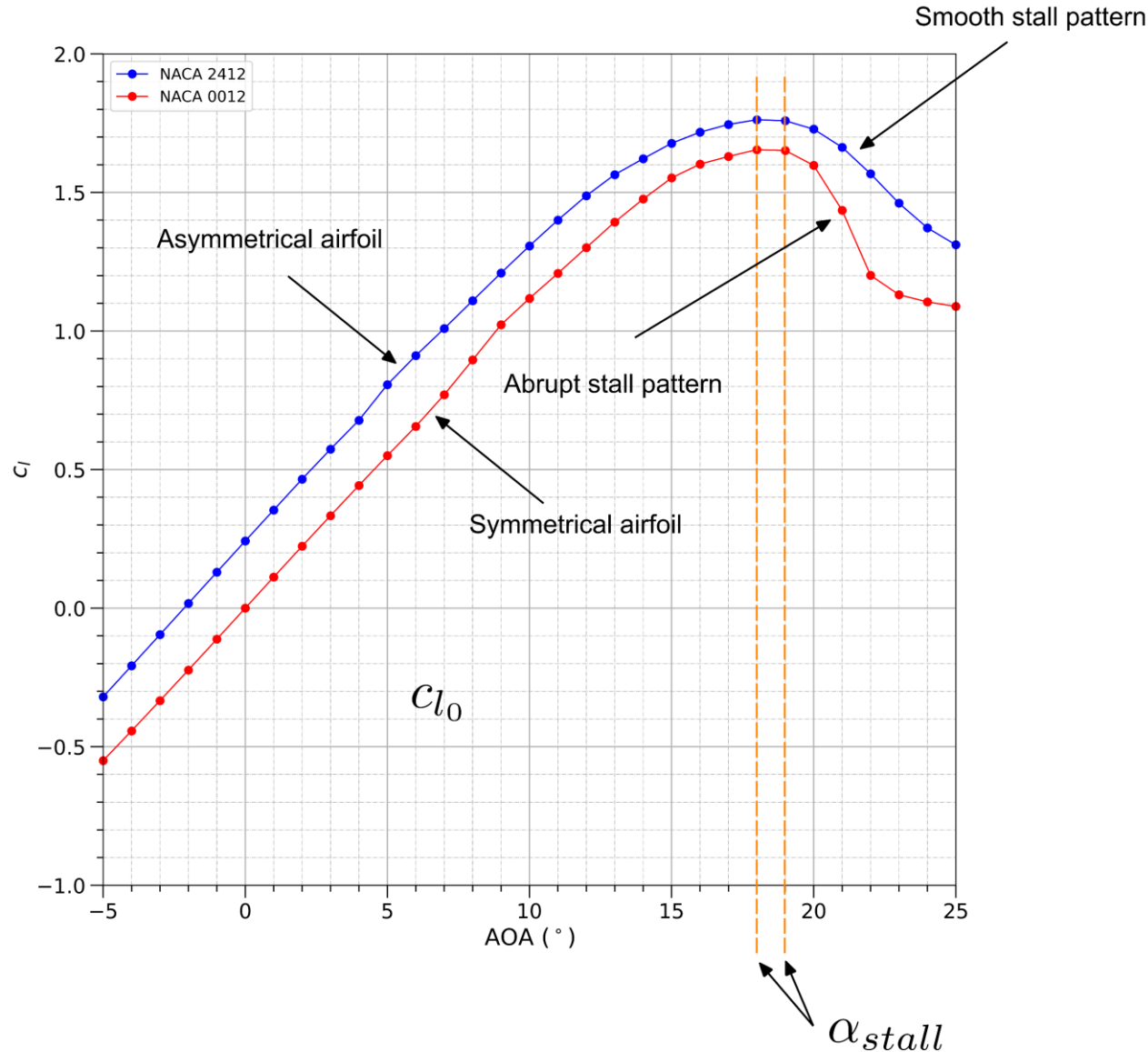
- Typical lift coefficient vs. AOA plot – Symmetric airfoil (NACA 0015) vs. Asymmetric airfoil (NACA 2412).



- Cambering (or curvature), helps to generate lift at zero angle of attack.
- Therefore, it increases the maximum lift coefficient.
- It also reduces the stall angle of attack.
- Positive camber shift the curve in the negative sense of the angle of attack.
- In general, cambering reduces the usable range of angles of attack from AOA equal to zero, up to the maximum lift coefficient.

Dissecting airfoil performance plots – Airfoil characteristics

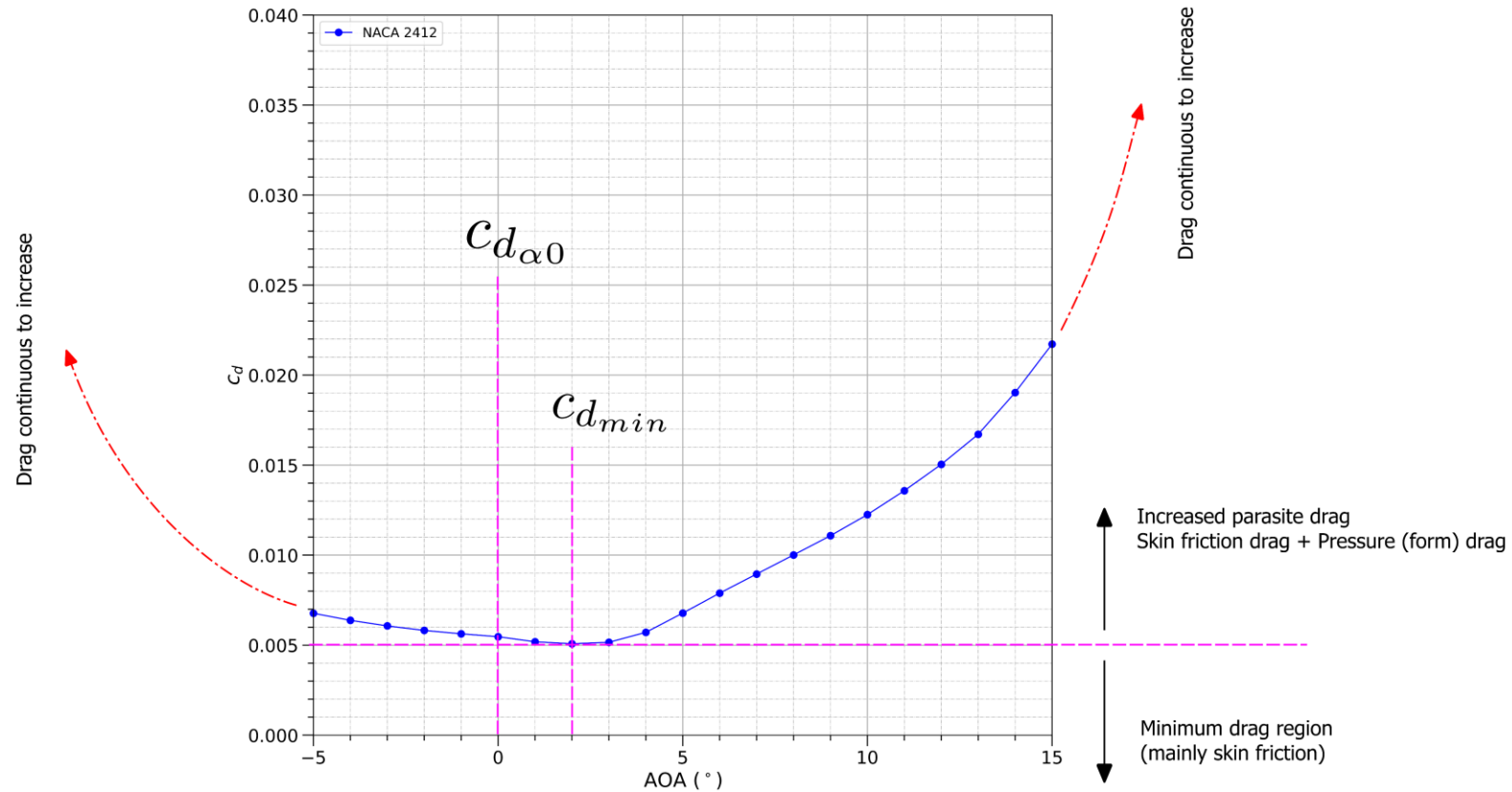
- Typical lift coefficient vs. AOA plot – Symmetric airfoil (NACA 0012) vs. Asymmetric airfoil (NACA 2412).



- Stall refers to the flow condition that follows the first peak of the lift curve.
- It is characterized by a decrease of lift and an increase of drag.
- Different airfoils can have different stall patterns.

Dissecting airfoil performance plots – Airfoil characteristics

- Typical drag coefficient vs. AOA plot.

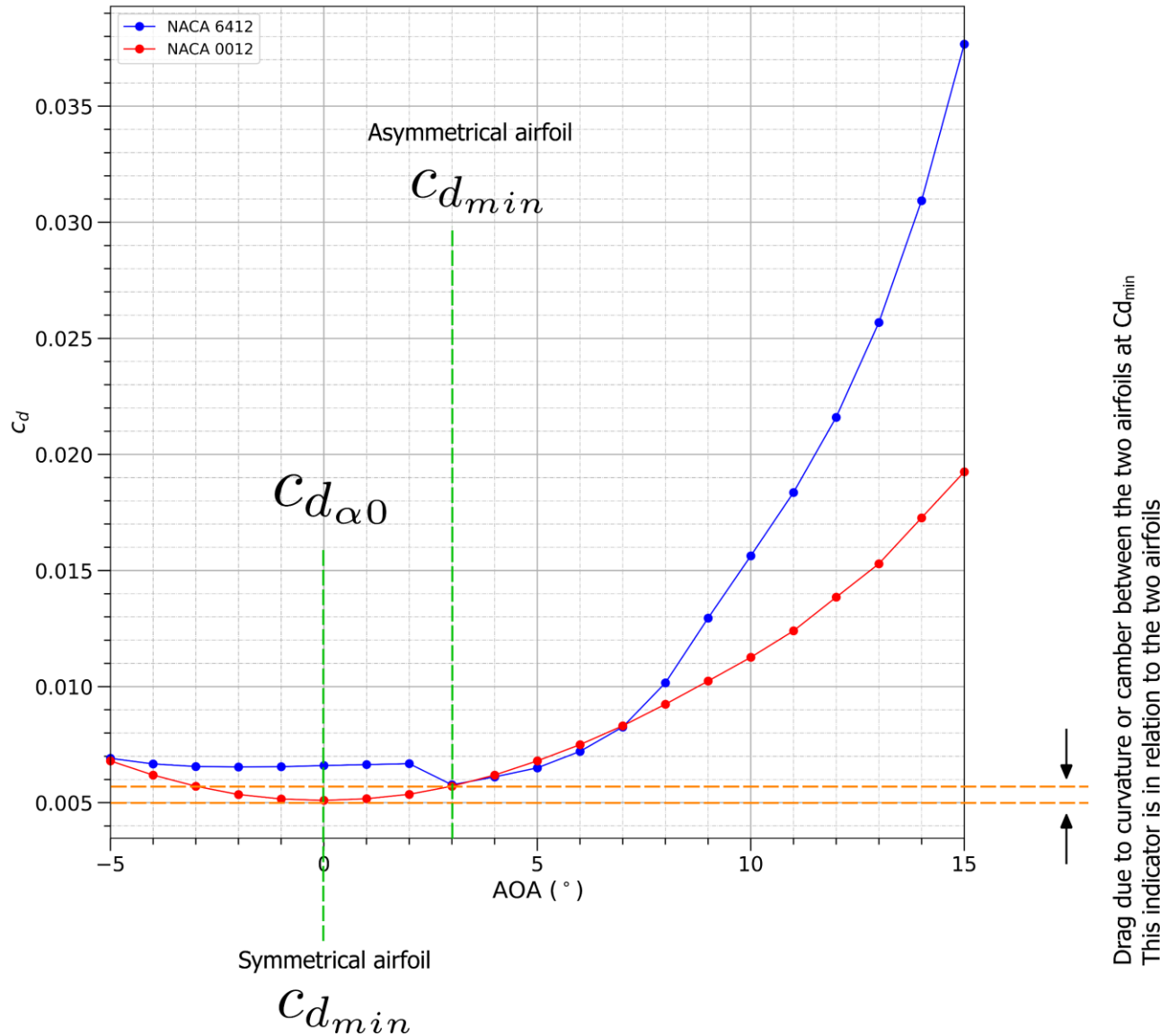


$C_{d_{min}}$ → Minimum drag coefficient

$C_{d_{\alpha 0}}$ → Drag coefficient at zero AOA

Dissecting airfoil performance plots – Airfoil characteristics

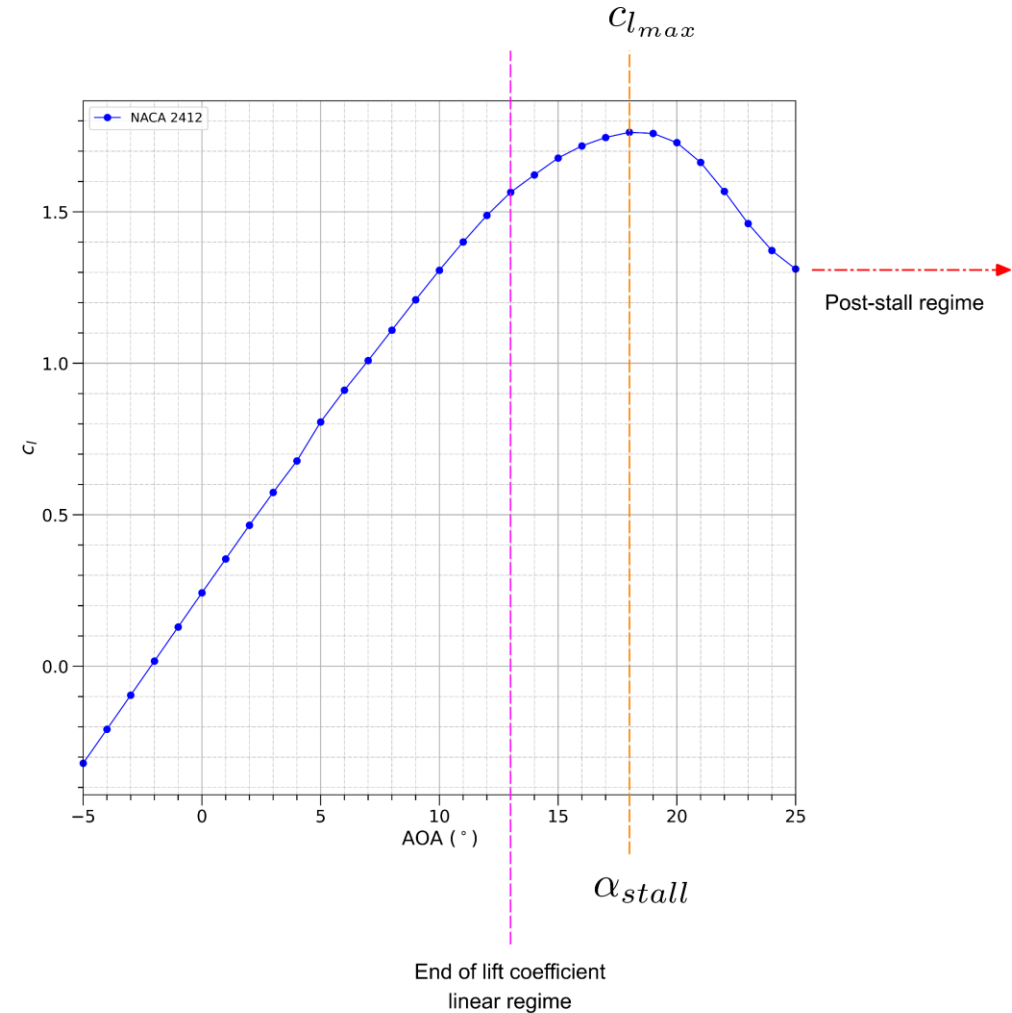
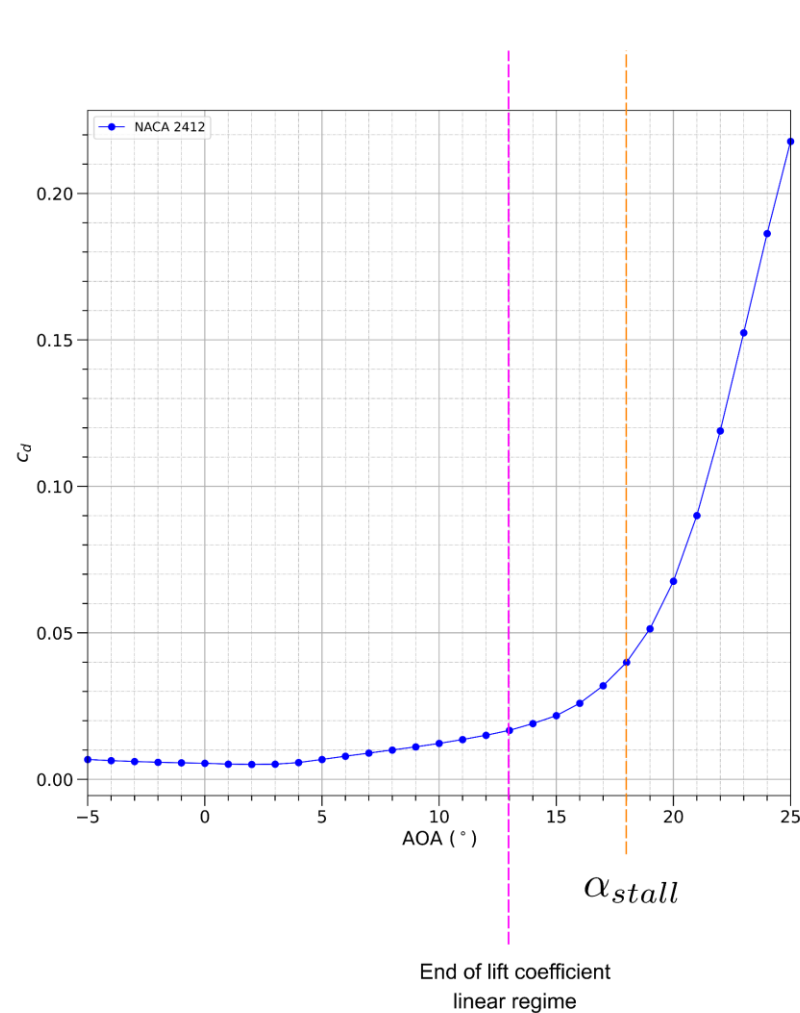
- Typical drag coefficient vs. AOA plot – Symmetric airfoil (NACA 0012) vs. Asymmetric airfoil (NACA 6412).



- Cambering (curvature), increases the minimum drag.
- The rise in minimum drag is due to airfoil curvature effects.
- Positive camber shift the curve in the positive sense of the angle of attack.
- The minimum drag in symmetrical airfoils is found when AOA is equal to zero.
- The region below $C_{d_{min}}$ is mainly skin friction drag.
- The drag due to curvature between the two airfoils is measured at $C_{d_{min}}$.

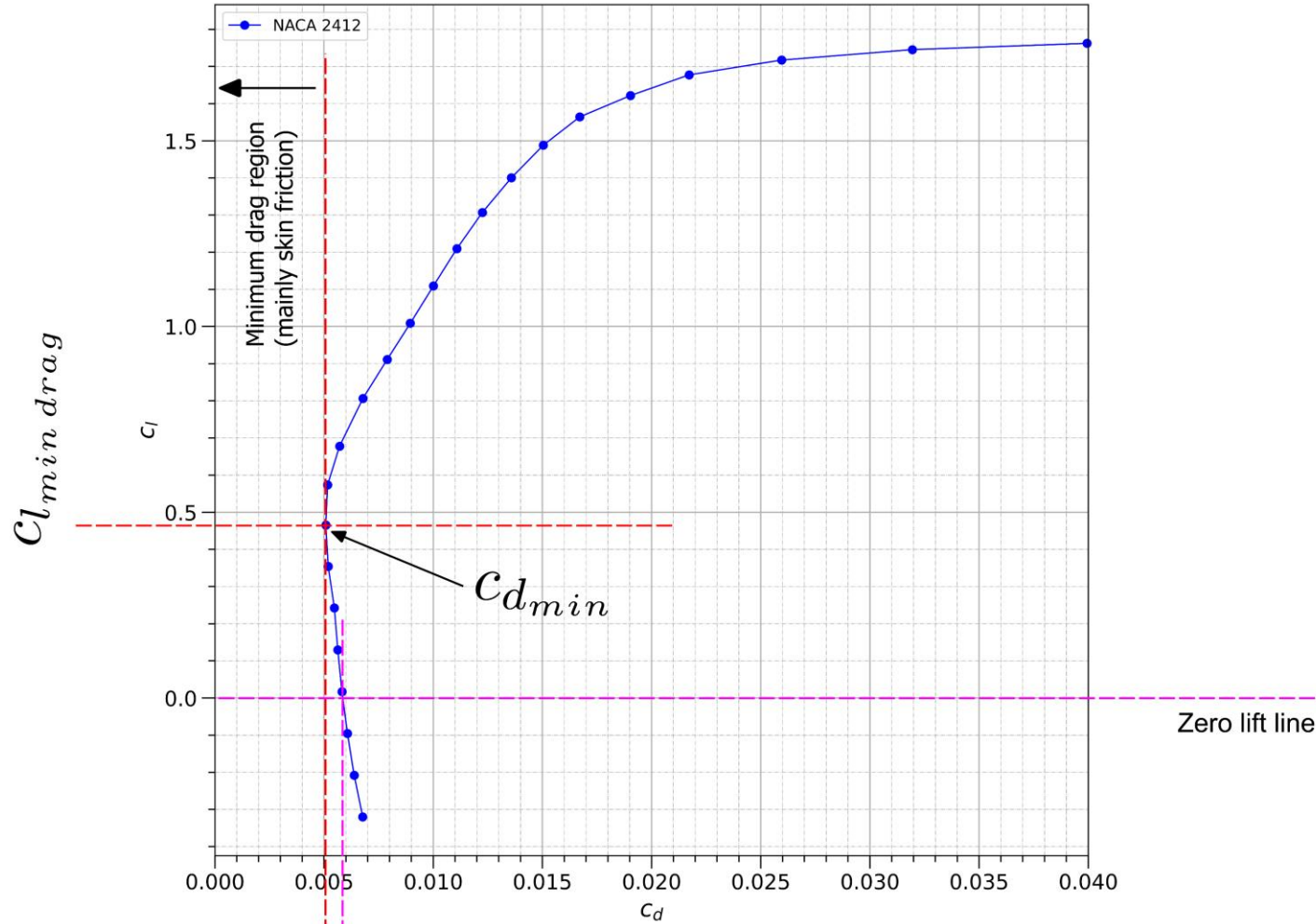
Dissecting airfoil performance plots – Airfoil characteristics

- Typical drag coefficient vs. AOA plot.
- After the end of the lift coefficient linear regime, and up to the maximum lift coefficient, and all the way into the post-stall region, the drag coefficient increases rapidly.



Dissecting airfoil performance plots – Airfoil characteristics

- Typical polar plot – Lift coefficient vs. Drag coefficient.



Drag due to curvature or camber of the single airfoil ($C_{d_0} - C_{d_{min}}$)

C_{d_0} or $C_{d_{l_0}}$

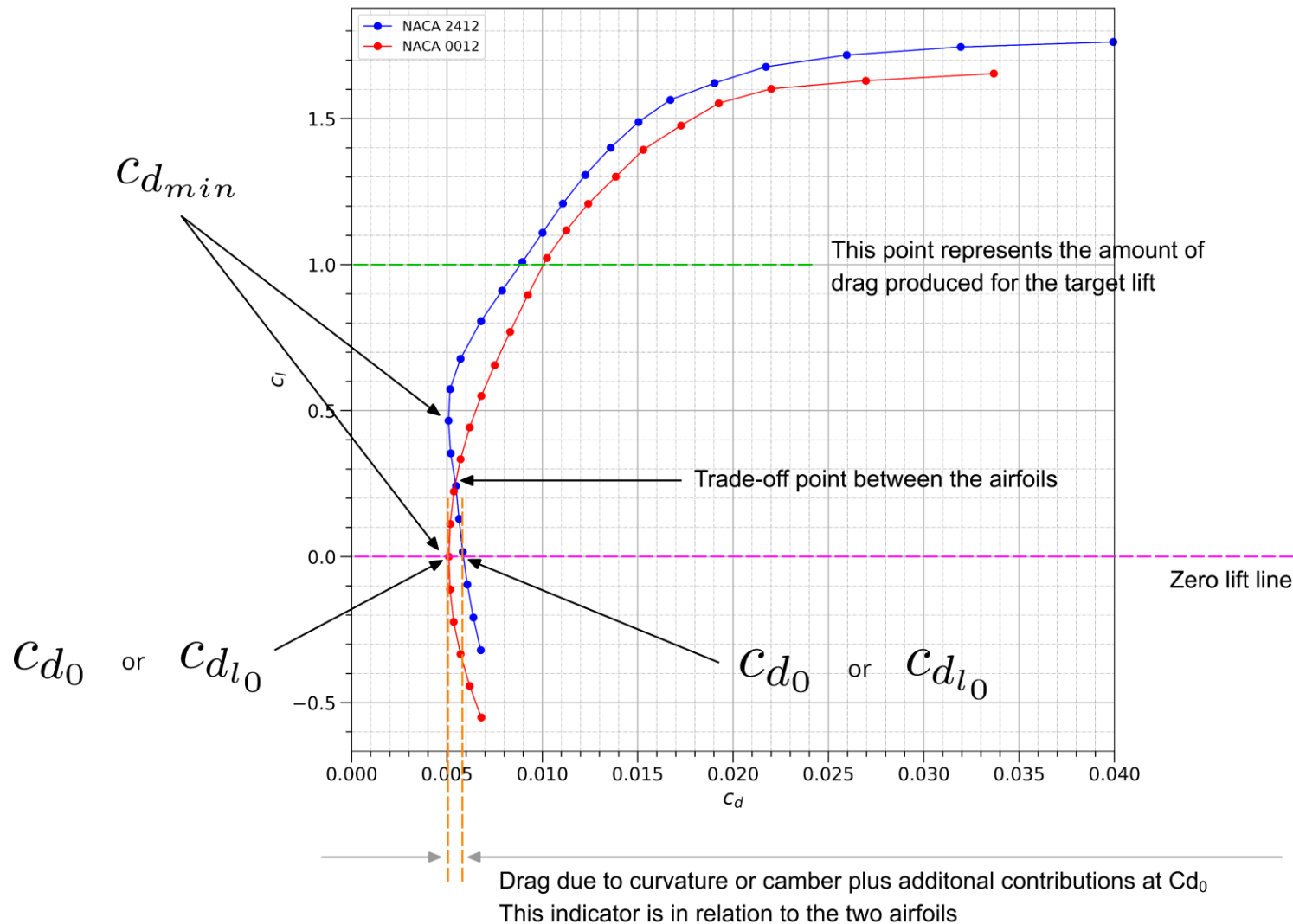
$C_{d_{min}}$
Minimum drag coefficient

C_{d_0} or $C_{d_{l_0}}$
Drag coefficient at zero lift

$C_{l_{min\ drag}}$
Lift coefficient at minimum drag

Dissecting airfoil performance plots – Airfoil characteristics

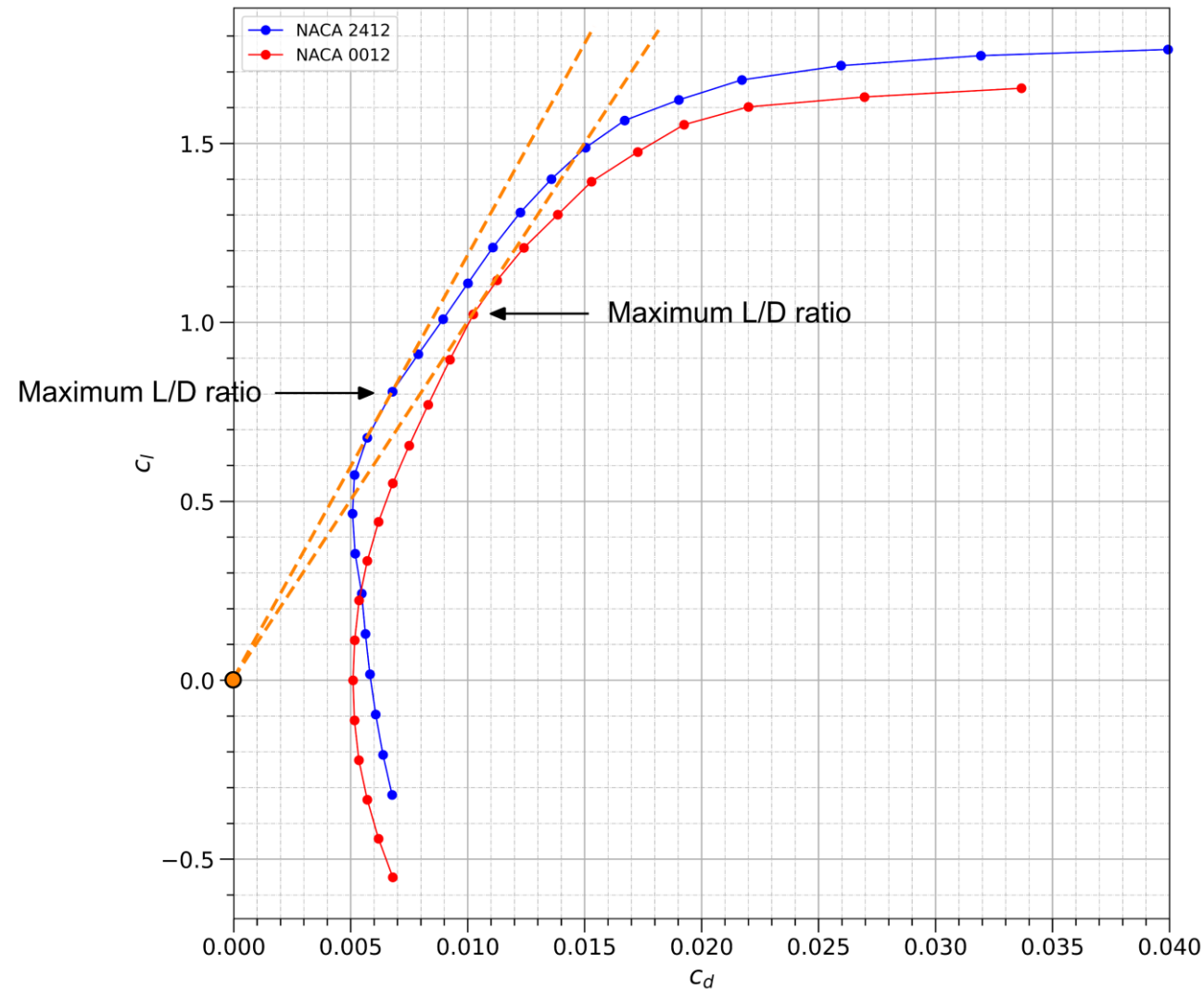
- Typical polar plot – Symmetric airfoil (NACA 0015) vs. Asymmetric airfoil (NACA 4415).
- In a few words, the polar plots are telling you how much drag the airfoil produces for a target lift.



- Cambering (curvature), increases the minimum drag. This rise is due to curvature.
- Camber also increases the drag at zero lift. Again, this increment is due to curvature, plus some additional contributions not so easy to quantify.
- Positive camber shift the curve in the positive sense of the angle of attack.
- For moderate curvature, the rise in minimum drag is not much.

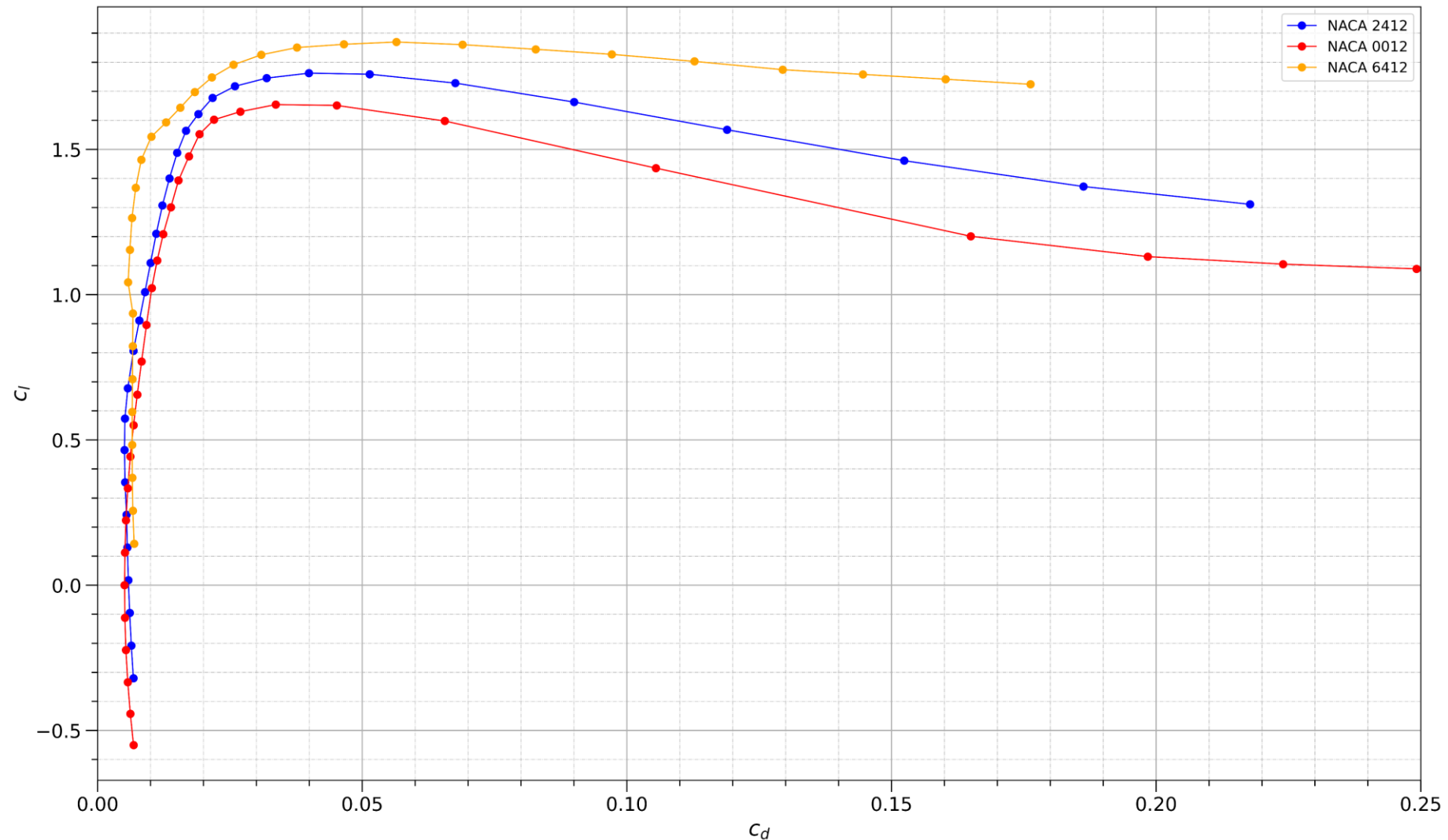
Dissecting airfoil performance plots – Airfoil characteristics

- Typical polar plot – Symmetric airfoil (NACA 0012) vs. Asymmetric airfoil (NACA 2412).
- If we start from $C_L = 0$ and we plot a line tangent to the polar lines, we obtain the maximum C_L/C_D ratio



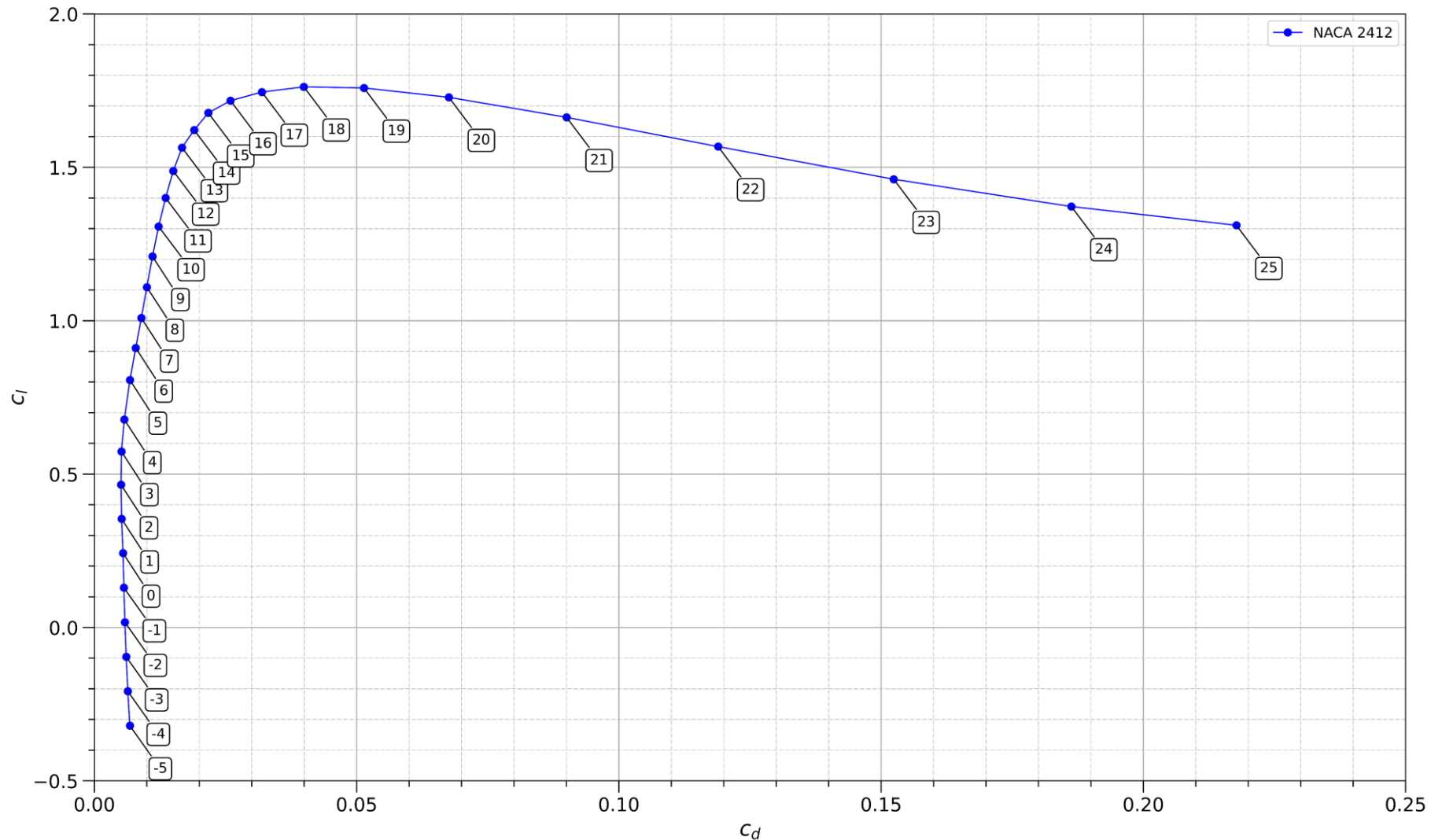
Dissecting airfoil performance plots – Airfoil characteristics

- Typical polar plot – Symmetric airfoil (NACA 0012) vs. Asymmetric airfoils (NACA 2412 & NACA 6412) .
- Hereafter, we are showing the complete polar. In the previous figures, we did not all the values for visibility reasons.



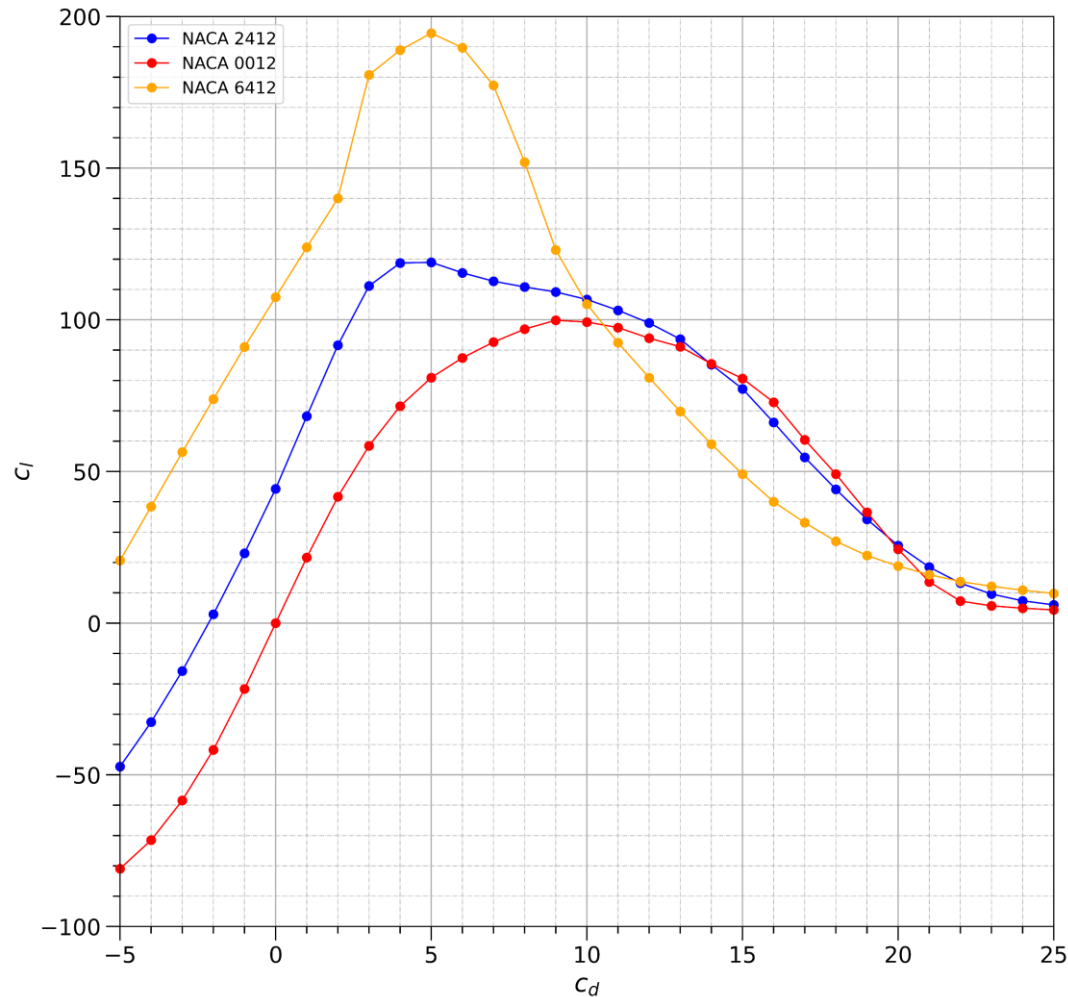
Dissecting airfoil performance plots – Airfoil characteristics

- Typical polar plot –Asymmetric airfoils (NACA 2412) .
- For easier interpretation, you can also add labels (angle of attack) to each point.



Dissecting airfoil performance plots – Airfoil characteristics

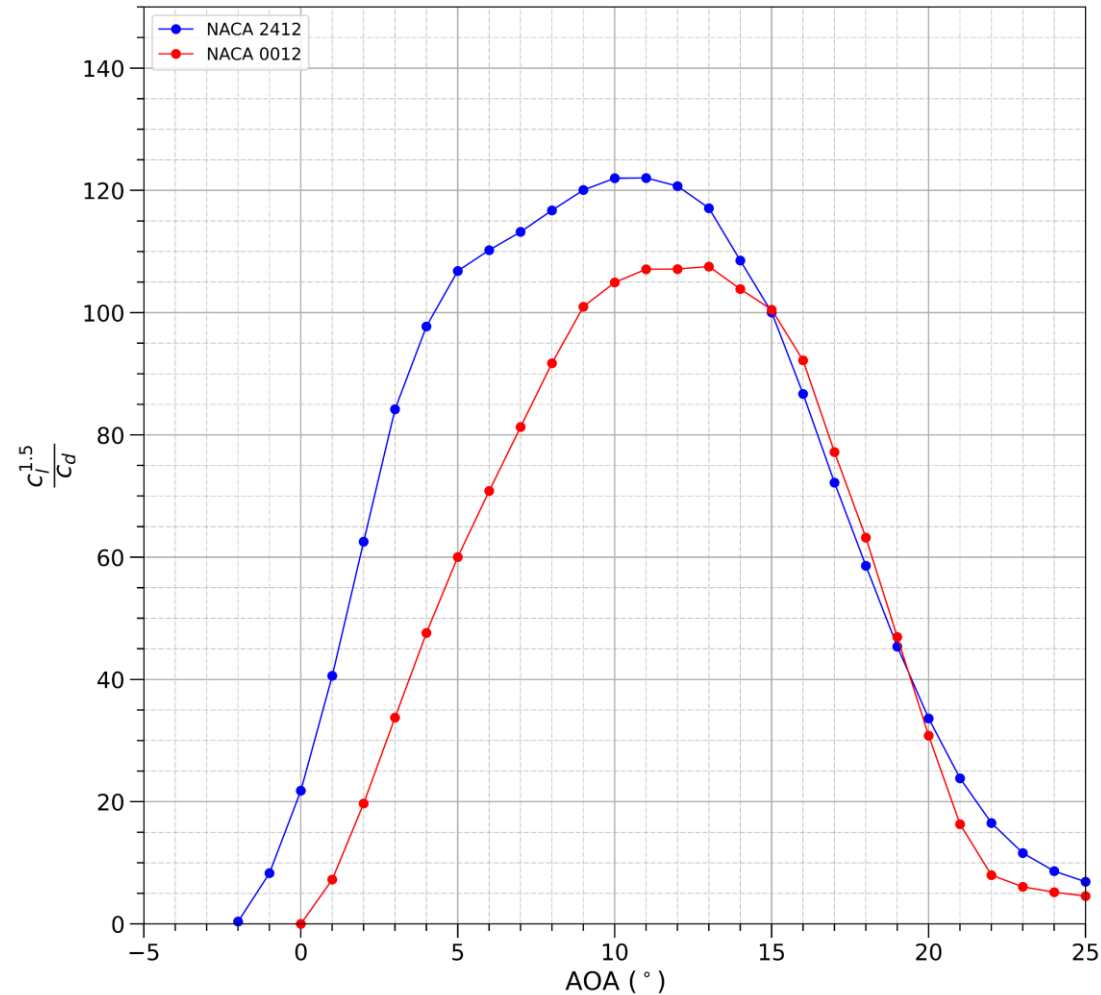
- Some additional plots that you might find useful.
- Lift-to-drag ratio $\frac{C_l}{C_d}$ vs. AOA.



- Lift-to-drag ratio is an indication of the efficiency of the airfoil.
- It tells how much drag the airfoil produces for a given lift value.
- Many metrics of airplane performance are obtained in flight at L/D maximum.
- Performance conditions that occur at L/D max include:
 - Maximum range of propeller-driven airplanes.
 - Maximum climb angle for jet-powered airplanes.
 - Maximum power-off glide ratio (for jet-powered or for propeller-driven airplanes).
 - Maximum endurance for jet-powered airplanes.
- Therefore, when designing a wing, is extremely important to have the L/D max as close as possible to cruise conditions (AOA and cruise velocity).

Dissecting airfoil performance plots – Airfoil characteristics

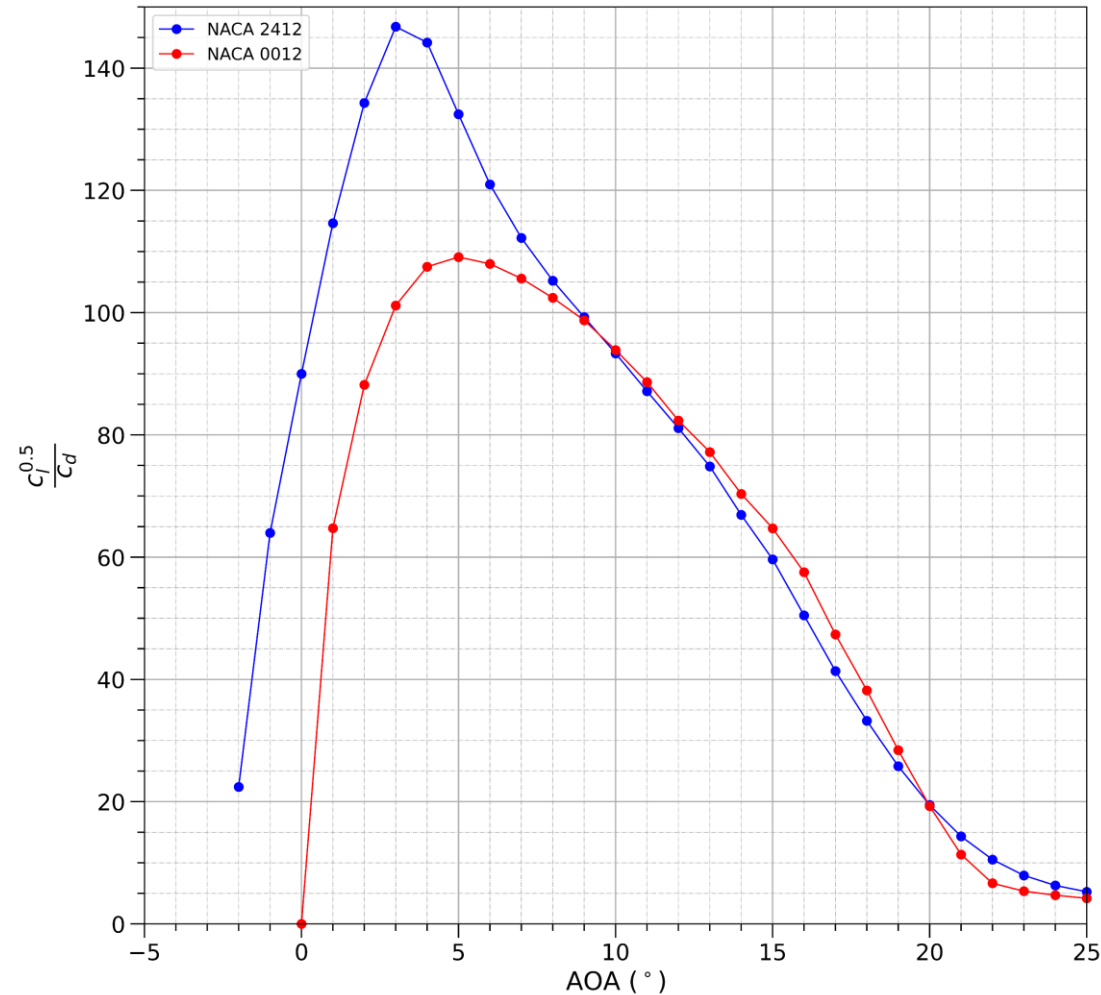
- Some additional plots that you might find useful.
- $\frac{c_l^{1.5}}{c_d}$ ratio vs. AOA.



- Mainly used in aircraft performance computations.
- Used for estimating the maximum endurance for reciprocating engine/propeller.

Dissecting airfoil performance plots – Airfoil characteristics

- Some additional plots that you might find useful.
- $\frac{c_l^{0.5}}{c_d}$ ratio vs. AOA.



- Mainly used in aircraft performance computations.
- Used for estimating the maximum range for reciprocating engine/propeller.

Dissecting airfoil performance plots – Airfoil characteristics

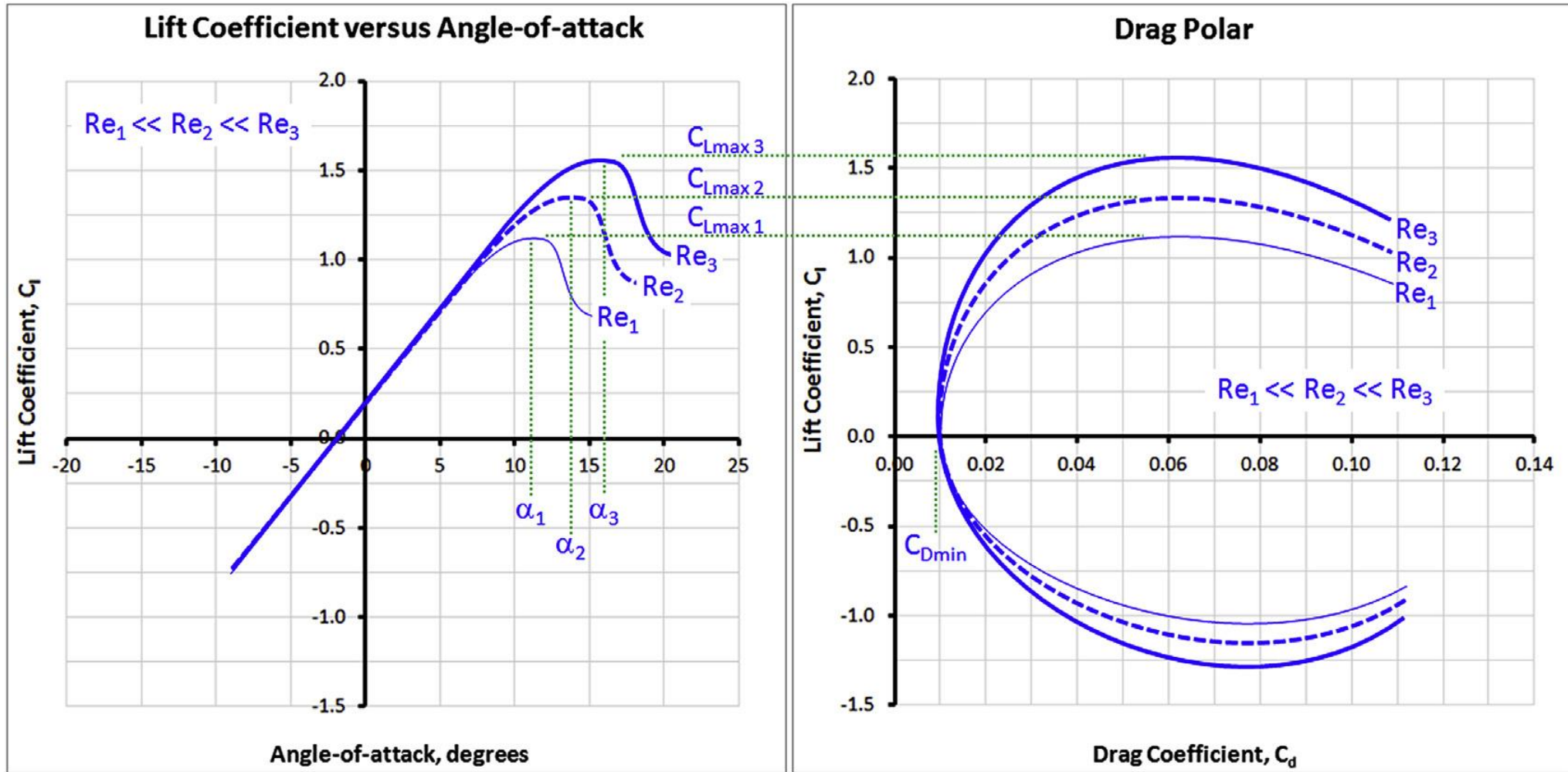
- All the previous plots can also be used with wings and aircraft configurations.
- The information conveyed by the plots and their interpretation is the same.

Aerodynamic performance curves

Extended comments

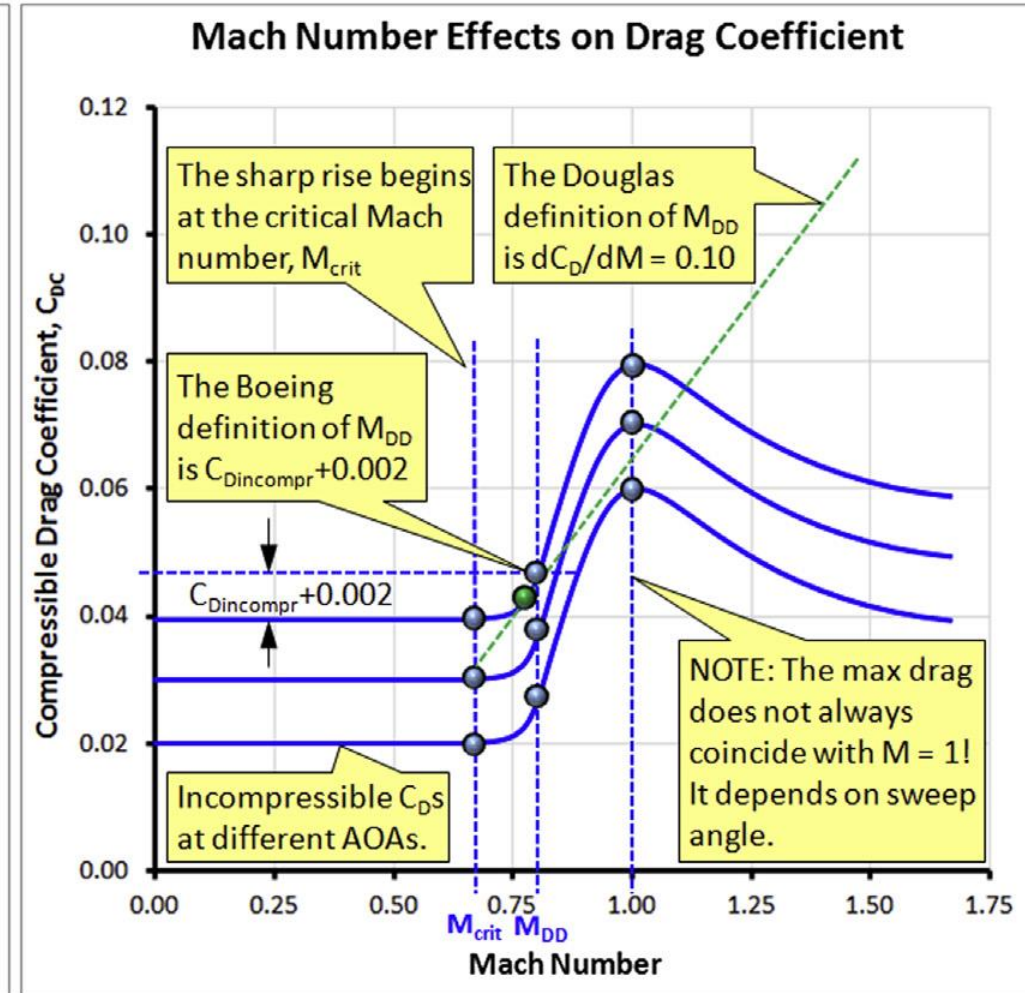
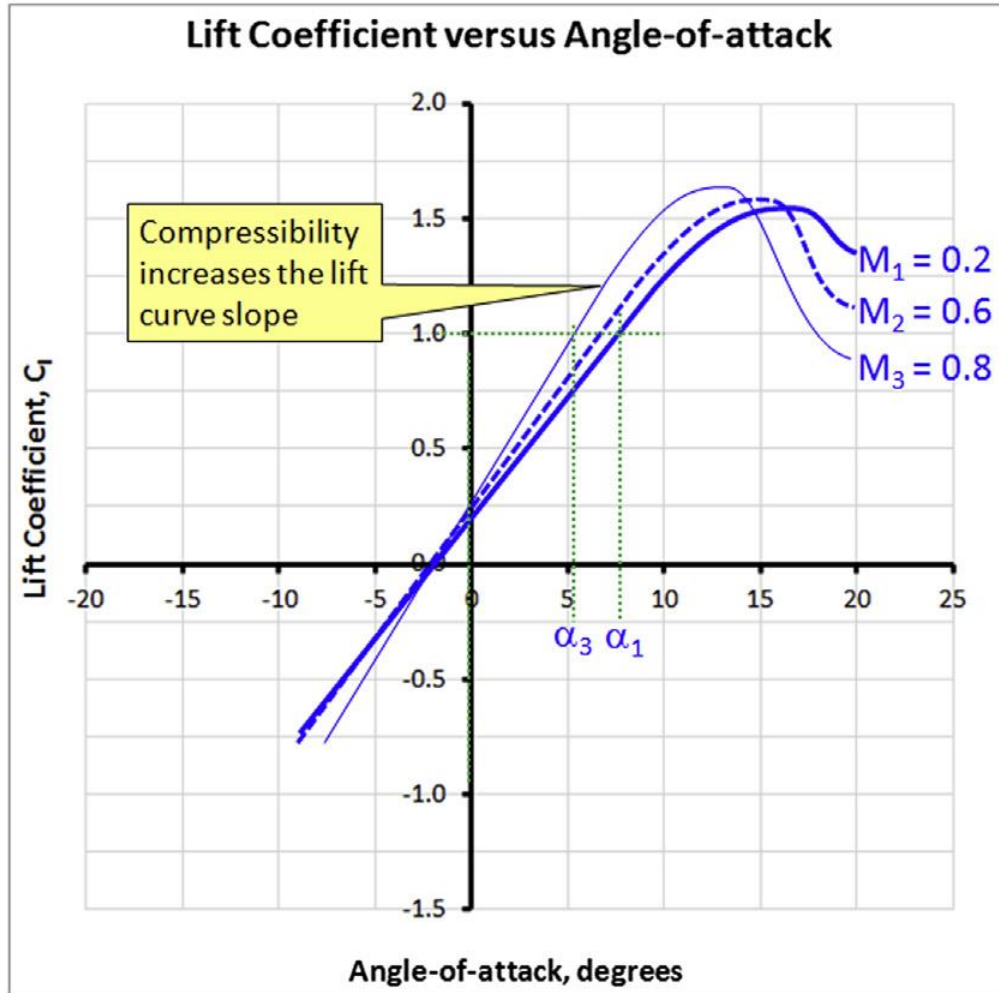
Aerodynamic performance curves – Extended comments

- The effect of Reynolds number on lift and drag.



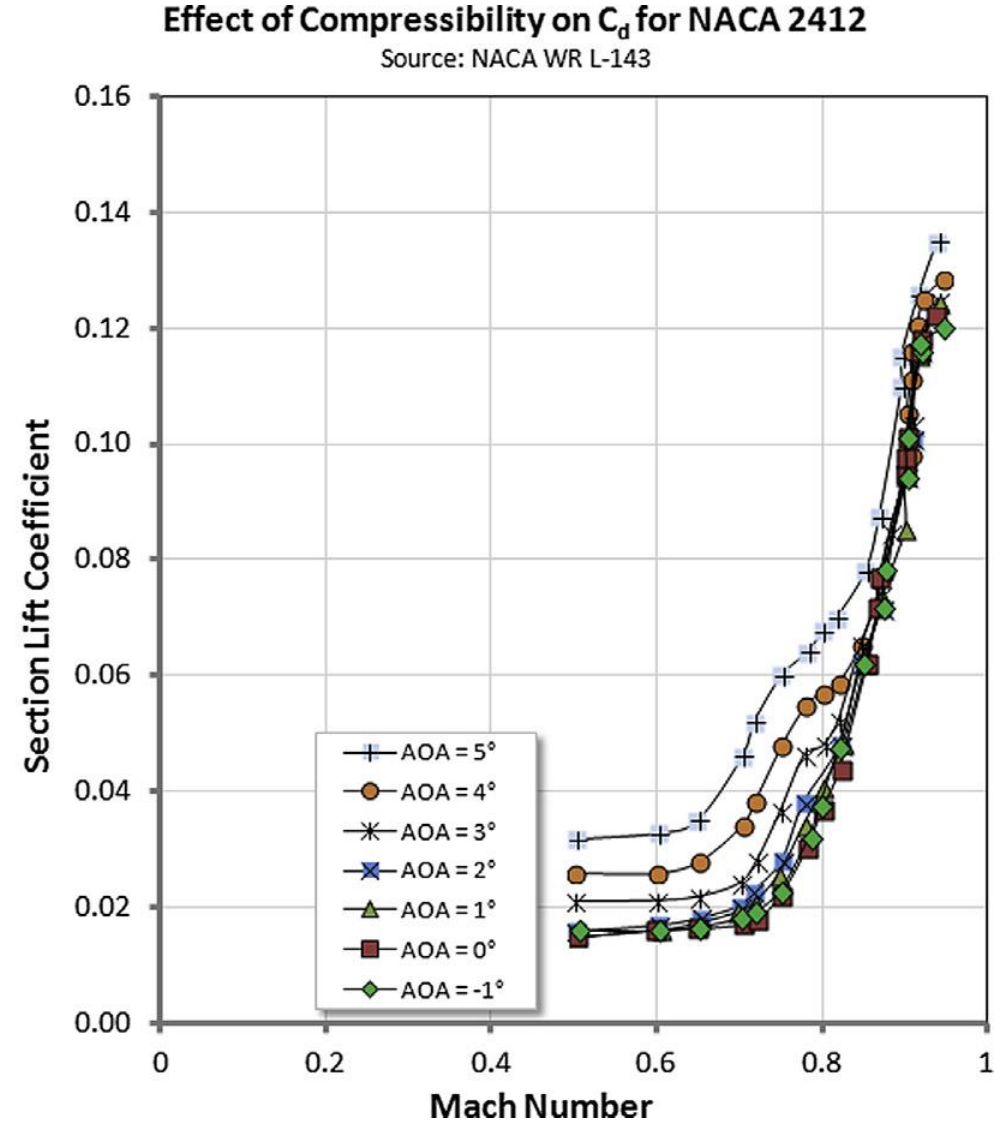
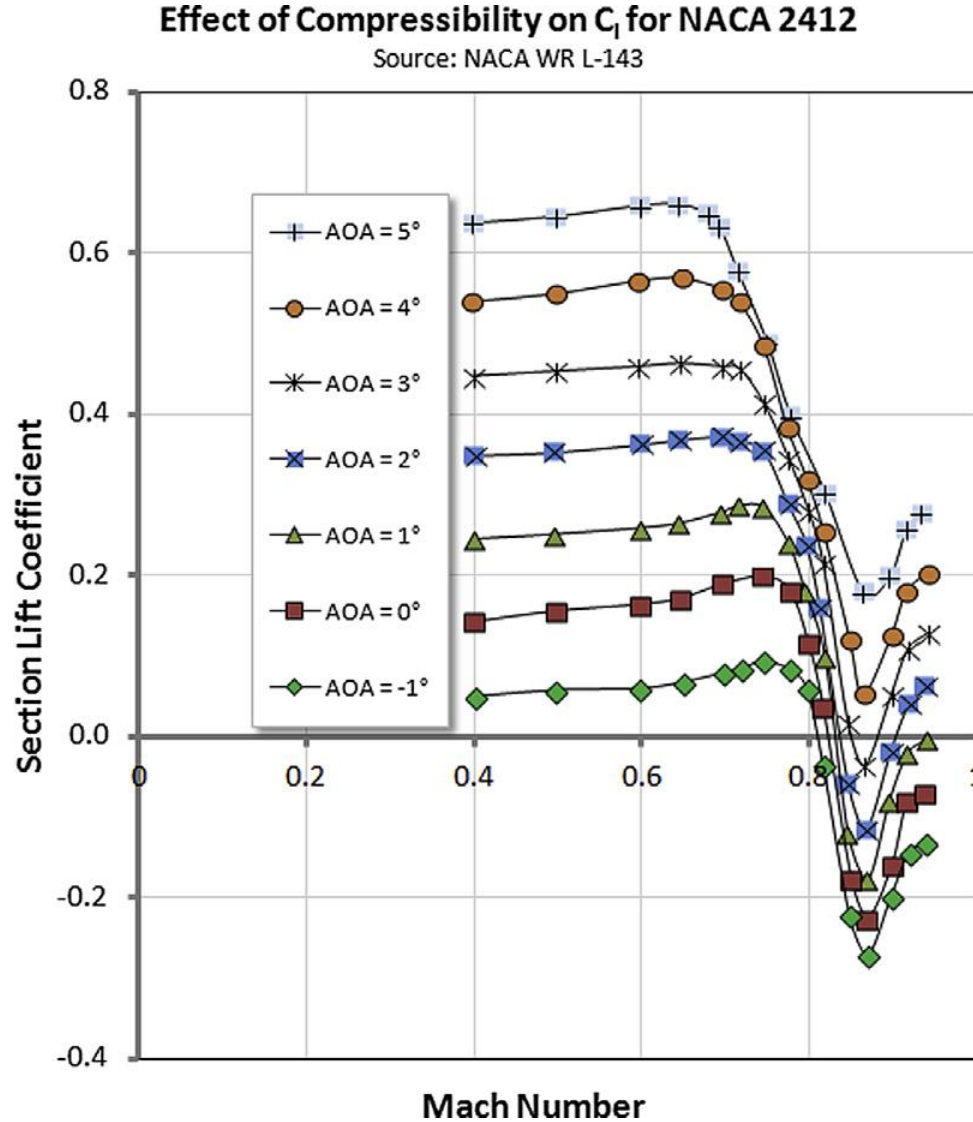
Aerodynamic performance curves – Extended comments

- Compressibility effects on lift and drag – High speed effects on lift and drag.



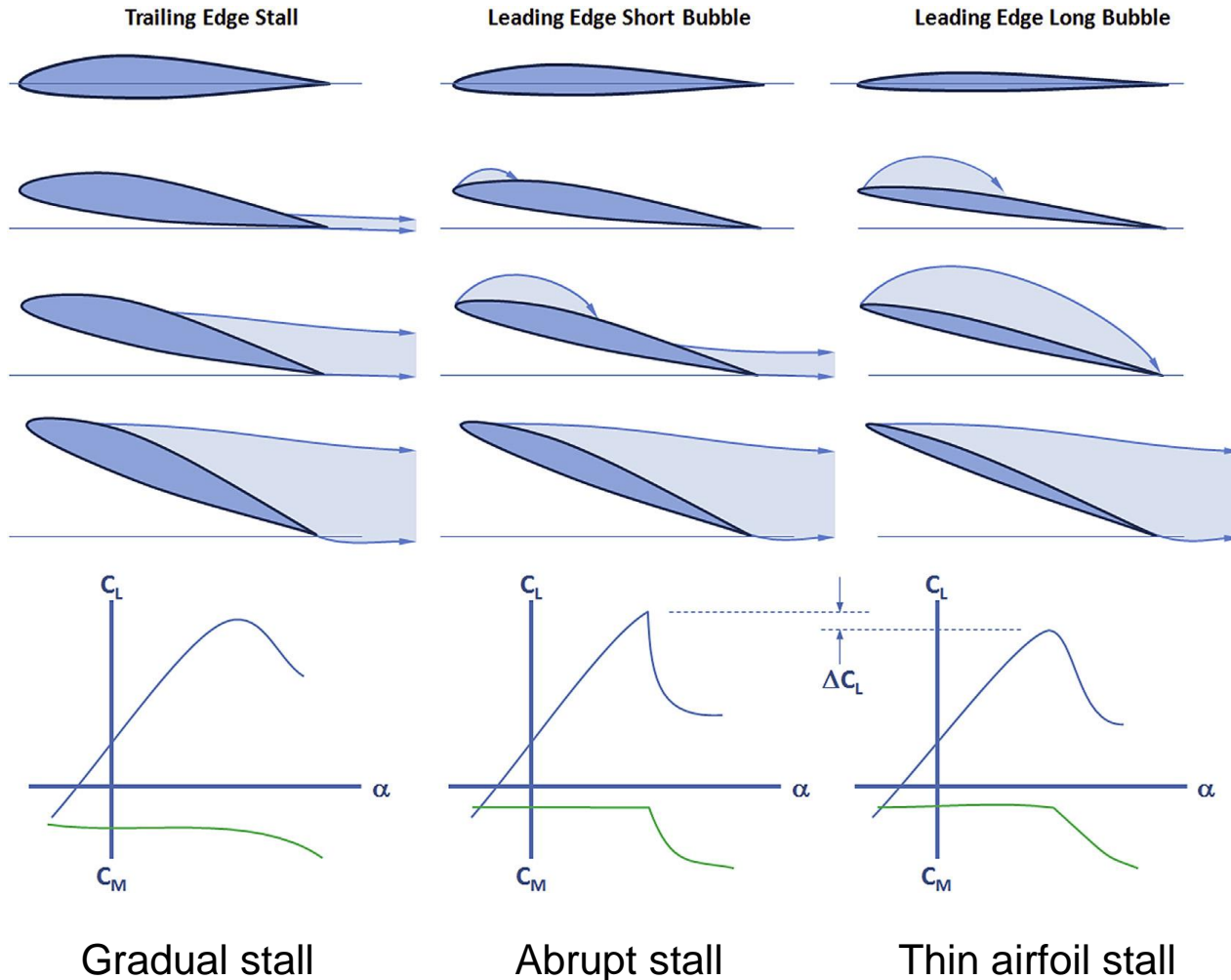
Aerodynamic performance curves – Extended comments

- Compressibility effects on lift and drag – High speed effects on lift and drag.



Aerodynamic performance curves – Extended comments

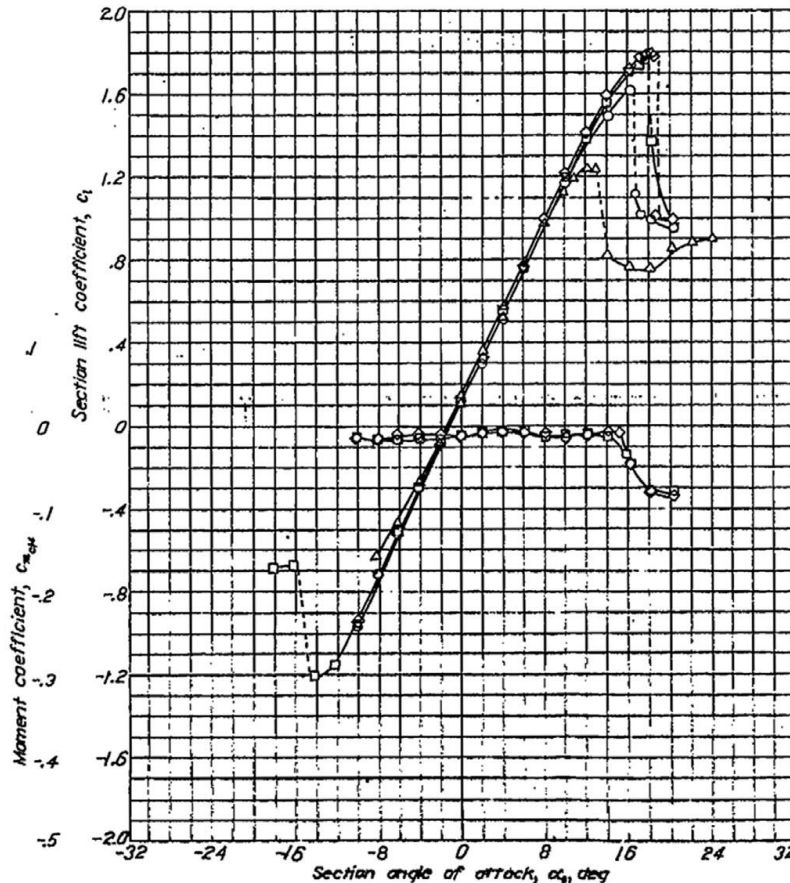
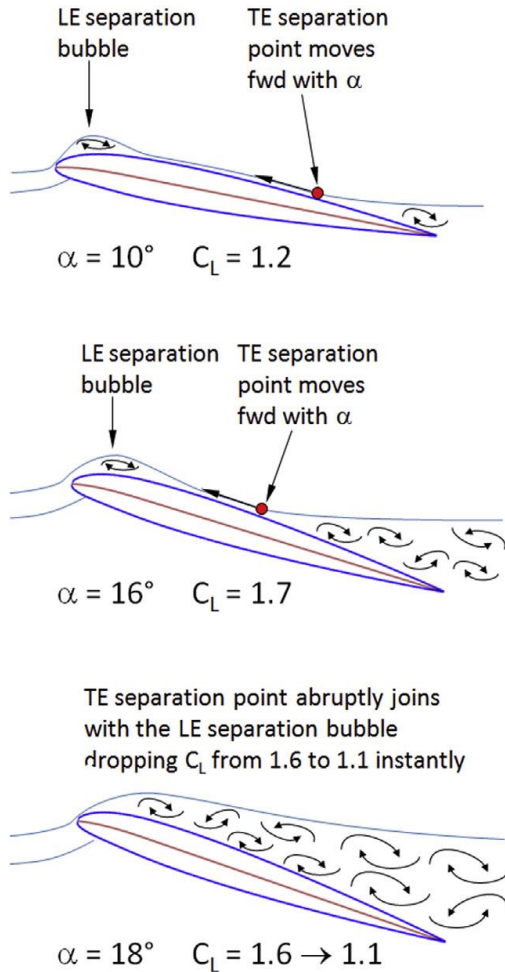
- Stall patterns of airfoils.



- Stall refers to the flow condition that follows the first peak of the lift curve.
- Stall places an upper limit on the maximum lift.
- It is characterized by a decrease of lift and an increase of drag.
- Stall is a consequence of the formation of a large separation region located between the leading edge and trailing edge of the airfoil.
- The thickness of the airfoil largely dictates how flow separation develops on the airfoil, but other parameters affect the maximum lift as well (e.g., maximum camber and its chordwise location, surface finish, Reynolds number, Mach number, free-stream turbulence).
- If the airfoil is thick with a rounded leading edge (thickness-to-chord ratio more than 12%), the separation tends to begin at the trailing edge and move forward as the AOA increases.
- On the other hand, if the airfoil is thin, the separation tends to begin at the leading edge in the form of a separation bubble.
- Trailing edge stall is the desirable stall pattern.

Aerodynamic performance curves – Extended comments

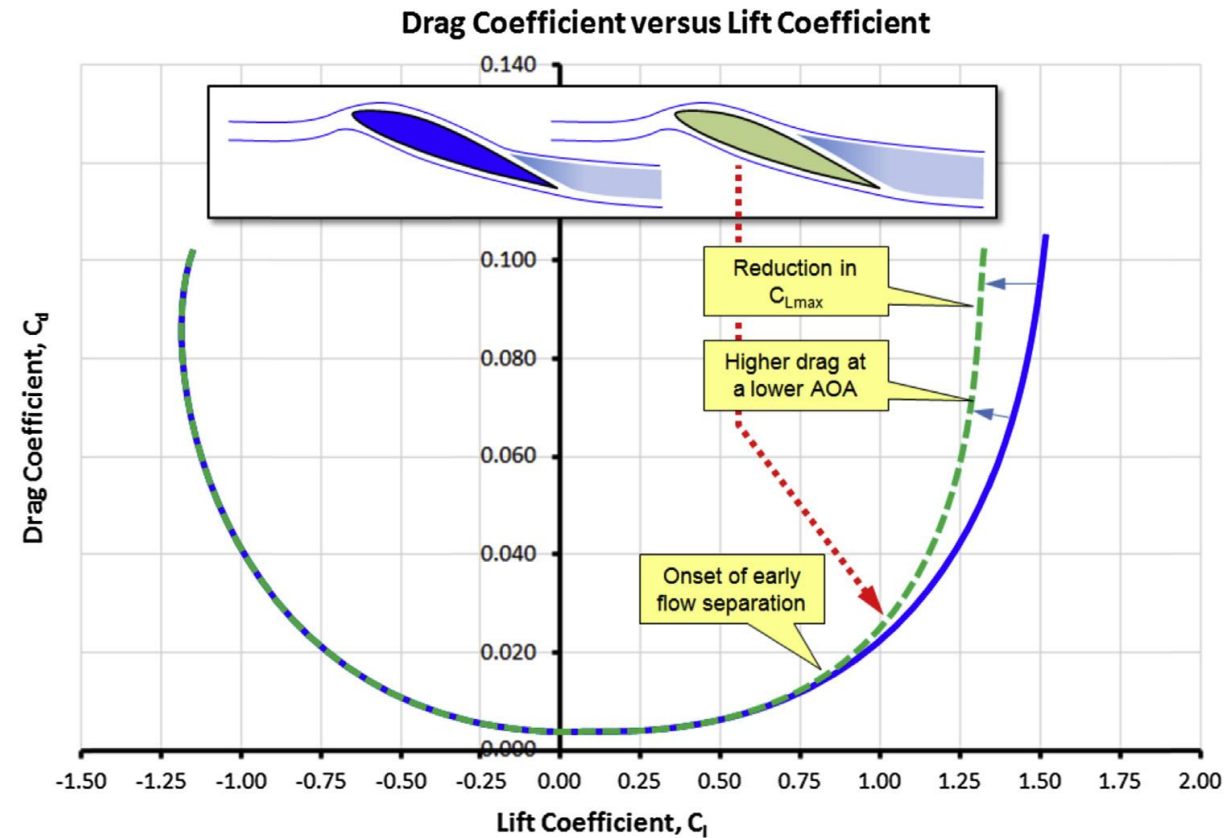
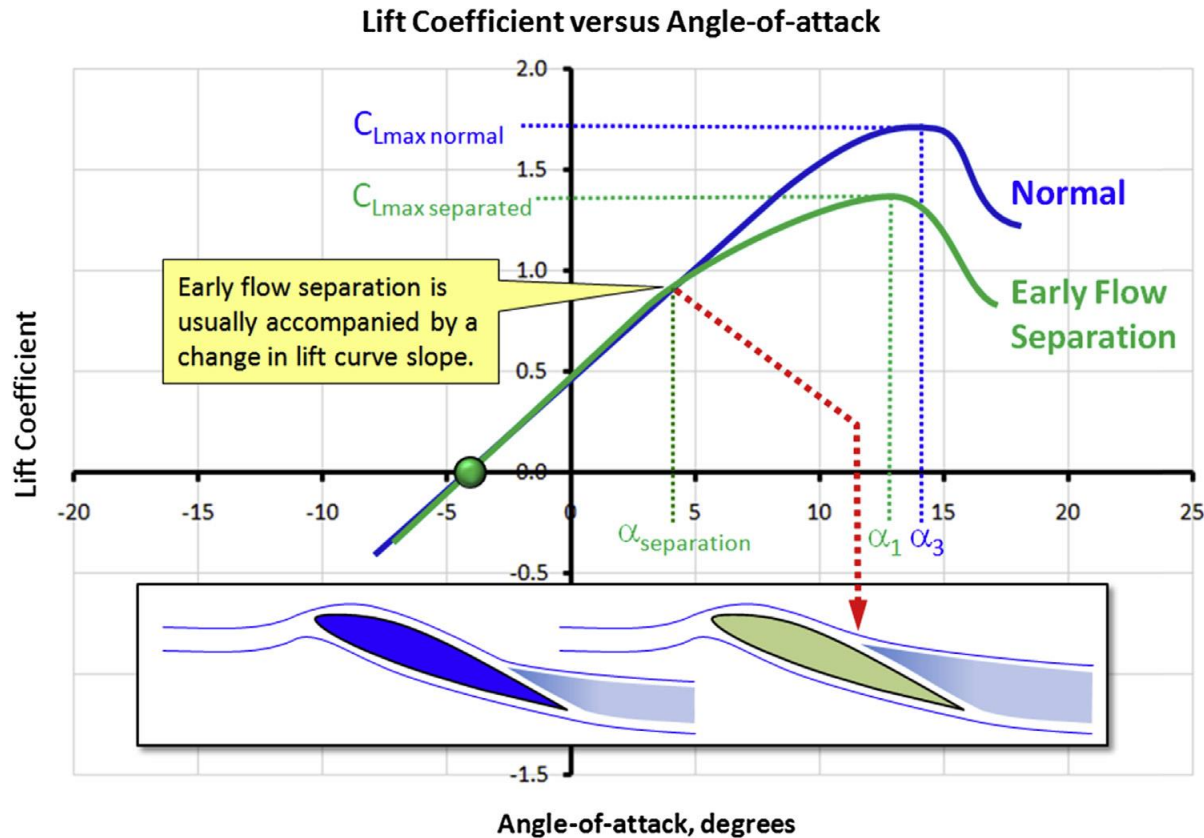
- Abrupt stall mechanism – NACA 23012 airfoil.



- Abrupt stall mechanism can be explained as a combination of leading-edge separation bubble and trailing-edge separation.
- Leading edge separation bubble may form on airfoils whose thickness-to-chord ratio is less than 12%.
- An example is the NACA 23012, where the sharp discontinuity in the curvature (at 15% of the chord) contributes to the formation of a separation bubble.
- As the AOA is increased, the airflow will detach behind the bubble, as illustrated in the figure.
- With further increase of AOA, the trailing edge separation point will continue to move forward.
- Eventually, the trailing edge separation will combine with the leading-edge separation bubble and an abrupt stall will take place.

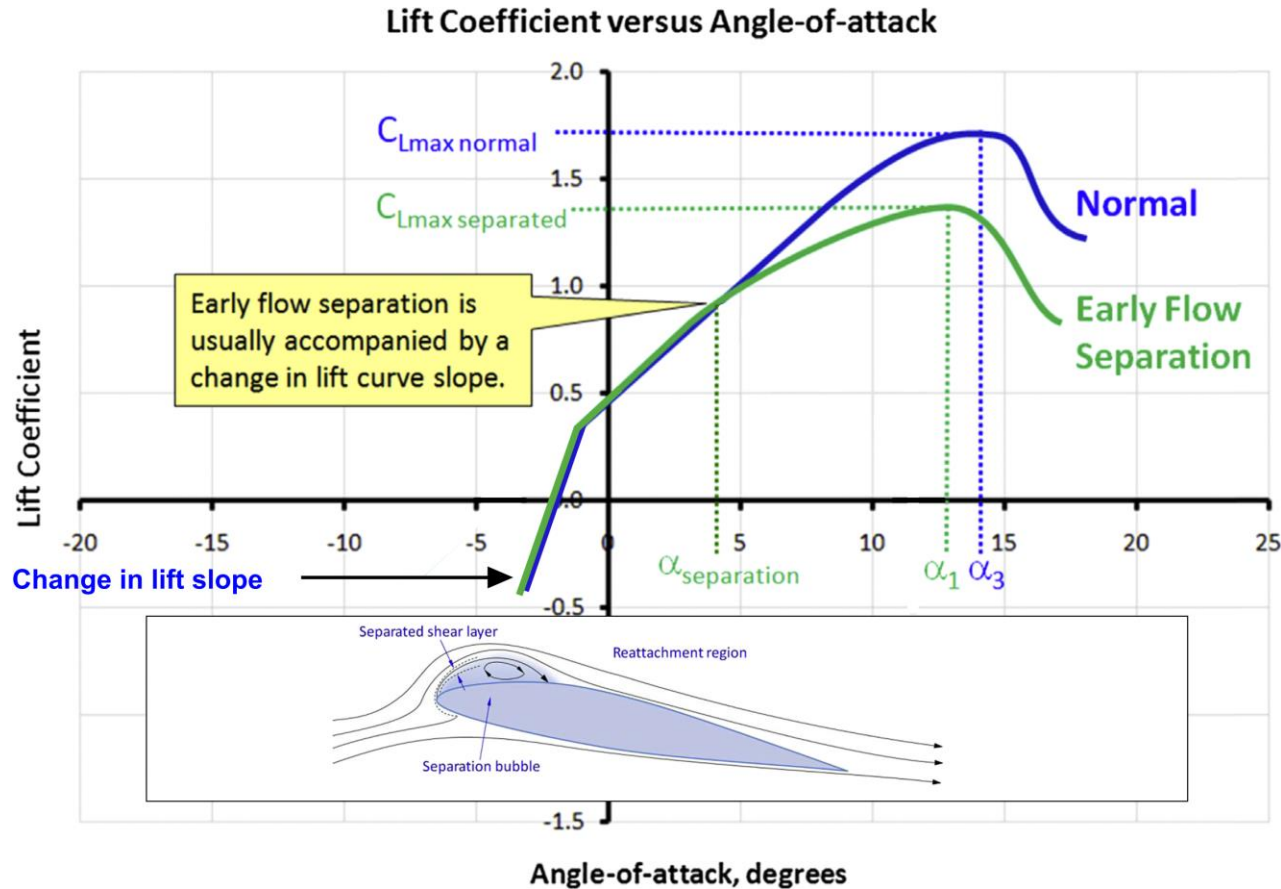
Aerodynamic performance curves – Extended comments

- Effect of early flow separation on lift and drag.
- Early separation can be the consequence of the pressure recovery region of the airfoil being too short, the trailing-edge region of the airfoil being too steep, or a discontinuity on the airfoil surface (e.g., the discontinuity caused by the presence of a control surface, surface contamination, ice formation, etc.).



Aerodynamic performance curves – Extended comments

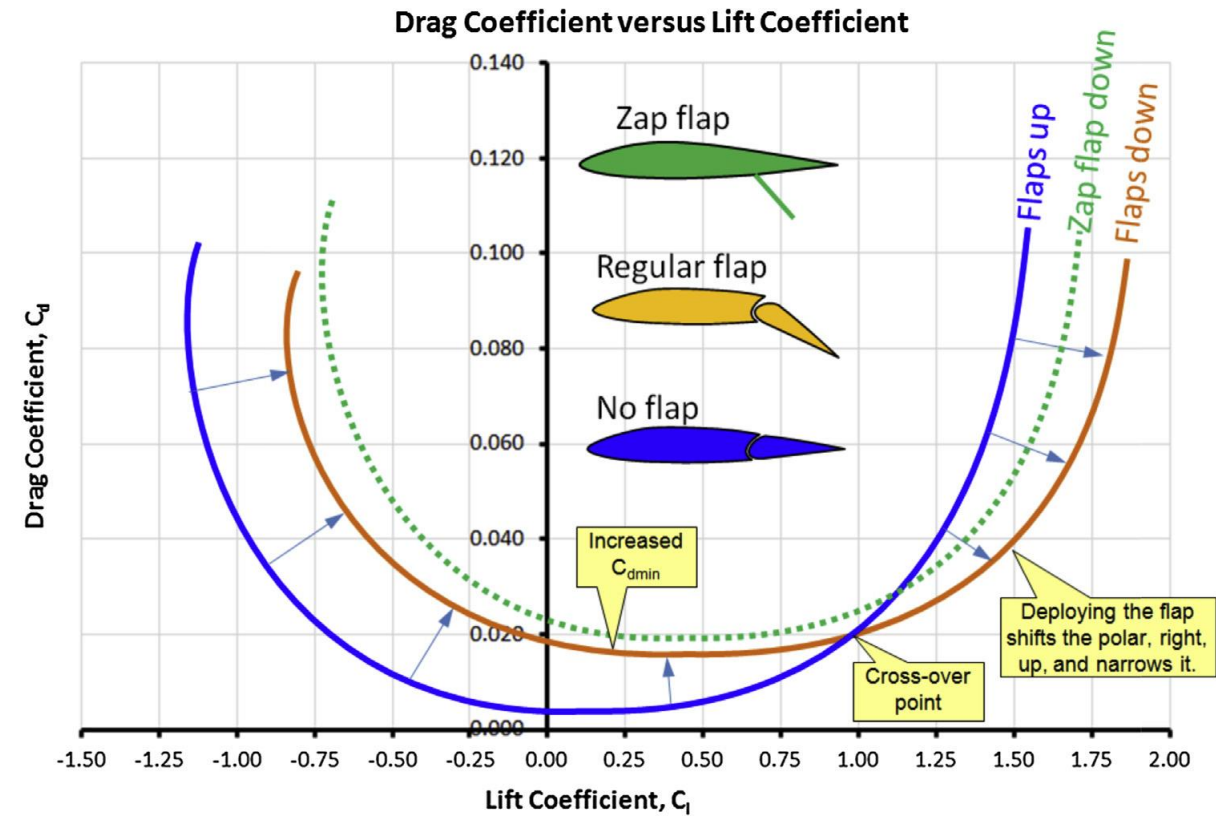
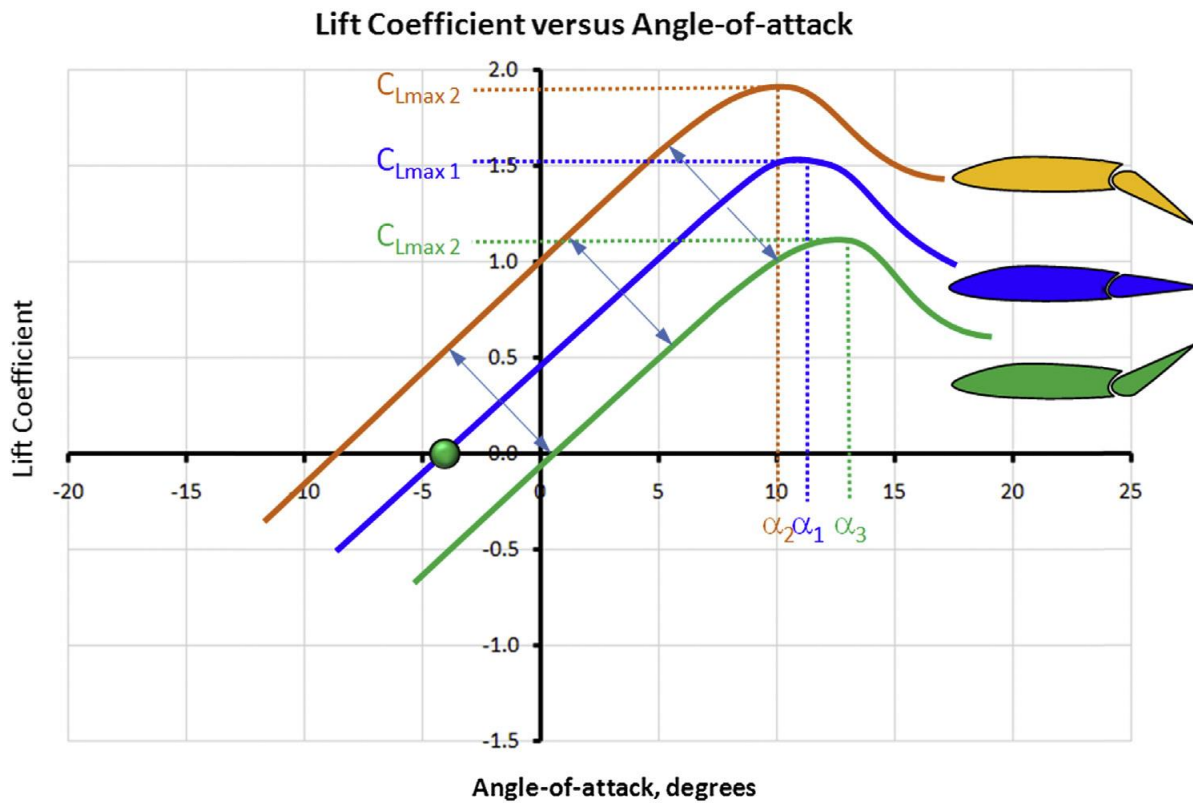
- Effect of leading-edge separation bubbles and early flow separation on lift.



- Sometimes you can find slightly different characteristics from what we just described.
- In this case, the lift curve has two approximately straight segments of different slopes.
- As it can be seen, at a moderate incidence, the slope takes a different, smaller value, leading to a smaller maximum lift coefficient.
- This change in the lift curve slope is due to a change in the type of flow near the nose of the airfoil.
- A separation bubble is responsible for the change in lift slope.

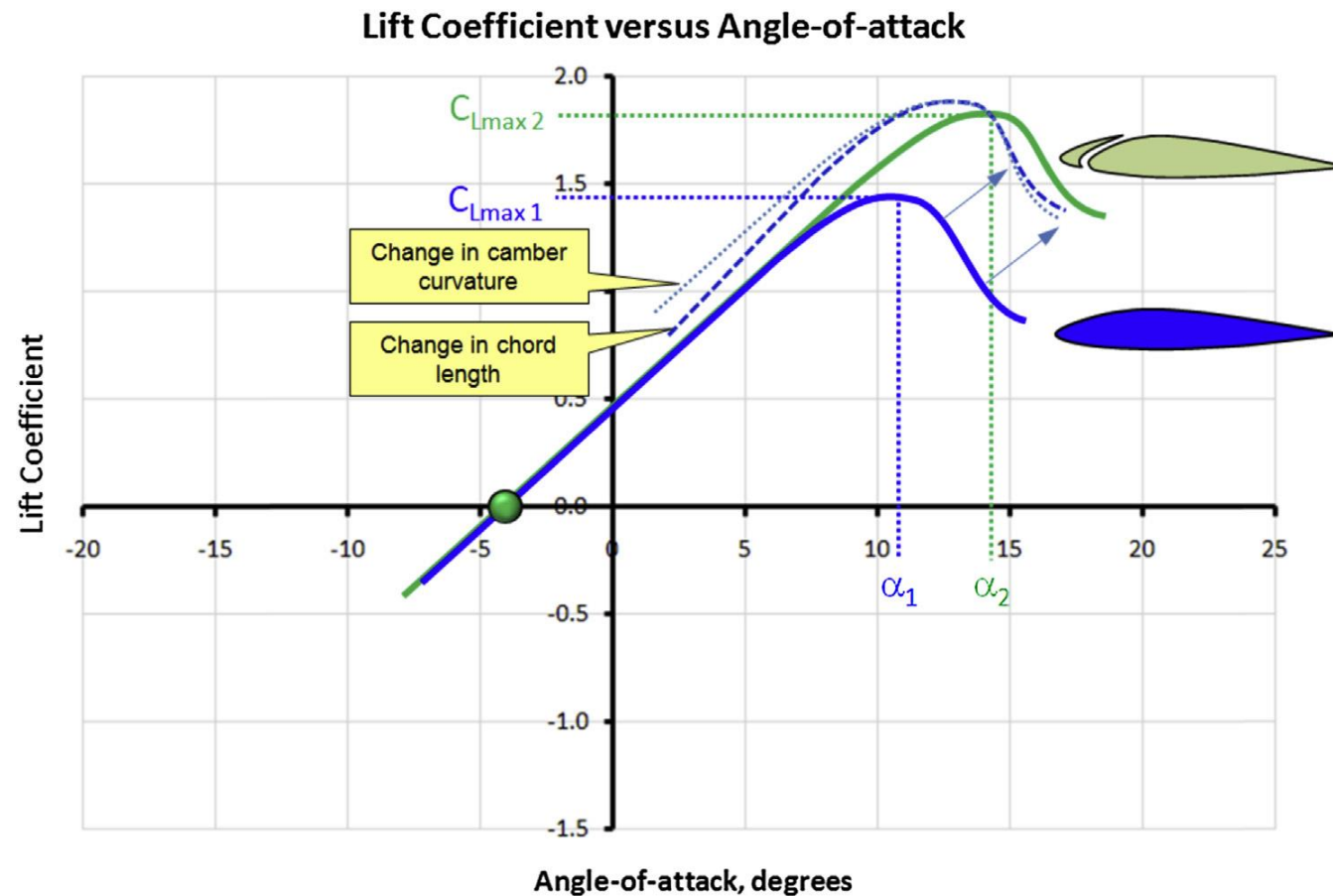
Aerodynamic performance curves – Extended comments

- The effect of high lift devices (HLD) on lift and drag – Flaps.
- In general, flaps increase lift and tend to decrease the stall angle a little bit.
- They also increase the drag.



Aerodynamic performance curves – Extended comments

- The effect of high lift devices (HLD) on lift and drag – Slats, slots, nose droops.
- Slats, slots, and nose droops delay the stall by increasing the maximum lift coefficient.
- They also slightly increase the drag.
- Flaps, slats, slots, and droops can be combined.

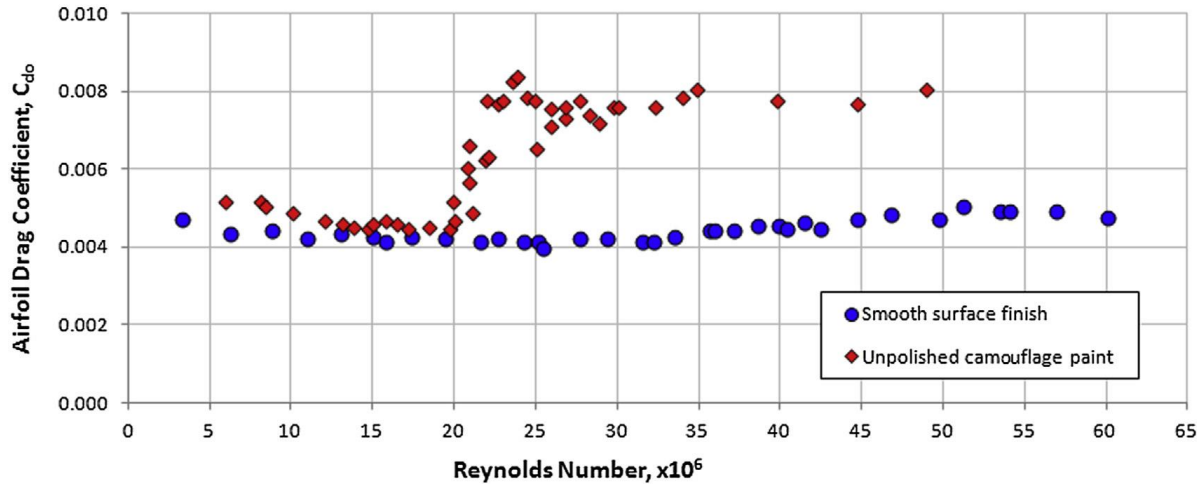


Aerodynamic performance curves – Extended comments

- Effect of surface finish and leading-edge contamination on lift and drag.

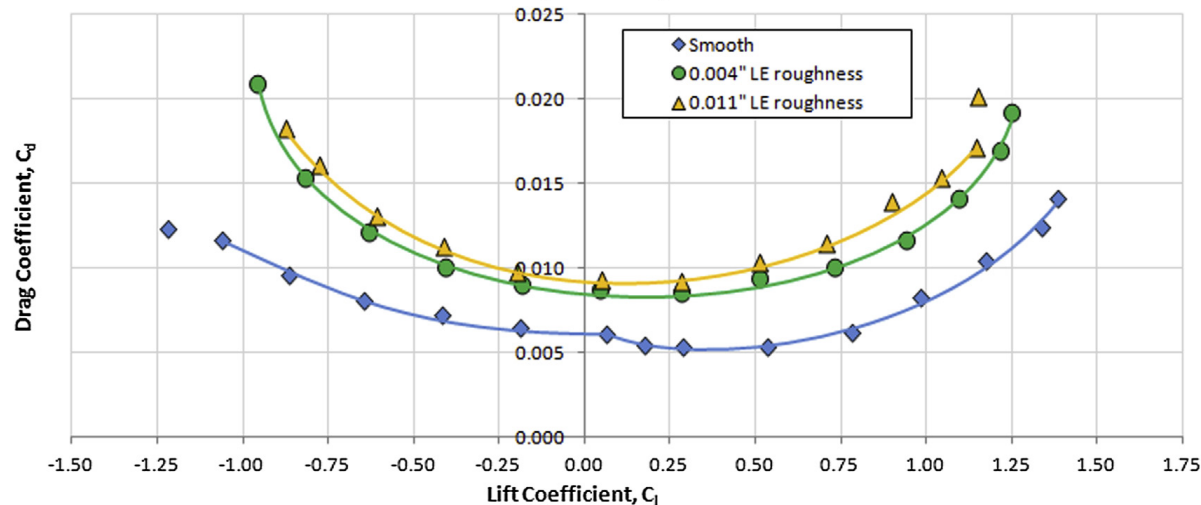
Airfoil Drag Coefficient versus RN for Two Surface Conditions

Chord: 60 inch, Source: NACA R-824



Impact of LE Roughness on Drag

Source: NACA R-824, $Re = 26 \times 10^6$, Chord = 36 in



- The quality of the surface finish is of great importance and its effect was investigated by NACA in the late 1930s [1].
- In reference [1], it was shown that surface roughness can cause a large increase in drag.
- It was also shown that smooth surfaces are important even when extensive laminar flow is not to be expected [2].
- However, it was also shown that surfaces do not have to be superbly smooth or polished.
- The effect of a contaminated leading edge (LE) is also presented in reference [2] and is reflected in the drag polar.
- The drag polar is shifted upwards because of leading-edge contamination.
- Reference [2] also shows that LE roughness reduces section lift-curve slope and maximum lift coefficient.

[1] NACA TN-695. The Effects of Some Surface Irregularities on Wing Drag. Hood, Manley J; 1939.

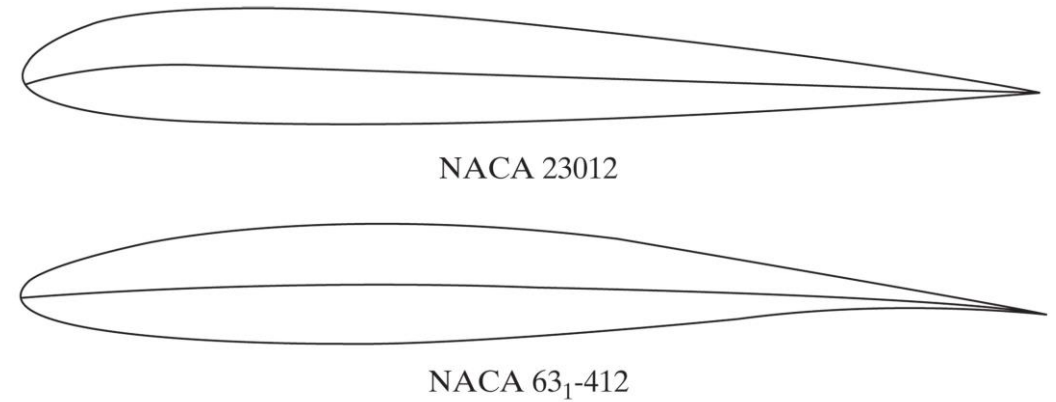
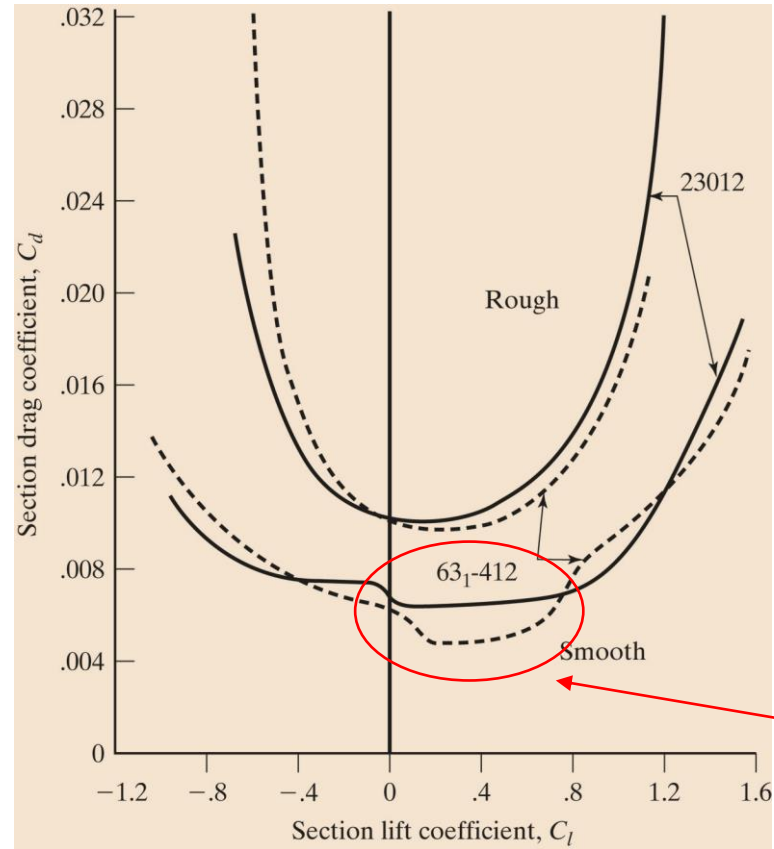
[2] NACA R-824. Summary of Airfoil Data. Abbott, Ira H., Albert E. von Doenhoff and Louis S. Stivers Jr; 1945.

Photo credit: General Aviation Aircraft Design: Applied Methods and Procedures. Butterworth-Heinemann, 2016. Copyright on the images is held by the contributors. Apart from Fair Use, permission must be sought for any other purpose.

Laminar flow airfoils

Laminar flow airfoils

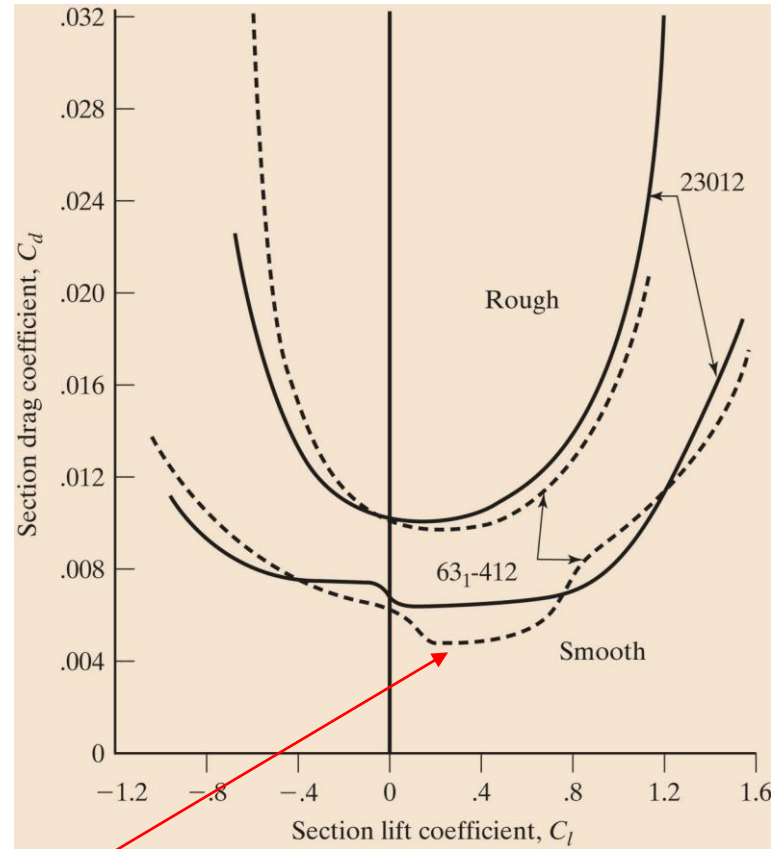
- Drag characteristics of NACA laminar flow airfoils and conventional airfoils sections with both smooth and rough leading edges.



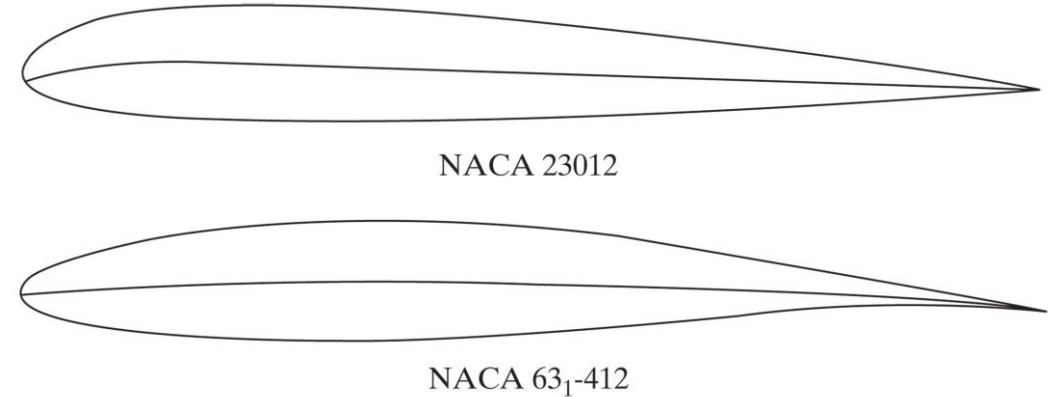
- The region highlighted in the figure is known as a drag bucket.
- Do you think this bucket has a positive or negative effect on the airfoil performance?

Laminar flow airfoils

- Drag characteristics of NACA laminar flow airfoils and conventional airfoils sections with both smooth and rough leading edges.



Drag bucket



- Drag reduction attained with laminar boundary layer.
- The bucket in the curve for the laminar flow airfoil occurs at angles of attack that normally might be required for cruise.
- The laminar-flow airfoil shows a potential drag reduction of up to 25% over the conventional airfoil.
- With no or minimal effect of the lift.

Laminar flow airfoils

- The P-51 was the first production aircraft to utilize laminar flow airfoils.
- Unfortunately, laminar flow airfoils do not function properly if the boundary layer transitions to turbulent, which can happen easily if the wing surface is not smooth.

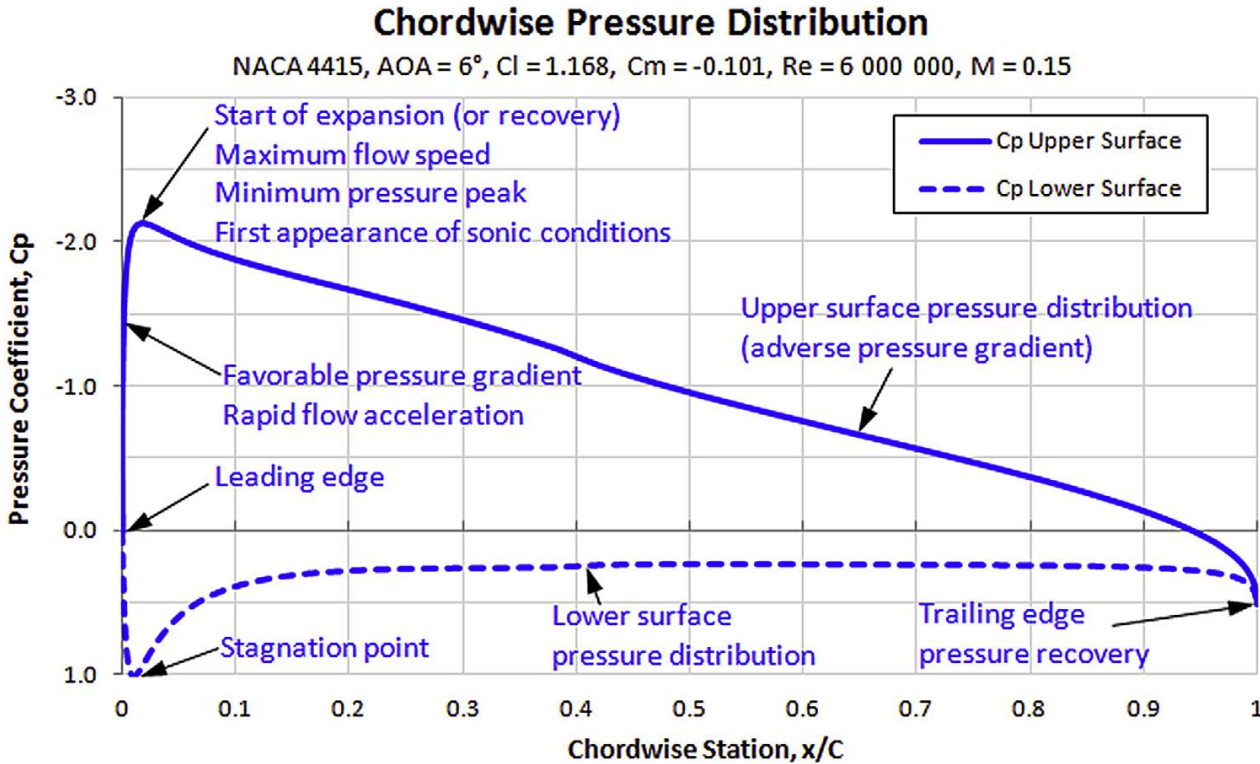


Airfoil pressure distribution

Pressure coefficient

Airfoil pressure distribution – Pressure coefficient

- Important properties of a pressure distribution curve for a typical airfoil – Pressure coefficient.



- The pressure coefficient is of considerable importance when studying airfoil performance.
- It represents the difference between the local static pressure and the freestream static pressure, non-dimensionalized by the freestream dynamic pressure.
- The incompressible pressure coefficient is defined as follows,

$$c_p = \frac{p - p_\infty}{0.5 \times \rho_\infty \times V_\infty^2}$$

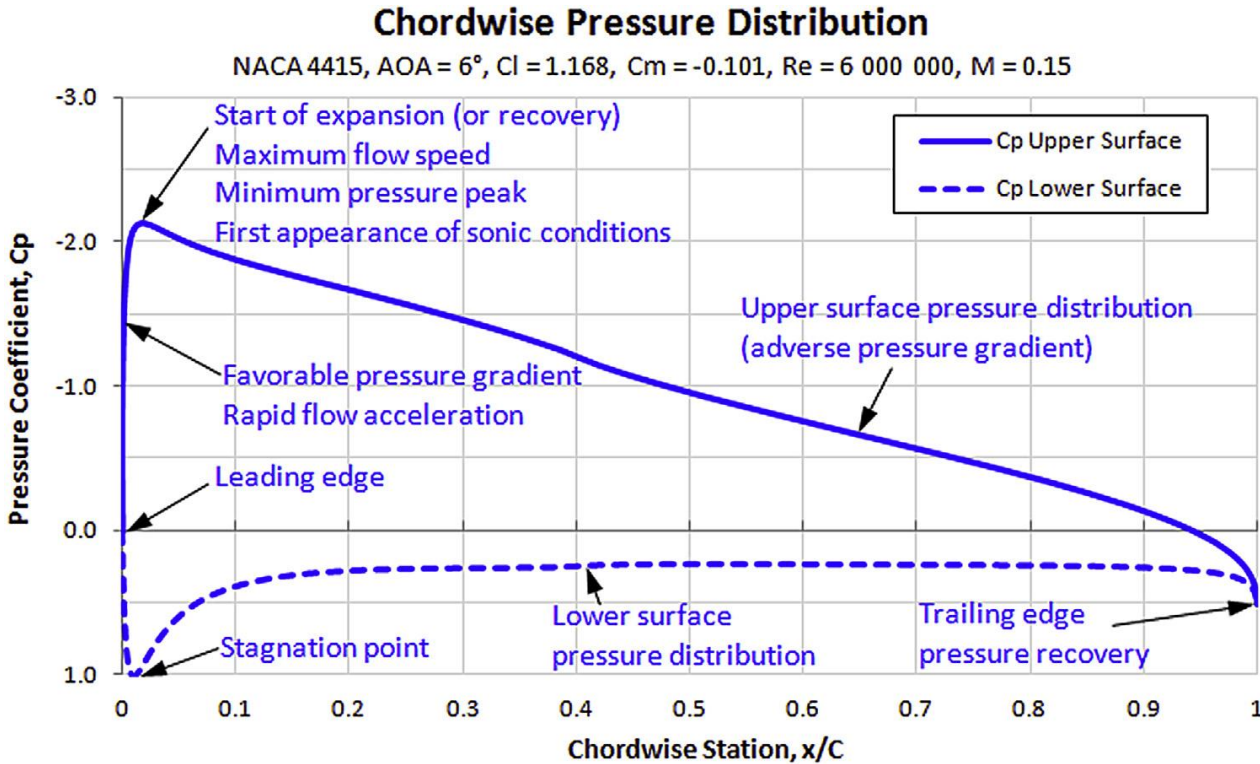
- It can also be written as follows (for incompressible flows),

$$c_p = 1 - \left(\frac{V}{V_\infty} \right)^2$$

- The maximum possible value of the pressure coefficient at the stagnation point in incompressible flows is 1.
- In compressible flows, it can become larger than one.

Airfoil pressure distribution – Pressure coefficient

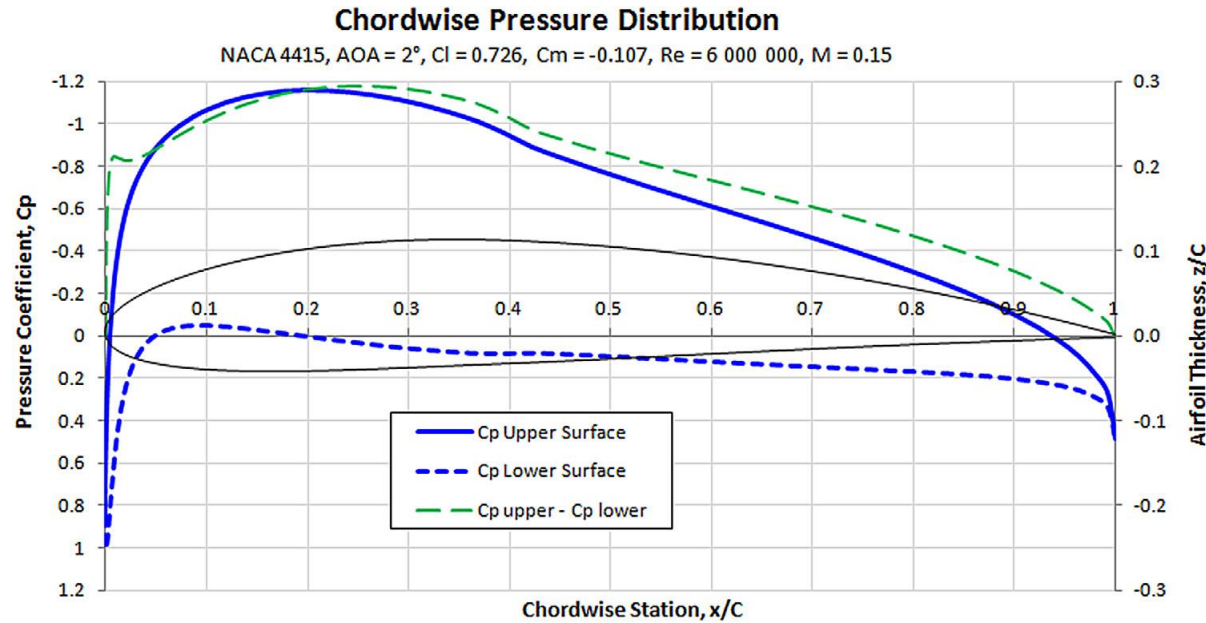
- Important properties of a pressure distribution curve for a typical airfoil – Pressure coefficient.



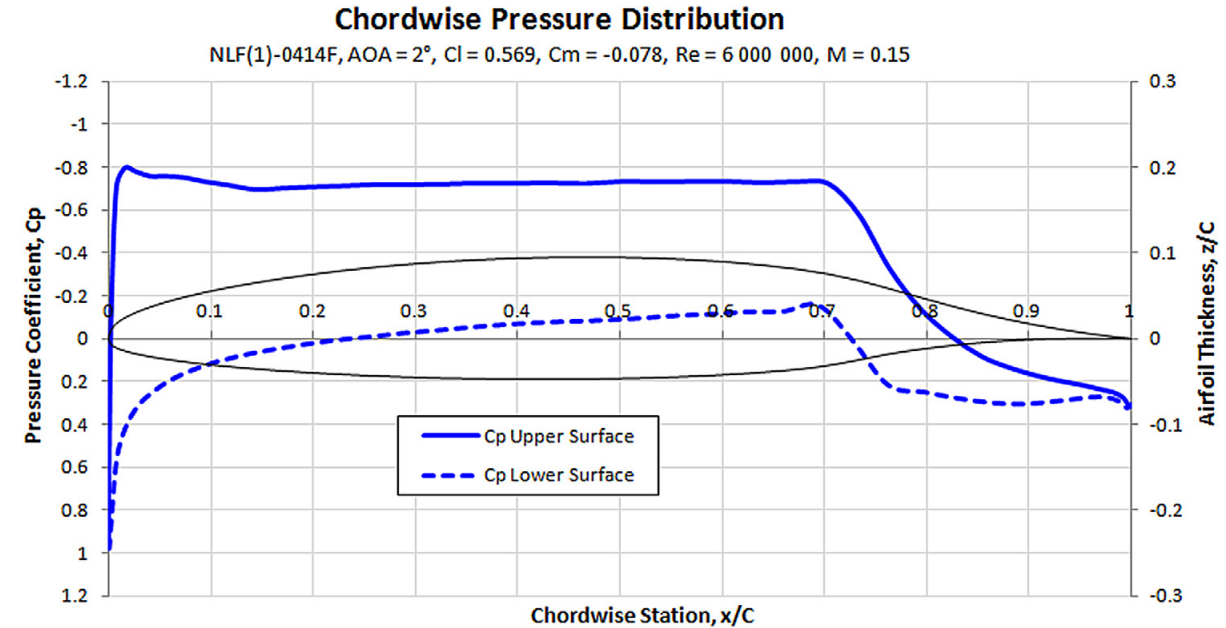
- The pressure coefficient starts from about 1.0 at the stagnation point near the leading edge.
- From the stagnation point, the pressure coefficient rises rapidly (pressure decreases) on both upper and lower surfaces, and finally recovers to a small value (hopefully) near the trailing edge.
- The pressure recovery region, is the area where the pressure increases from its minimum value to the value at the trailing edge.
- This area is also known as adverse pressure gradient region, and it is associated with boundary layer transition and separation (if the gradient is large).
- Trailing edge pressure determines the severity of adverse gradient.
 - Large positive values imply more severe adverse pressure gradients.
- The favorable pressure gradient region leads to laminar flow and lower drag.
 - Favorable pressure gradient is highly desirable as it reduces boundary layer transition.
- The pressure coefficient distribution can be controlled by adjusting the curvature and thickness distribution of the airfoil.

Airfoil pressure distribution – Pressure coefficient

- Pressure coefficient distribution of different airfoils.



A. Conventional pressure distribution

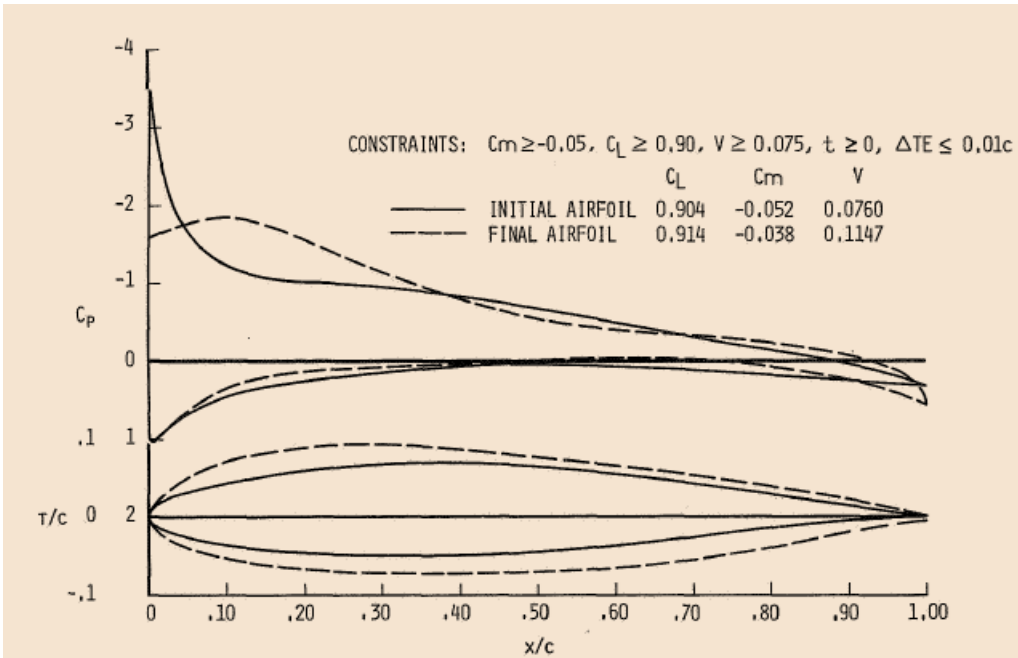


B. Stratford like pressure distribution

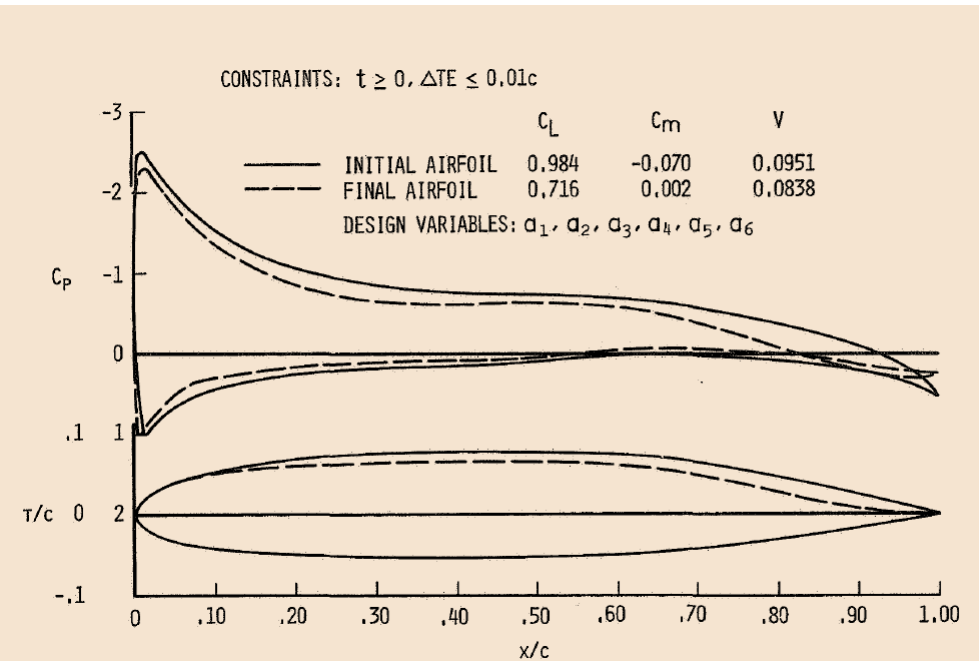
- In figure A, a favorable pressure gradient extends aft for about 20% of the chord. In other words, the laminar boundary layer is promoted only over the first 20% of the chord length.
- The pressure distribution shown in figure B forms a distinct flat pressure contour on the upper surface. This contour is commonly referred to as a rooftop or Stratford pressure distribution. Such a distribution promotes an extensive laminar boundary layer.
- Modern airfoils are specifically designed to generate a chordwise pressure distribution along the upper surface that is uniform across much of the chord, as shown in figure B.

Airfoil pressure distribution – Pressure coefficient

- Design of airfoils using pressure coefficient distribution.



Upper surface adverse pressure gradient minimization

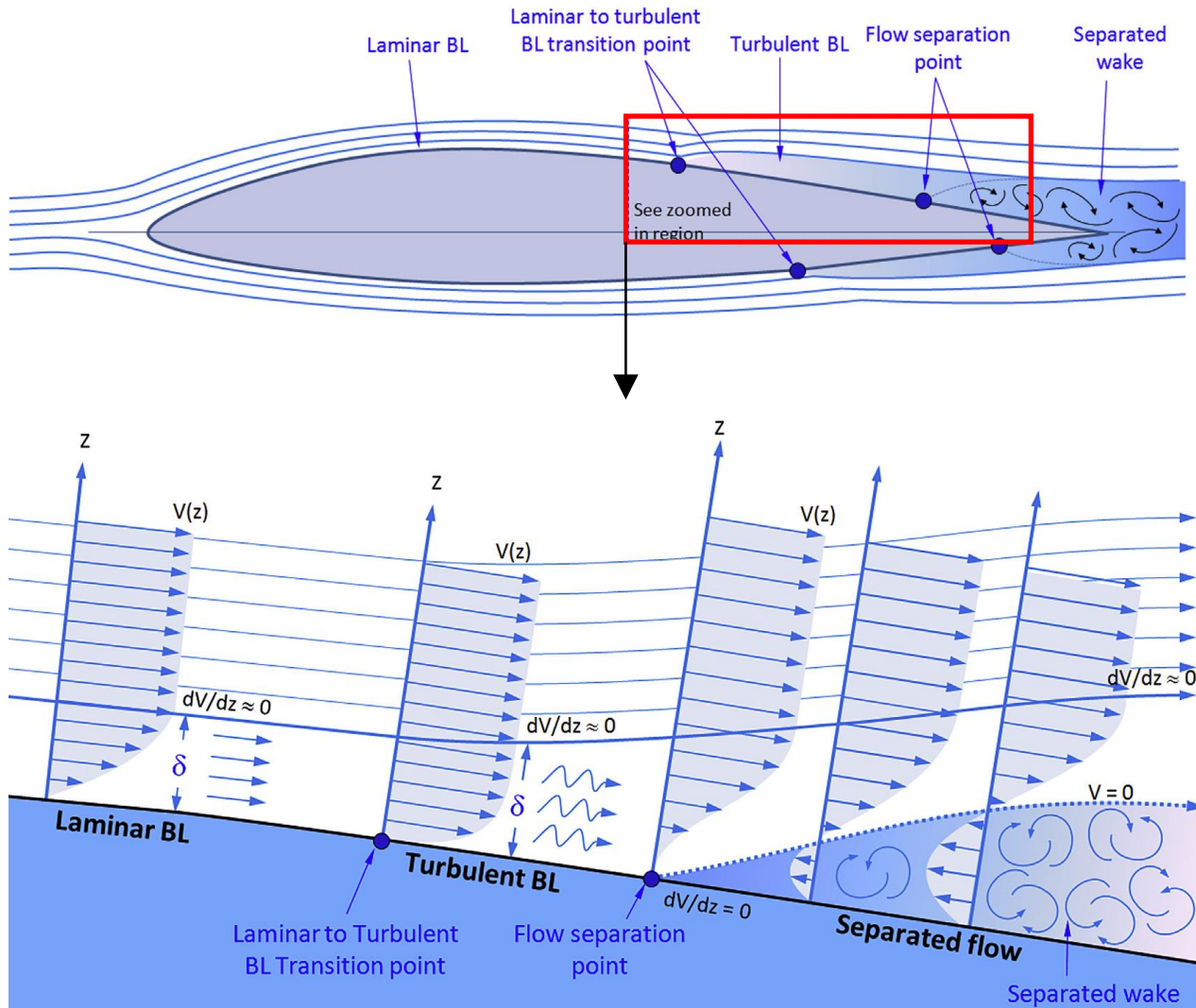


Pitching moment minimization

Effect of turbulence on airfoil performance

Effect of turbulence on airfoil performance

- Boundary layer, flow separation and turbulence.



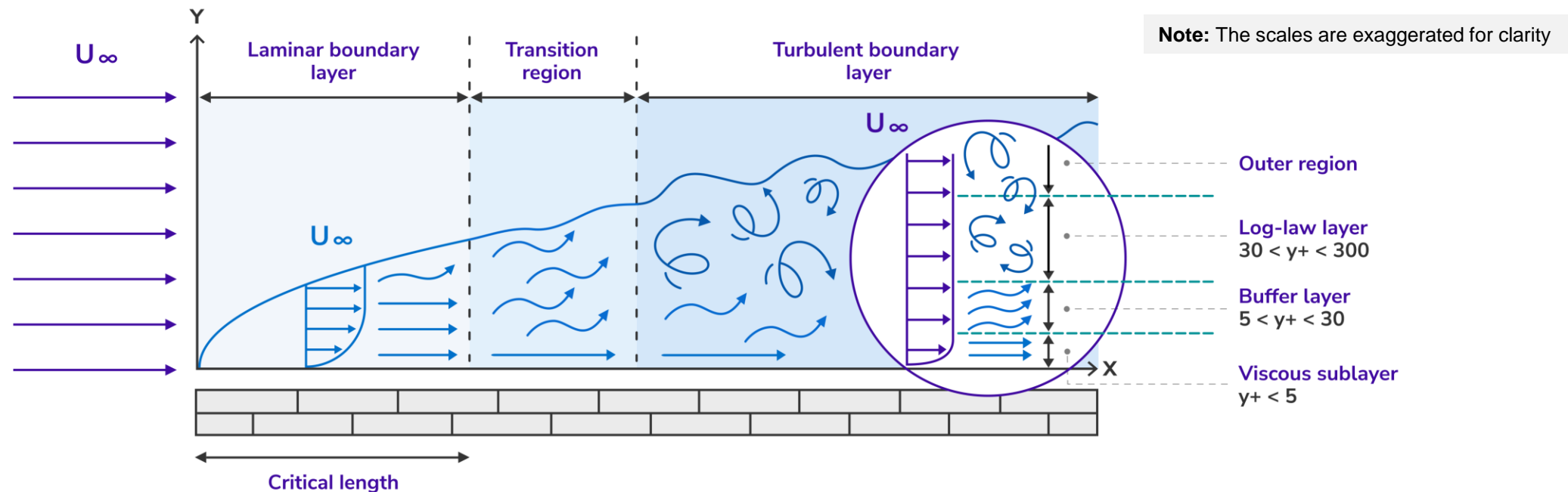
In the illustration, the turbulent velocity profile has been averaged (in reality there are fluctuations).

- Turbulence has a direct effect on the velocity profiles close to the walls and mixing of transported quantities.
- In the laminar boundary layer (BL), the skin friction is low.
 - However, the laminar BL is prone to separation and the formation of laminar separation bubbles (LSB), that might negatively affect the aerodynamic performance.
- In the turbulent BL, the skin friction is high, but it is less prone to separation (due to a more energetic flow), and rarely you will see separation bubbles.
- The flow separation causes a large increase in drag and reduction in lift.
- The pitching moment may increase or diminish depending on the geometry.
- In the boundary layer along the airfoil surface, you can find a laminar region, a turbulent region, and a transition region.
 - Depending on the Reynolds number, surface finish, and geometry, the extension in percentage of the chord of these regions is different.

Photo credit: General Aviation Aircraft Design: Applied Methods and Procedures. Butterworth-Heinemann, 2016. Copyright on the images is held by the contributors. Apart from Fair Use, permission must be sought for any other purpose.

Effect of turbulence on airfoil performance

- In airfoils and slender bodies, transition happens approximately at Reynolds number equal to 500 000.
- The transition region is defined as the region where transition from laminar to turbulent flow happens.
- Transition to turbulence is a very elusive and difficult to predict phenomenon.
- The transition region can be very short, and it can be affected by many factors.
 - Maybe the factor with the strongest influence is the pressure gradient.
 - Pressure gradient is directly related to the geometry but can also be controlled using active systems.
- Transition to turbulence can happen earlier or later than predicted due to external perturbations.
 - Early transition means that the transition takes place earlier than anticipated. In the same way, delayed transition refers to the opposite.



Boundary layer (Laminar-Transitional-Turbulent flow)

Effect of turbulence on airfoil performance

- Factors that may change the Reynolds number; and therefore, transition to turbulence:
 - Geometry.
 - Surface smoothness (or roughness).
 - Surface temperature.
 - Compressibility effects.
 - Atmospheric conditions (rain, strong winds, snow).
 - Suction or blowing (openings, boundary layer control devices).
 - Leading edge quality (insect, dirt erosion, icing).
 - Noise.
- In wind tunnel experiments and in numerical simulations, transition can be triggered artificially.
 - We will study this using xfoil.

Effect of turbulence on airfoil performance

- Laminar and turbulent flows – Flow around two spheres

- Laminar boundary layer.
- Low skin friction.
- Large pressure drag.
- Total drag larger than that of figure b.



(a) $C_D \approx 0.4$



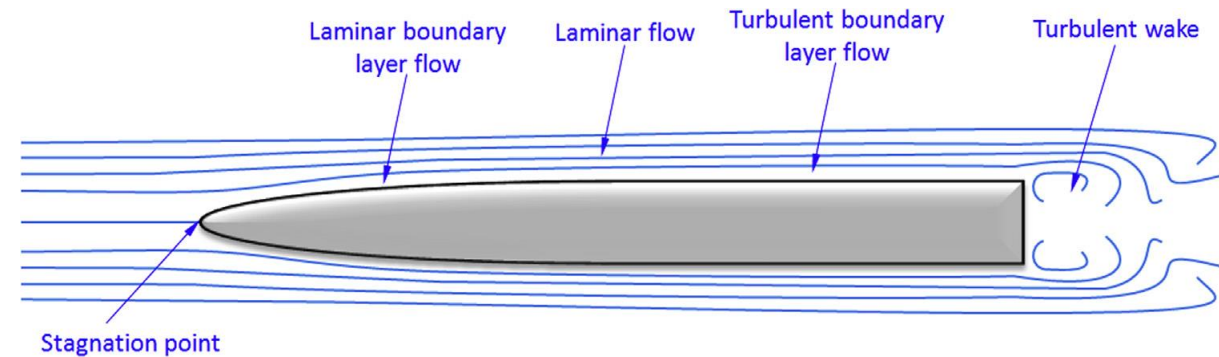
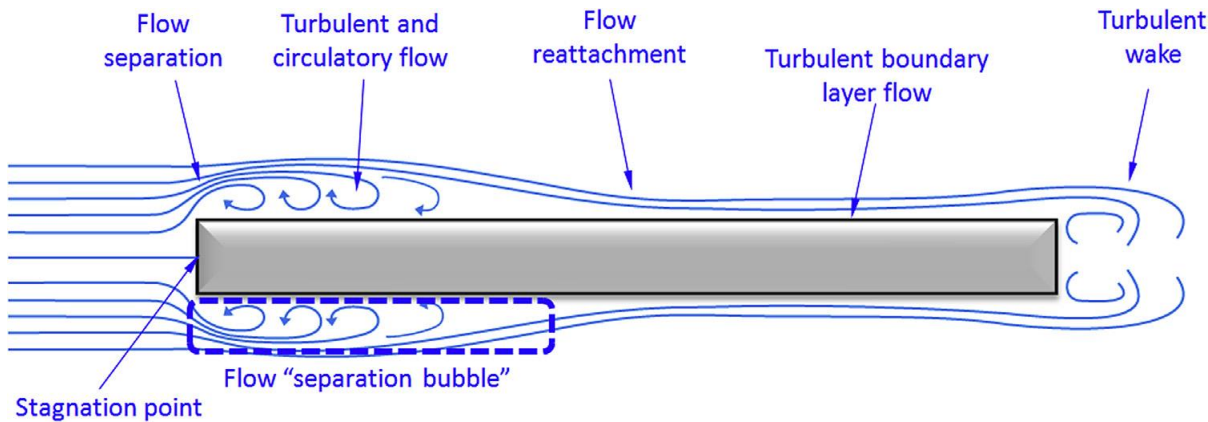
(b) $C_D \approx 0.2$

- Turbulent boundary layer.
- High skin friction.
- Reduced pressure drag.
- Total drag lower than that of figure a.

Flow around two spheres. Left image (a): smooth sphere. Right image (b): sphere with rough surface at the nose

Effect of turbulence on airfoil performance

- To avoid flow separation and recirculation bubbles, the external geometry of an airplane should be shaped so the areas of flow separation are minimized, or even better, eliminated.
 - Flow separation considerably increases drag, specifically, pressure drag.
- This simple guideline applies to the fuselage, wings, control surfaces, aerodynamic fairings, appendages, and so on.
- In airplanes, everything is rounded.



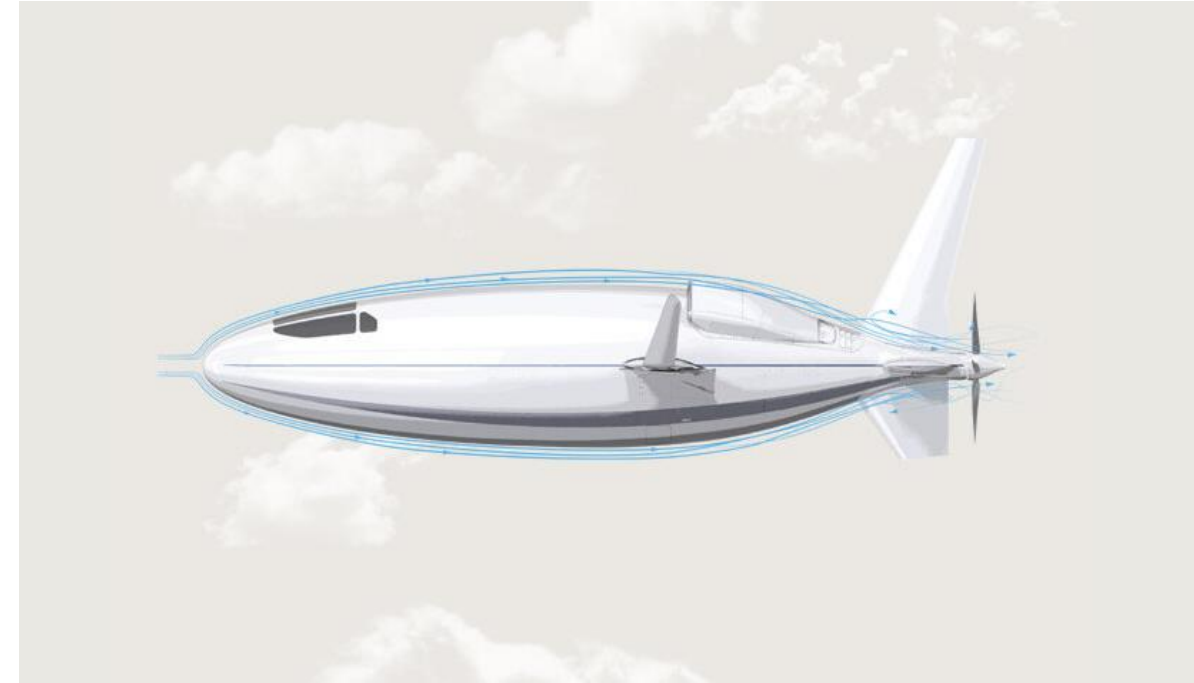
Effect of turbulence on airfoil performance

- To avoid flow separation and recirculation bubbles, the external geometry of an airplane should be shaped so the areas of flow separation are minimized, or even better, eliminated.



Old vs. new: Piper PA-31 (left aircraft) next to the Otto Celera 500L (right aircraft). Extensive use of laminar flow surfaces in the Otto Celera 500L results in approximately 59% reduction in drag compared to a similar sized conventional aircraft.

Photo credit: <https://edition.cnn.com/travel/article/celera-500l-business-aircraft-future/index.html>.



Prolate spheroid fuselage to reduce flow separation and promote laminar boundary layer. The design of the Celera 500L fuselage takes advantage of an optimum length-to-width ratio to maximize laminar flow (these benefits do not scale for large jet transports).

Photo credit: <https://www.ottoaviation.com/technology>

Effect of turbulence on airfoil performance

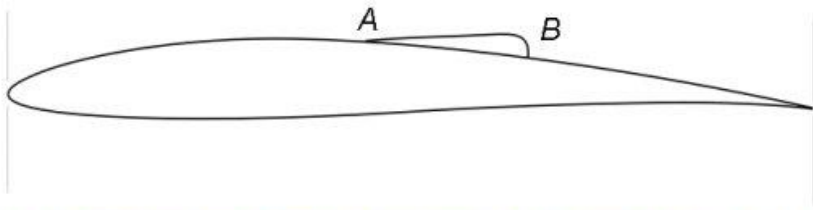
- Among many high efficiency aerodynamic concepts, the Otto Celera 500L uses a prolate spheroid fuselage to reduce flow separation and promote laminar boundary layer.
- Extensive use of laminar flow surfaces results in approximately 59% reduction of drag compared to a similar sized conventional aircraft.
- Other advanced aerodynamic concepts used in the Celera 500L: winglets, high aspect ratio wings, wing planform optimized for elliptical lift distribution, NLF airfoils, ventral fins, elliptical planform horizontal stabilizers, laminar flow control, pusher propeller, reduced excrescence and interference drag.



Laminar separation bubbles (LSB)

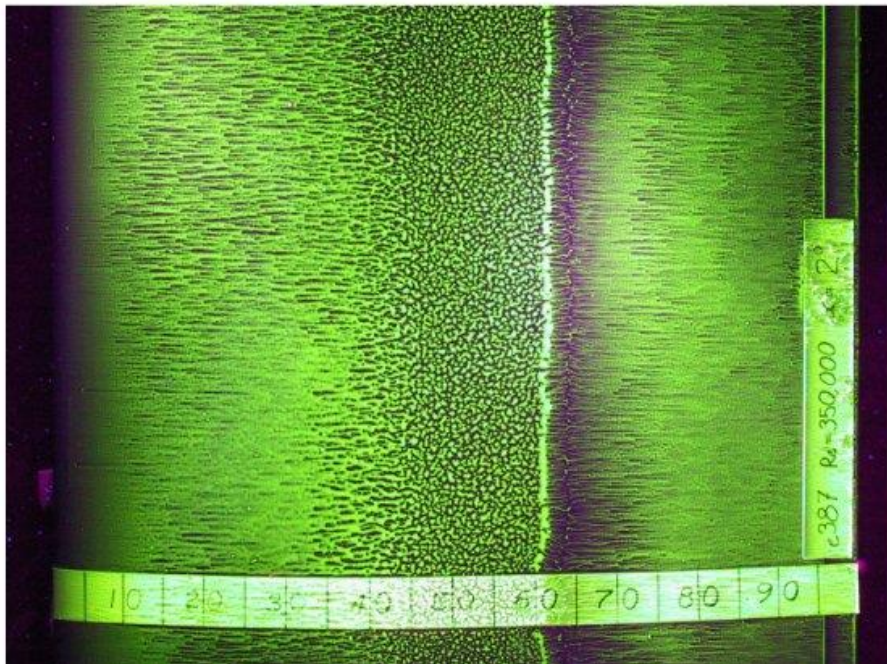
Laminar separation bubbles (LSB)

- Laminar separation bubbles (LSB), are very characteristics of low Reynolds number airfoils.
- LSB cause an increase in drag.
- These separation bubbles can be visualized by injecting smoke into the boundary layer or by using oil flow visualization.



E387 airfoil oil flow visualization at a Reynolds number of 350 000 and angle of attack of 2 degrees.

- In the image, the laminar flow smoothly streaks the oil, until point **A** where laminar separation starts.
- Beyond this point and inside the bubble, there is very little flow, and the oil does not change; it takes an orange-peel textured look.
- At reattachment, point **B**, the flow is quite unsteady and vigorous. In this point the flow impinges on the surface and creates high shear stress that scours away the oil.
- The flow moves some oil upstream and some oil downstream as the downflow splashes onto the surface, effectively creating a continental divide defined by a very fine dividing line.
- The oil moving upstream pools into what we call the oil accumulation line, while the oil going downstream moves towards the trailing edge.
- The flow upstream of the LSB, is fully turbulent.



Laminar separation bubbles (LSB)

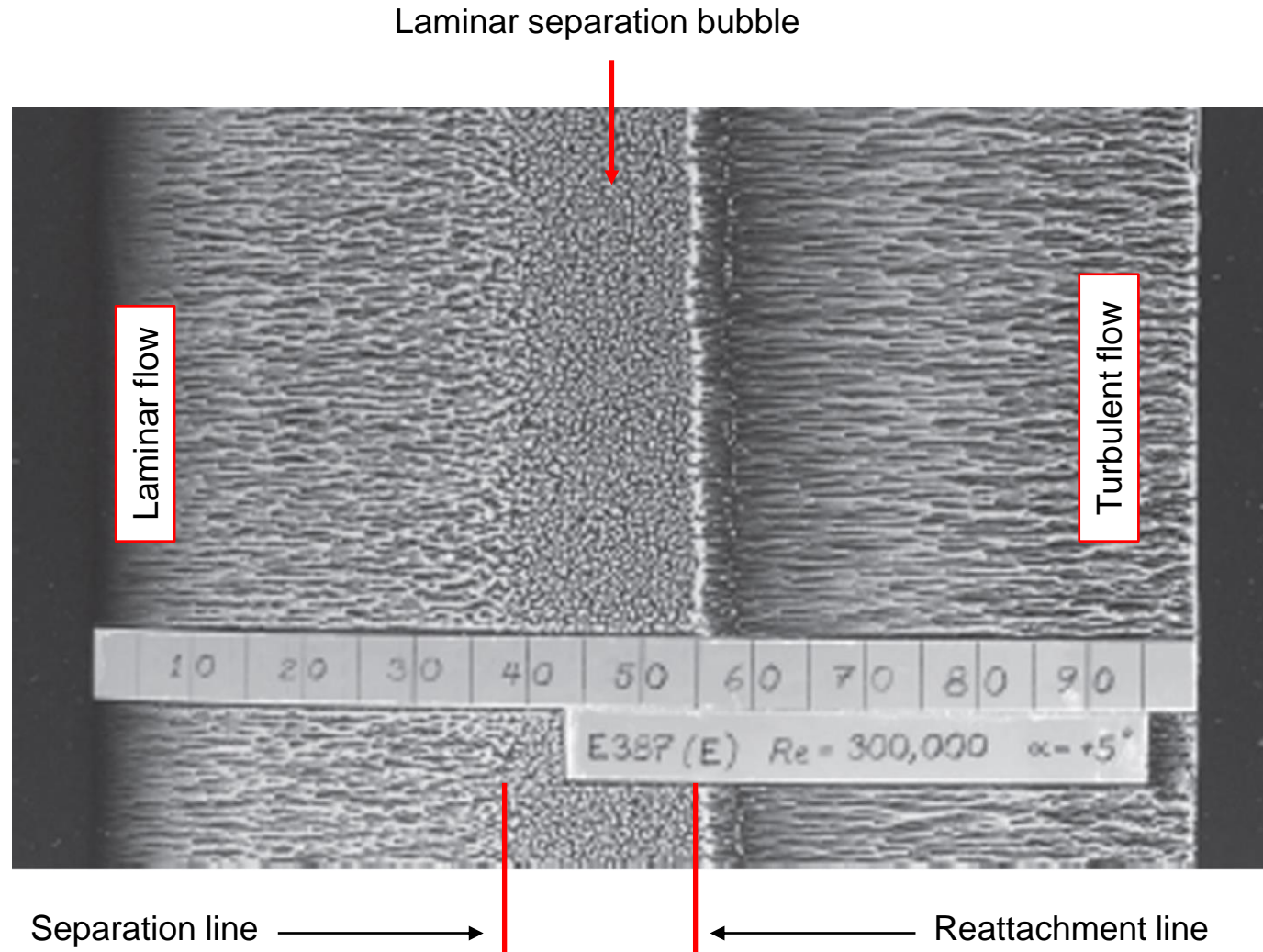
- Laminar separation bubbles (LSB), are very characteristics of low Reynolds number airfoils.
- LSB cause an increase in drag.
- These separation bubbles can be visualized by injecting smoke into the boundary layer or by using oil flow visualization.



Smoke flow visualization of a laminar separation bubble on the Eppler 387 airfoil at a chord Reynolds number of 100 000 and 2 degrees angle of attack.

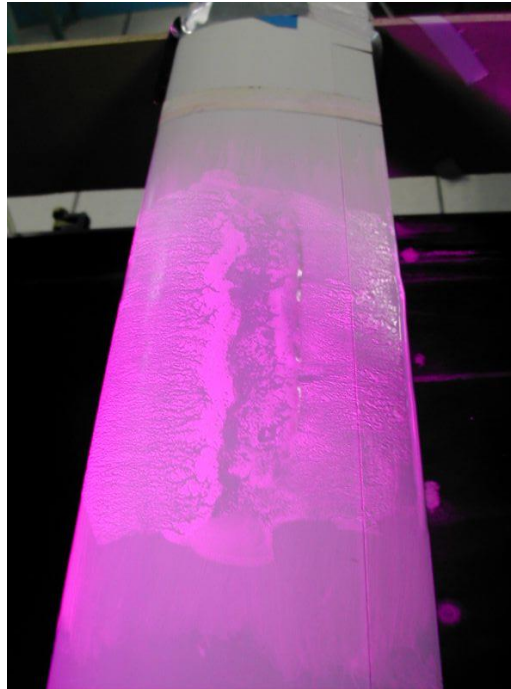
Laminar separation bubbles (LSB)

- Visualization of a Laminar separation bubble (LSB) on the E387 airfoil by using surface oil flow.
- Separation and reattachment zones are visible.



Laminar separation bubbles (LSB)

- Laminar separation bubbles can cause large increase in drag.
- LSB can also cause early stall and stability problems.
 - The LSB influences greatly the pressure distribution over the airfoil surface, hence the pitching moment.
- LSB can be popped (eliminated) by forcing transition to turbulence.
- In the figure, a trip strip is used to force transition to turbulence.



No trip strip

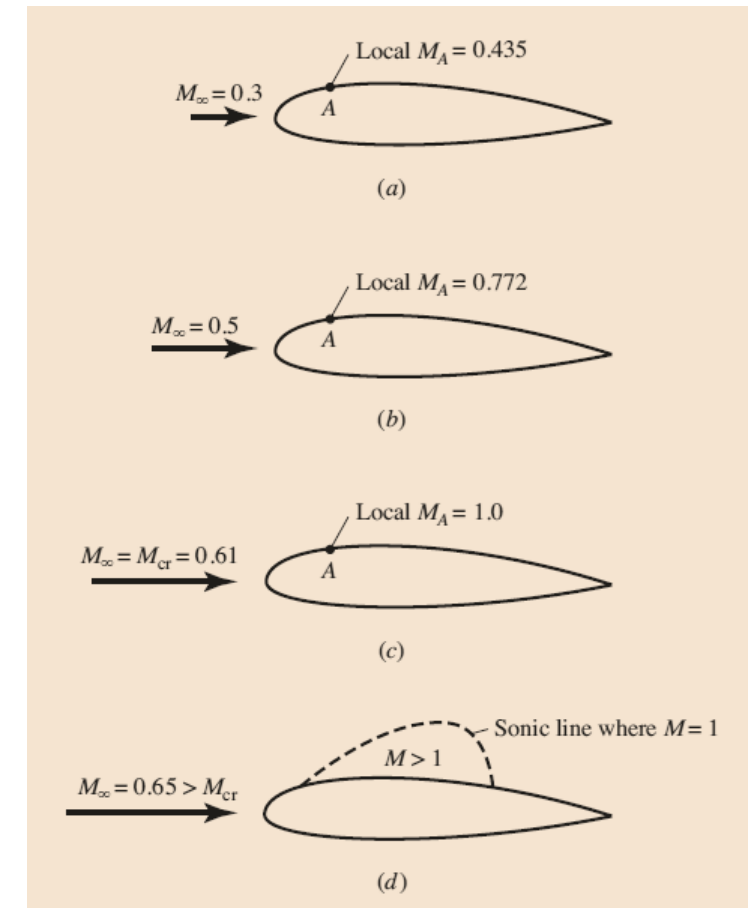


Zigzag trip strip

Critical Mach number Compressibility corrections

Critical Mach number – Compressibility corrections

- Critical Mach number M_{cr} .
 - The critical Mach number is the freestream Mach number at which sonic flow is first achieved on the airfoil surface.
 - In the figure $M_{cr} = 0.61$ (image c).
 - Determining the critical Mach number is very important in high-speed aerodynamics.
 - At values slightly above M_{cr} , the airfoil experiences a dramatic increase in drag coefficient due to the appearance of shock waves.
 - When using panel methods, is not possible to capture shock waves.
 - However, by using the incompressible pressure distribution $c_{p,0}$ and compressibility corrections, we can roughly estimate the critical Mach number of the airfoil.



- As we keep increasing the freestream Mach number, the local Mach number on point A increases.
- Recall that point A corresponds to the minimum pressure; therefore, maximum velocity.
- At a given freestream Mach number, the local Mach number on the airfoil surface may become sonic (image c).

General knowledge, as our focus is low speed aerodynamics.

Critical Mach number – Compressibility corrections

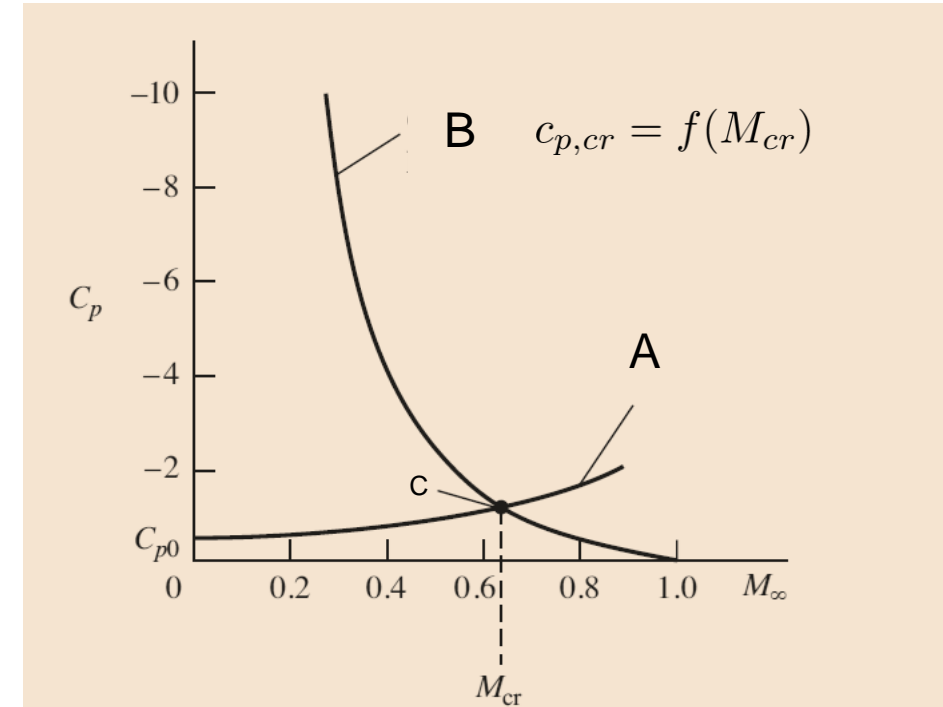
- For a given airfoil, the critical Mach number M_{cr} can be estimated as follows,
 - Obtain the incompressible pressure coefficient distribution $c_{p,0}$.
 - Using any of the compressibility corrections available in the literature (e.g., Prandtl-Glauert, Karman-Tsien, Laitone), compute the corrected pressure coefficient at the minimum incompressible pressure coefficient location.
 - For example, using the Karman-Tsien correction the corrected pressure coefficient at the minimum incompressible pressure coefficient location is computed as follows,

$$c_{p,corrected} = \frac{c_{p,0}}{\sqrt{1 - M_\infty^2} + \frac{M_\infty^2}{1 + \sqrt{1 - M_\infty^2}} \frac{c_{p,0}}{2}} \quad \text{E1}$$

- Plot the critical pressure coefficient $c_{p,cr}$ (equation E2), and the corrected pressure coefficient (at the minimum incompressible pressure coefficient location) in function of the Mach number.
- The point where these two curves intersect, represents the critical Mach number.

$$c_{p,cr} = \frac{2}{\gamma M_\infty^2} \left[\left(\frac{1 + \frac{\gamma - 1}{2} M_\infty^2}{1 + \frac{\gamma - 1}{2}} \right)^{\frac{\gamma}{\gamma - 1}} - 1 \right] \quad \text{E2}$$

General knowledge, as our focus is low speed aerodynamics.

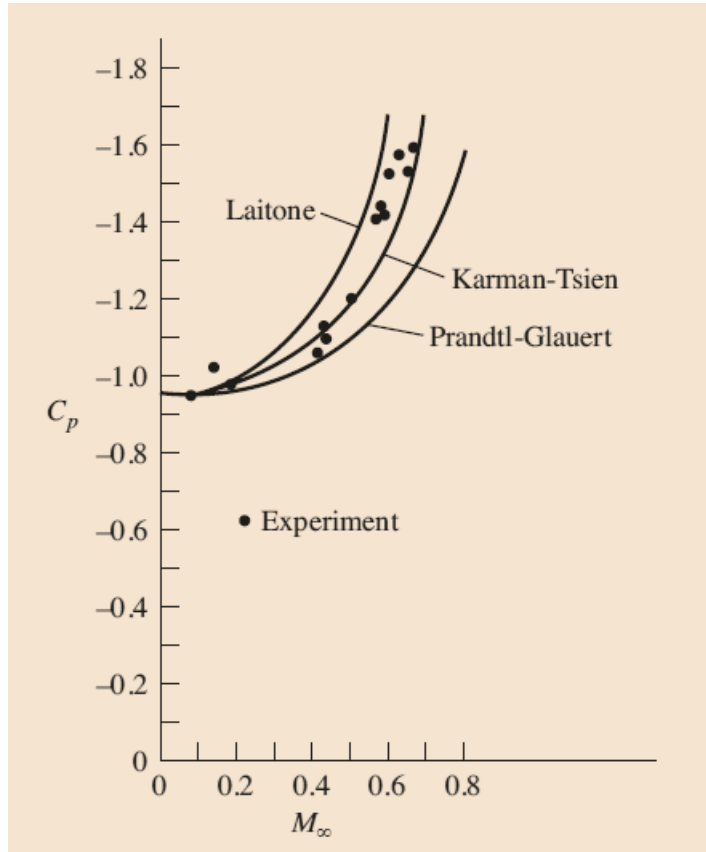


- In the figure, curve A is computed using equation E1 (Karman-Tsien compressibility correction), and curve B is computed using equation E2.
- The point where curve A and curve B intersect, represents the critical Mach number of the airfoil that is being studied.
- Equation E1 depends on the incompressible pressure coefficient distribution (therefore the geometry) and the Mach number.
- Equation E2, depends only on the freestream Mach number (isentropic relation).

Critical Mach number – Compressibility corrections

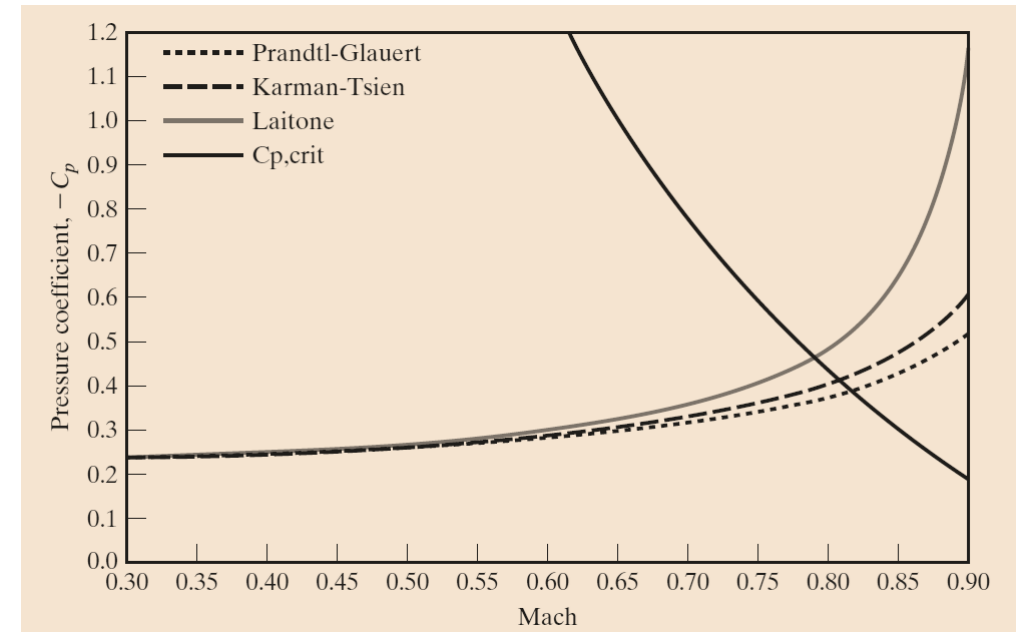
- Comparison of three compressibility correction rules.

General knowledge, as our focus is low speed aerodynamics.



Three compressibility corrections compared with experimental results for an NACA 4412 airfoil at an angle of attack of 1.53 degrees.

Photo credit: Fundamentals of aerodynamics, J. Anderson, McGraw-Hill, 2016.



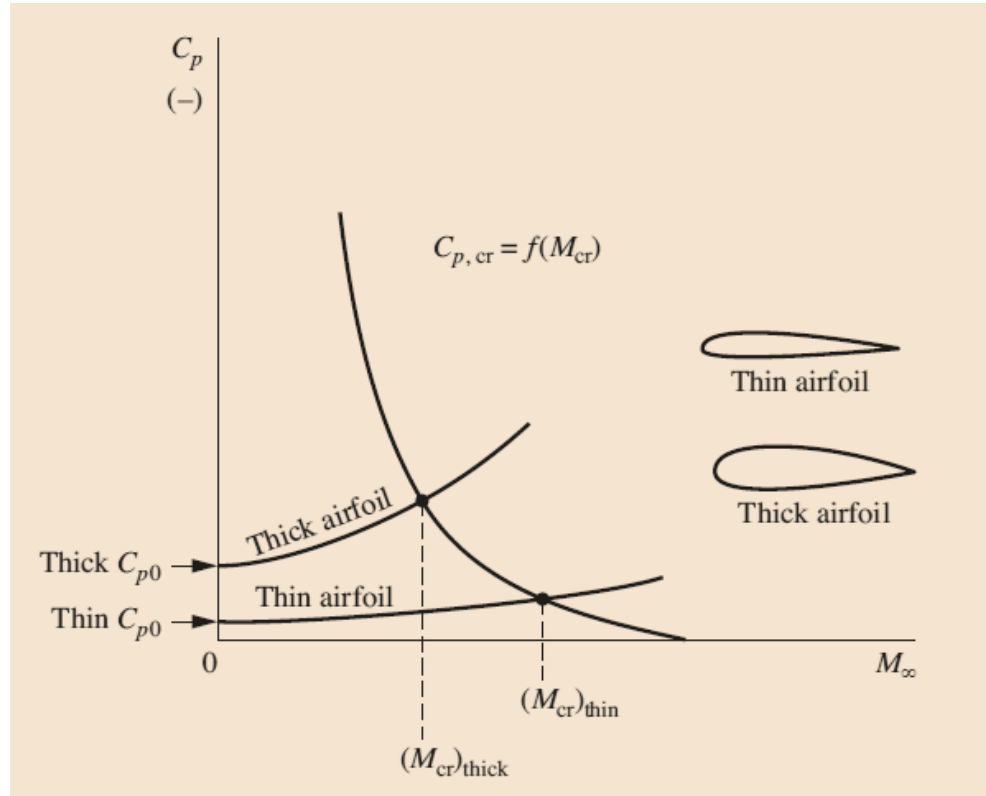
Comparison of three compressibility correction rules, showing large variation in critical Mach number estimate.

Photo credit: Aerodynamics for Engineers (6th Edition). J. Bertin, R. Cummings. Pearson, 2013.

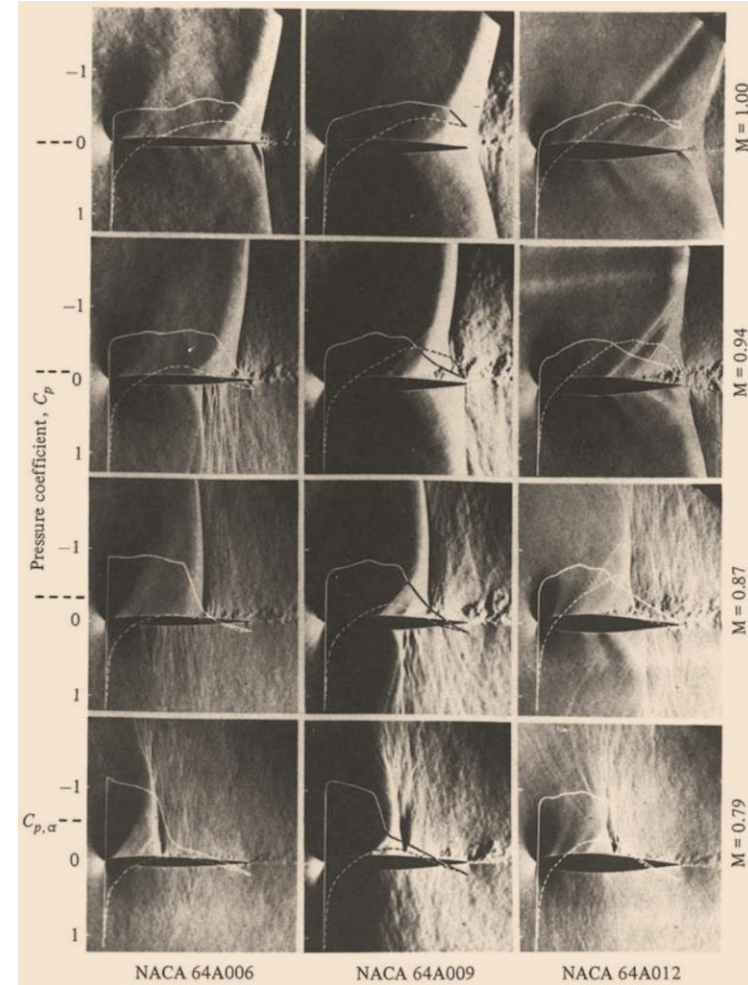
Critical Mach number – Compressibility corrections

- Effect of the airfoil geometry on the critical Mach number and the critical pressure coefficient.

General knowledge, as our focus is low speed aerodynamics.



Effect of airfoil thickness on critical Mach number

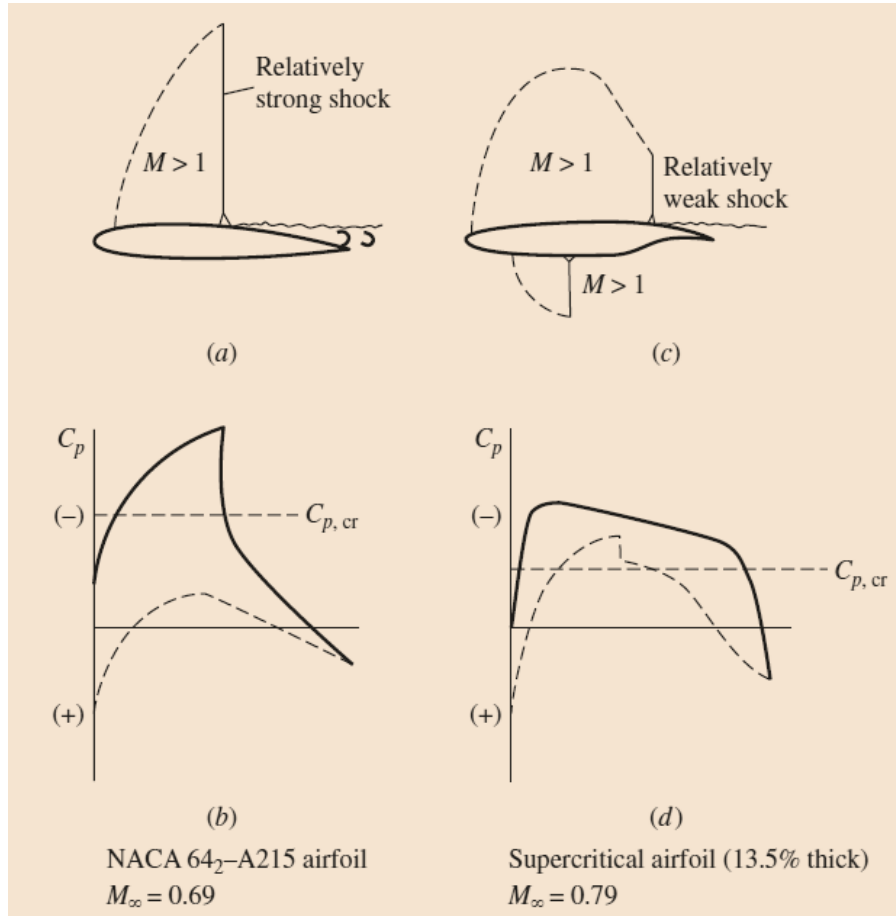


Schlieren pictures and pressure distributions for transonic flows over several NACA airfoils.

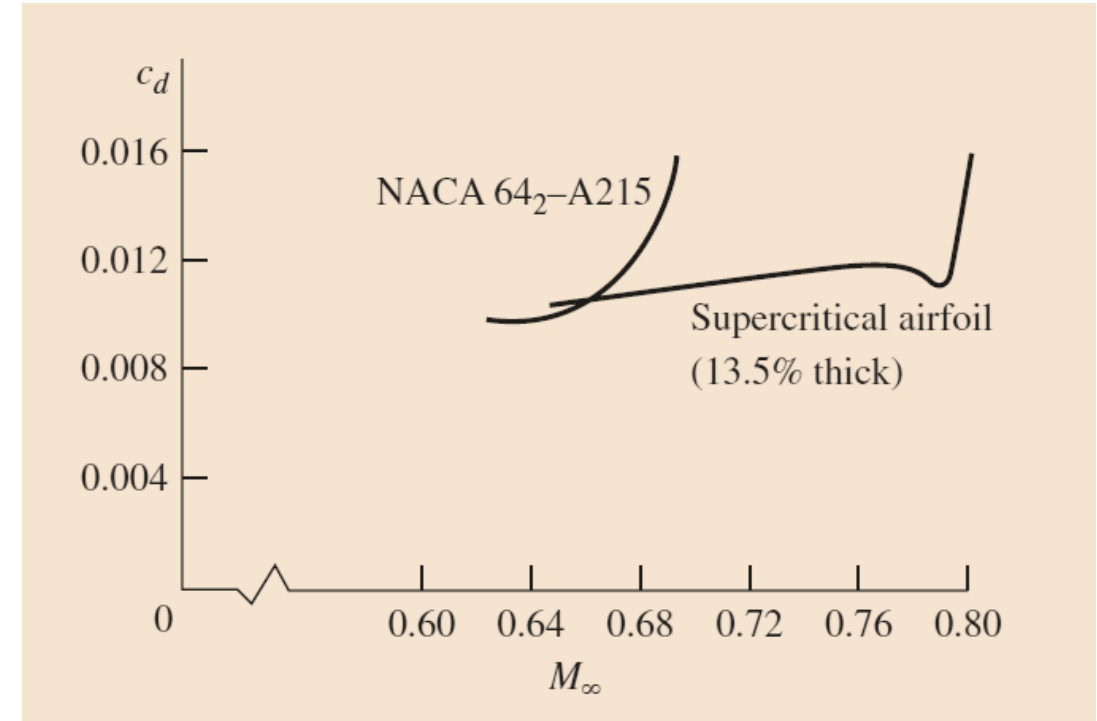
Critical Mach number – Compressibility corrections

- Effect of the airfoil geometry on the critical Mach number and the critical pressure coefficient.

General knowledge, as our focus is low speed aerodynamics.



Standard NACA 64-series airfoil compared with a supercritical airfoil at cruise conditions. Data source, NASA TMX-1109.

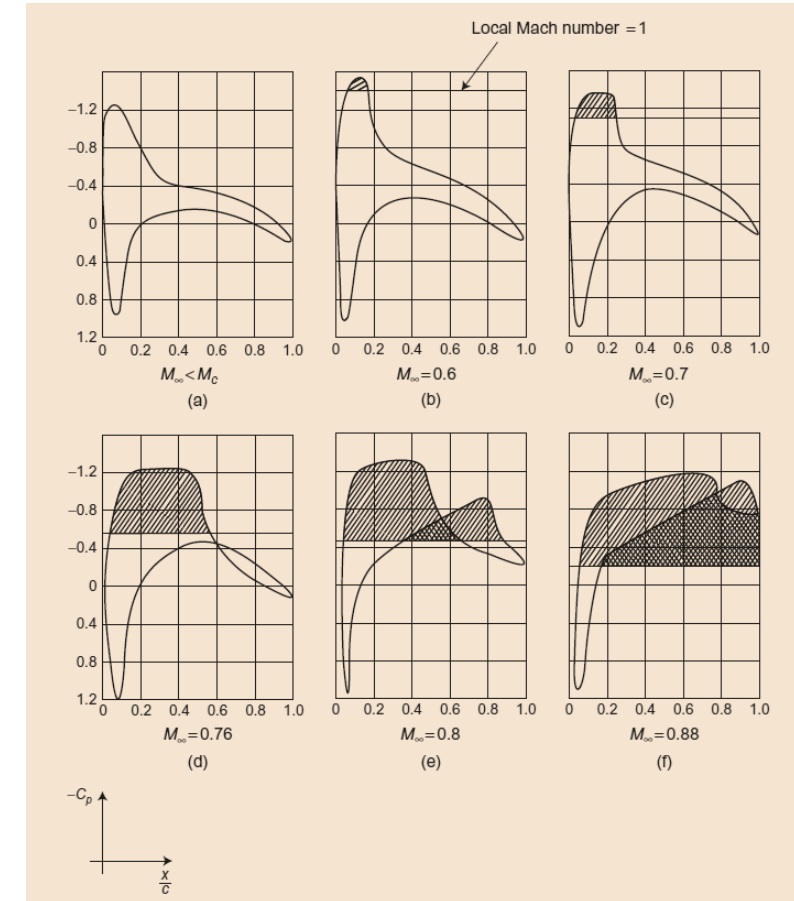
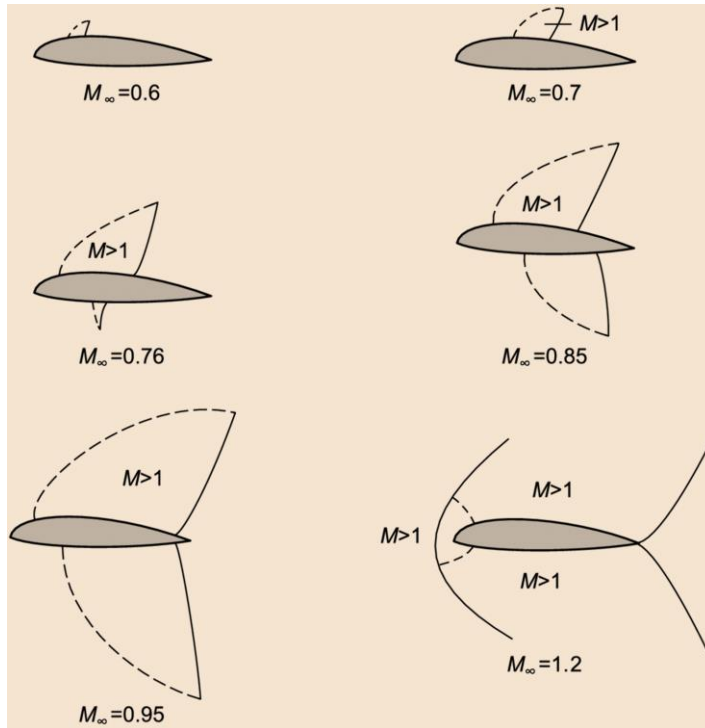


The drag-divergence properties of a standard NACA 64-series airfoil and a supercritical airfoil.

Critical Mach number – Compressibility corrections

- Flow development and pressure distribution on an airfoil.

General knowledge, as our focus is low speed aerodynamics.

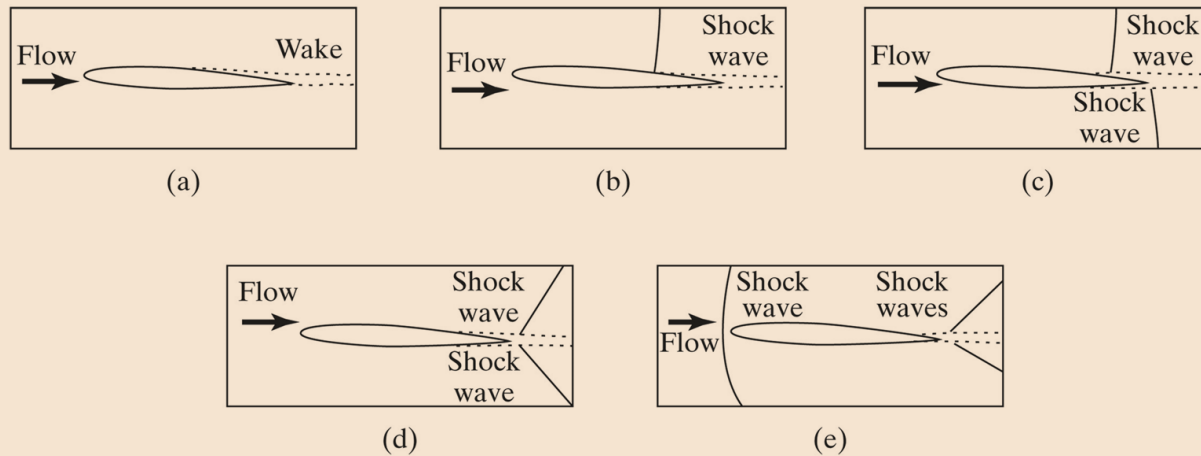


Shock waves

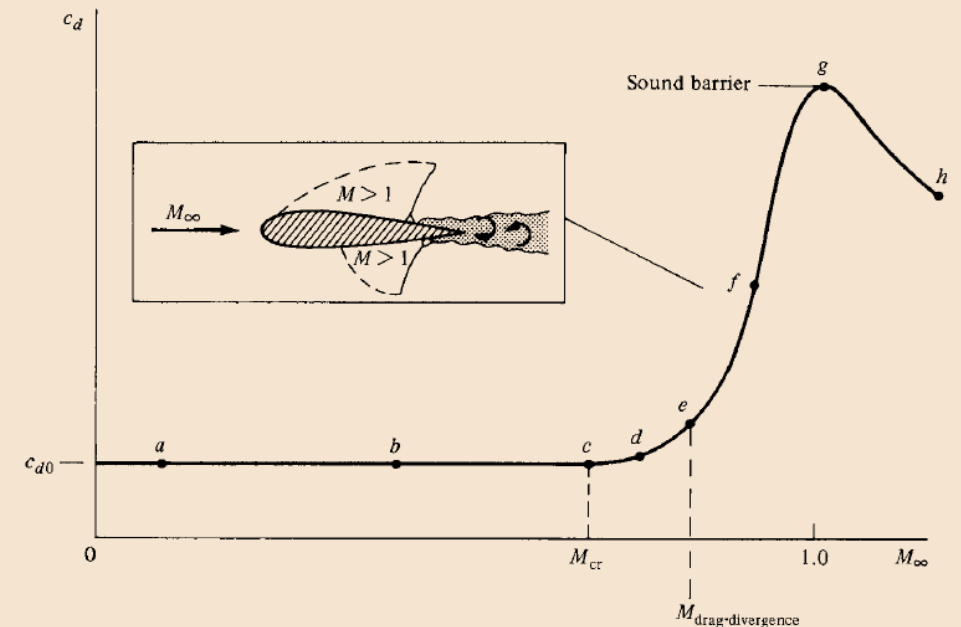
Shock waves

General knowledge, as our focus is low speed aerodynamics.

- Flow around an airfoil at high speed.
 - As soon as the critical Mach number (M_{cr}) has been reached, a sonic point appears on the airfoil surface.
 - At a Mach number just slightly higher than the critical Mach number, the drag increases very fast due to the appearance of shock waves. This is known as drag divergence Mach number (M_{dd}).
 - In order to capture the shock wave location and to predict the wave drag, specialized methods must be used.



Flow field around an airfoil in transonic streams (a) Mach number $M = 0.75$; (b) Mach number $M = 0.81$; (c) Mach number $M = 0.89$; (d) Mach number $M = 0.98$; (e) Mach number $M = 1.4$.
Photo credit: Aerodynamics for Engineers (6th Edition). J. Bertin, R. Cummings. Pearson, 2013.



Sketch of the variation of profile drag coefficient with freestream Mach number.
Photo credit: Fundamentals of aerodynamics, J. Anderson, McGraw-Hill, 2016

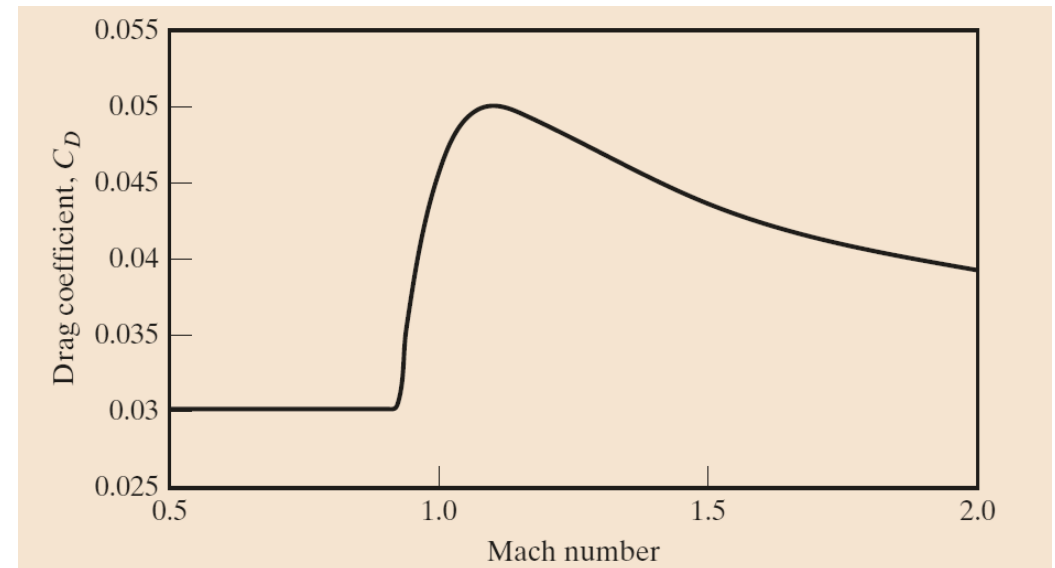
Shock waves

General knowledge, as our focus is low speed aerodynamics.

- Flow around an airfoil at high speed.
 - As soon as the critical Mach number (M_{cr}) has been reached, a sonic point appears on the airfoil surface.
 - At a Mach number just slightly higher than the critical Mach number, the drag increases very fast due to the appearance of shock waves. This is known as drag divergence Mach number (M_{dd}).
 - There are no reliable analytic methods for predicting the drag divergence Mach number, although practically every aircraft manufacturer has some rule of thumb for estimating the value.



F-4C zero-lift drag coefficient. F-4C which was flown at 35 000 ft in level acceleration; $W = 38\,924$ lb with 4 AIM-7 missiles.



F-4C zero-lift drag coefficient. At a Mach number just slightly higher than the critical Mach number, the drag increases very fast due to the appearance of shock waves.

Shock waves

- Effect of the Mach number and shock waves on the aerodynamic performance.
 - The main consequences of shock waves on the aerodynamic performance are the rapid increment of the drag and the lost of lift.

General knowledge, as our focus is low speed aerodynamics.



F-111 flying at transonic speeds with shock waves clearly visible.

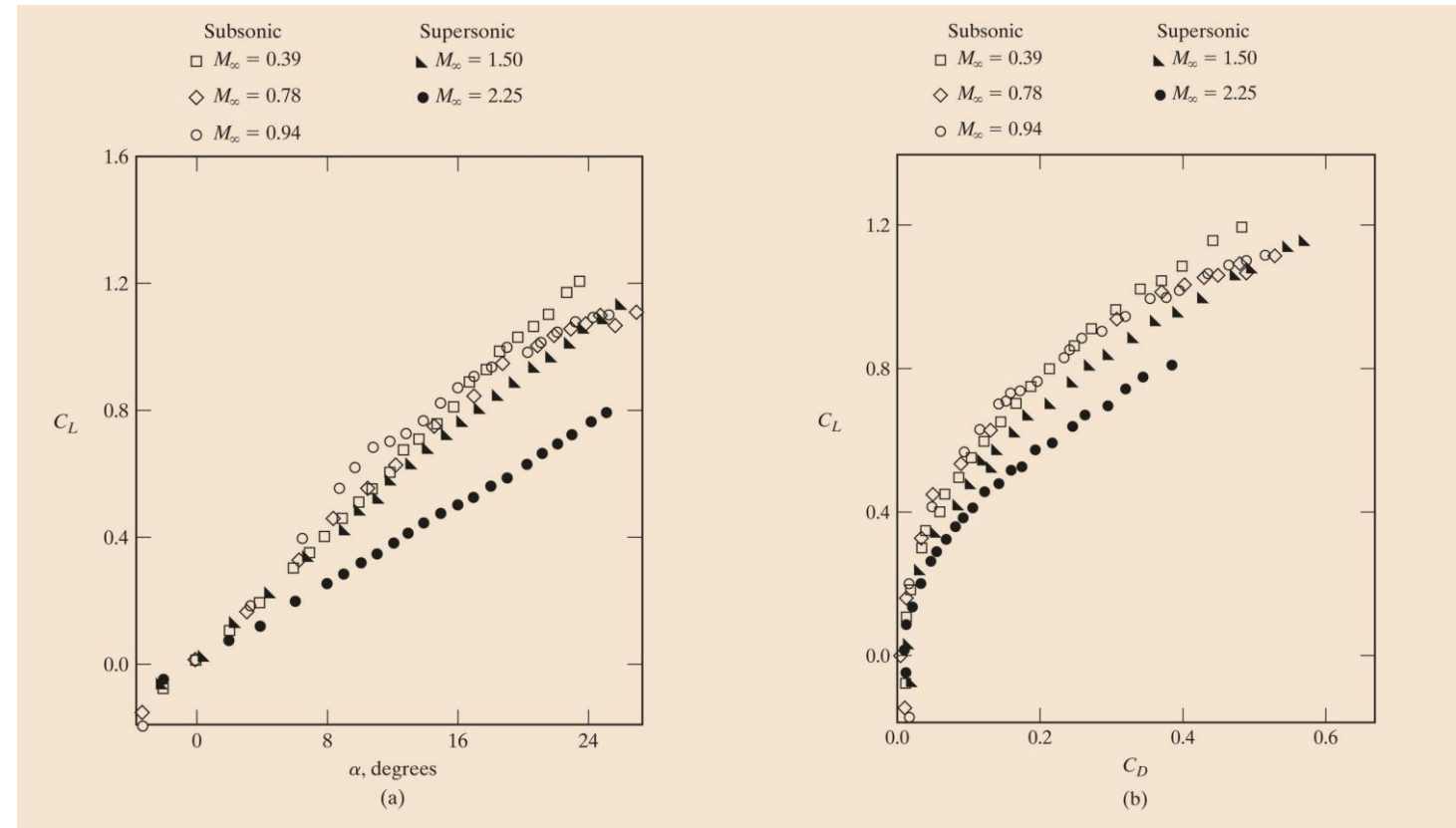
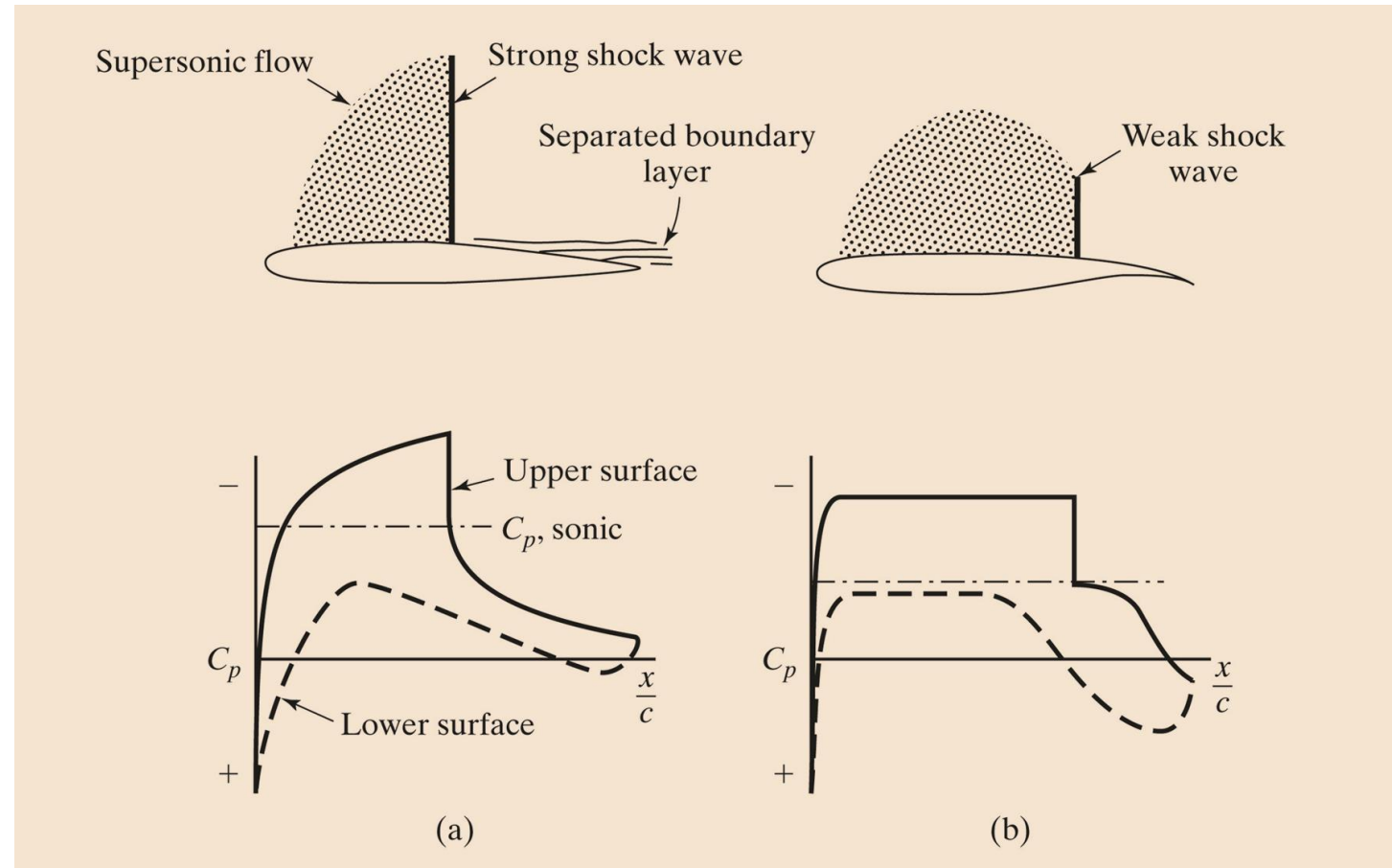


Figure a: Effect of Mach number on the lift-coefficient/angle-of-attack correlation for a rectangular wing, AR = 2.75.
 Figure b: Effect of the Mach number on drag polars for a rectangular wing, AR = 2.75.

Shock waves

- To delay the onset of the critical Mach number and to diminish the intensity of the shock wave (therefore the wave drag), special airfoils are used.

General knowledge, as our focus is low speed aerodynamics.



Comparison of transonic flow over a NACA 64A series airfoil with that over a supercritical airfoil section: (a) NACA 64A series, $M = 0.72$; (b) supercritical airfoil, $M = 0.80$.

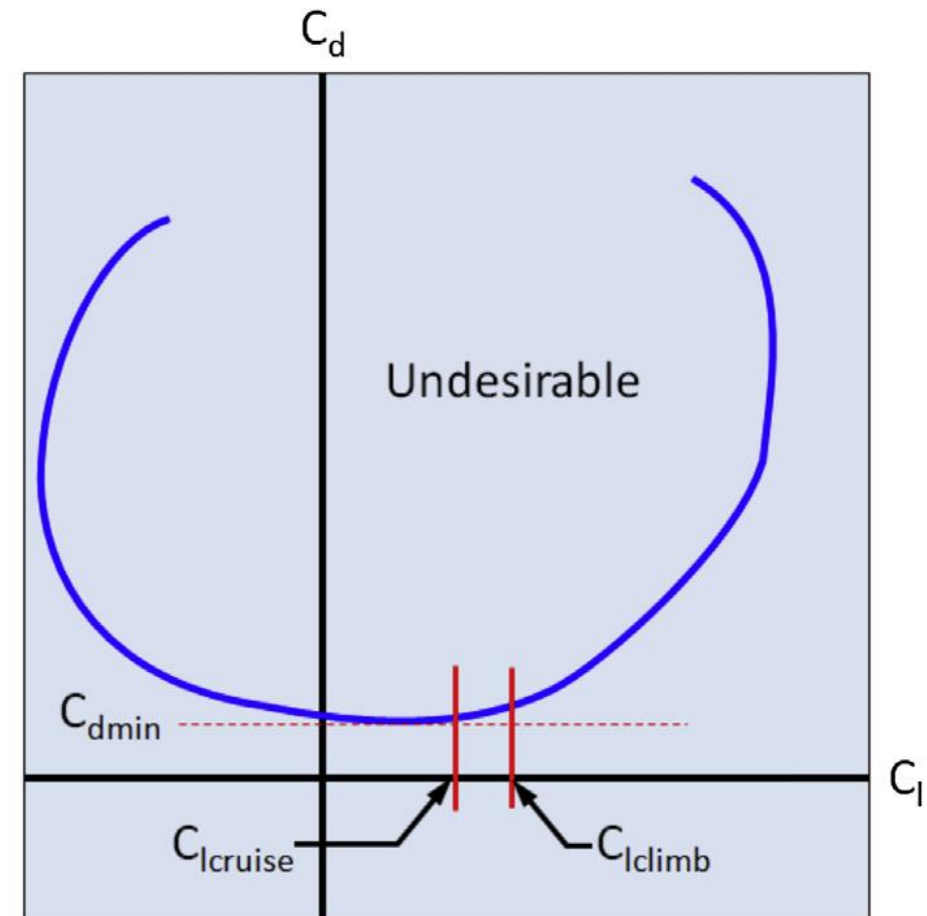
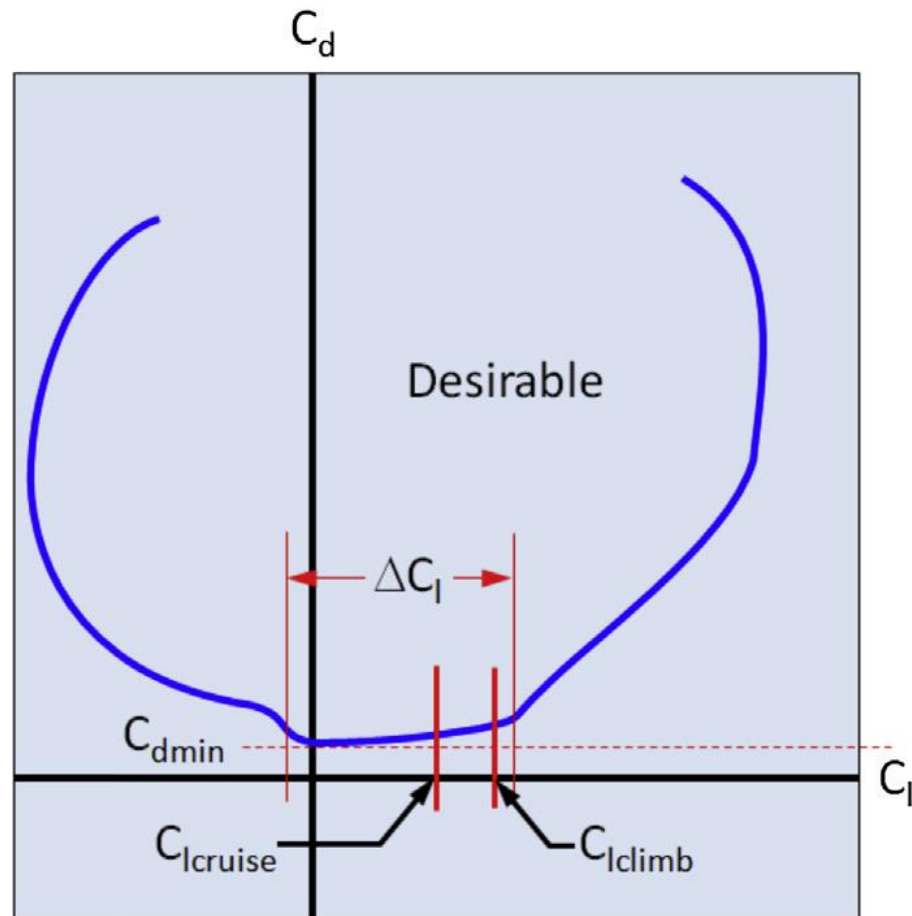
Airfoil selection

Airfoil selection

- The selection of airfoils is often a challenging task for aircraft designers.
- The airfoil have a profound effect on the performance and handling qualities of the aircraft, as well as the structure and weight.
- When selecting (or designing) an airfoil, the following aerodynamics and geometric characteristics should be kept in mind:
 - Impact on drag.
 - Impact on flow separation.
 - Impact on maximum lift coefficient and stall handling.
 - Impact on pitch-down moment and longitudinal trim.
 - Critical Mach number.
 - Impact on wing-fuselage interaction.
 - Impact on structural depth.
 - Internal volume for fuel storage.

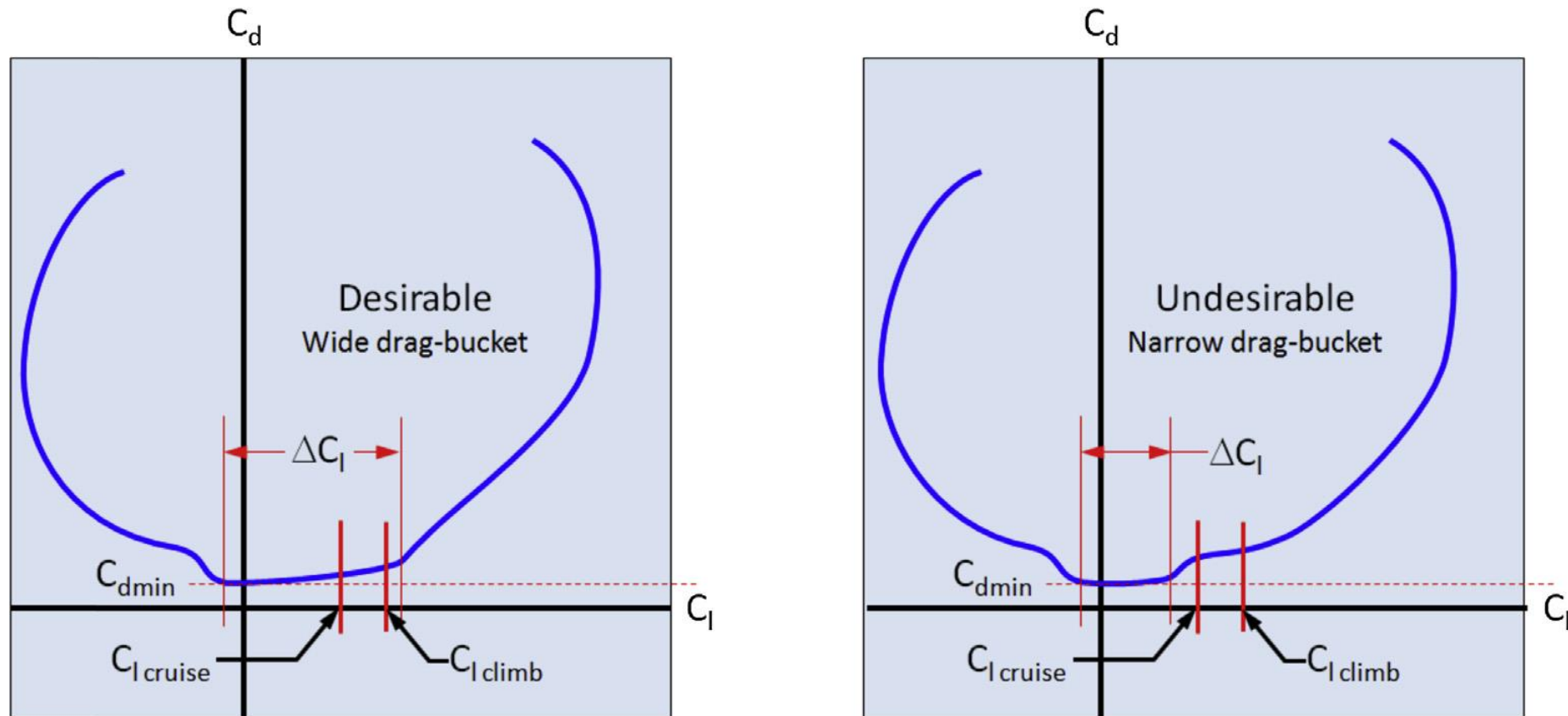
Airfoil selection

- A drag polar featuring a wide drag bucket (left figure) is always more desirable than a drag polar without one (right figure) or one with a narrow drag bucket.
- The drag bucket is a feature typical of laminar-flow airfoils (e.g., NACA 6-series or NASA NLF airfoils).



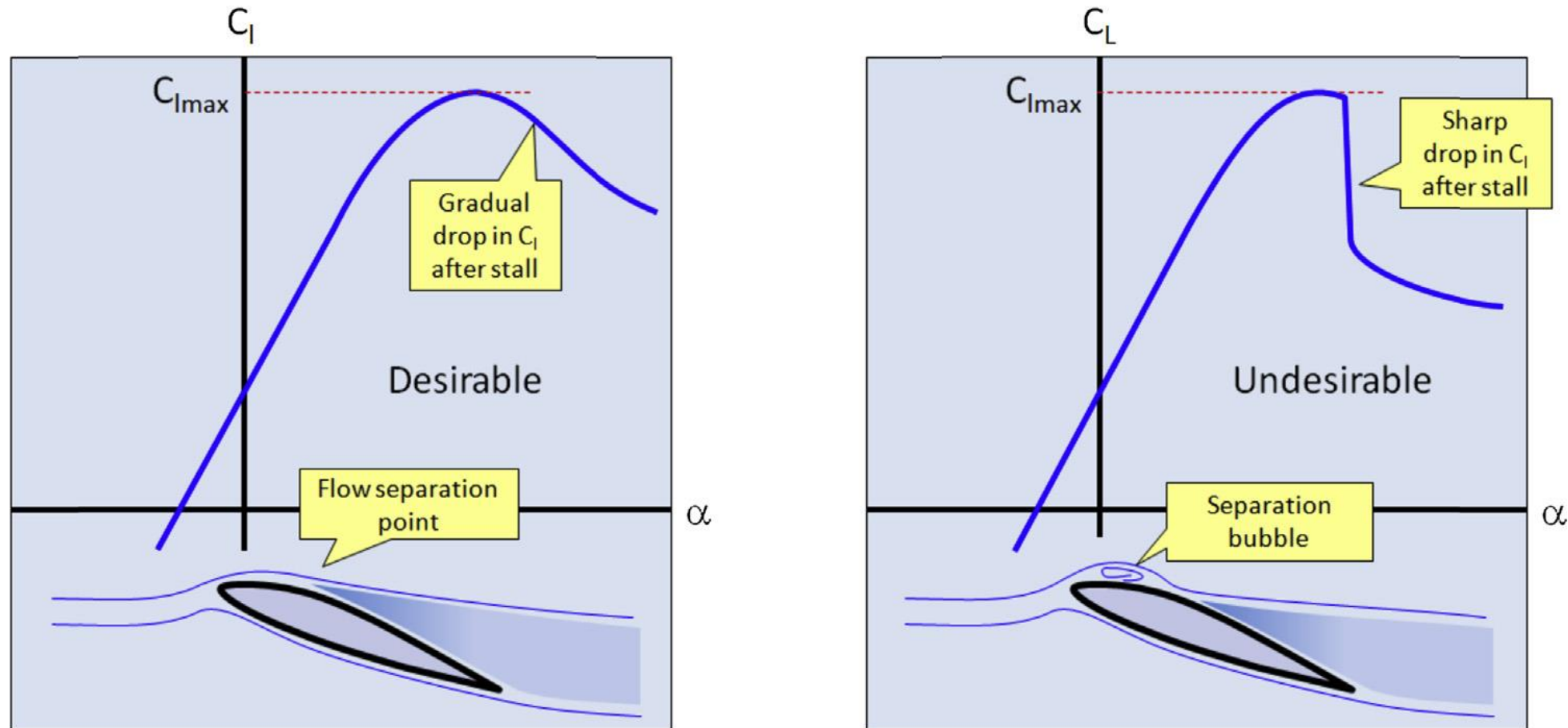
Airfoil selection

- A drag polar featuring a wide drag bucket (left figure) is always more desirable than a drag polar without one (right figure) or one with a narrow drag bucket.
- It is also desirable to have the maximum lift-to-drag ratio as close as possible to cruise conditions.



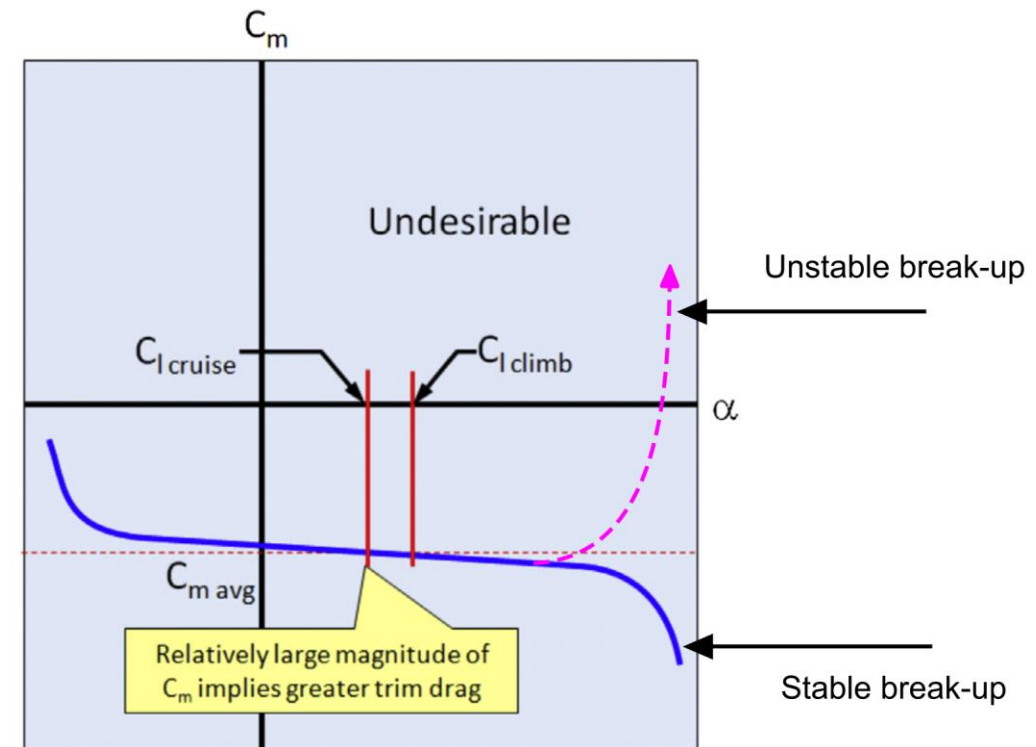
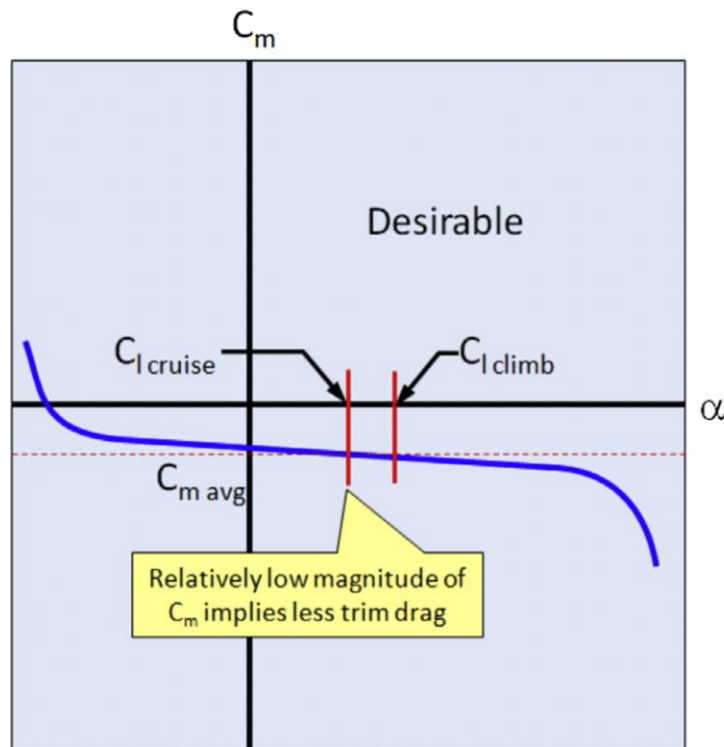
Airfoil selection

- An abrupt stall pattern (right figure) is undesirable.
- In general, gradual stall (left figure) is preferred over abrupt stall (right figure).
- High maximum lift coefficient values in combination with a steep lift curve slope are also desirable.



Airfoil selection

- We did not talk much about pitching moment, but this is an important quantity that you should also keep an eye on.
- Pitching moment is used to define the stability of the aircraft.
- Most of the airfoils have a negative pitching moment, and its value depends on the pressure distribution.
- The larger the magnitude of pitching moment coefficient (right figure) the greater will be the trim drag (drag generated by the stabilizing surfaces to trim the aircraft).
- Stable break-up is preferred over unstable break-up.

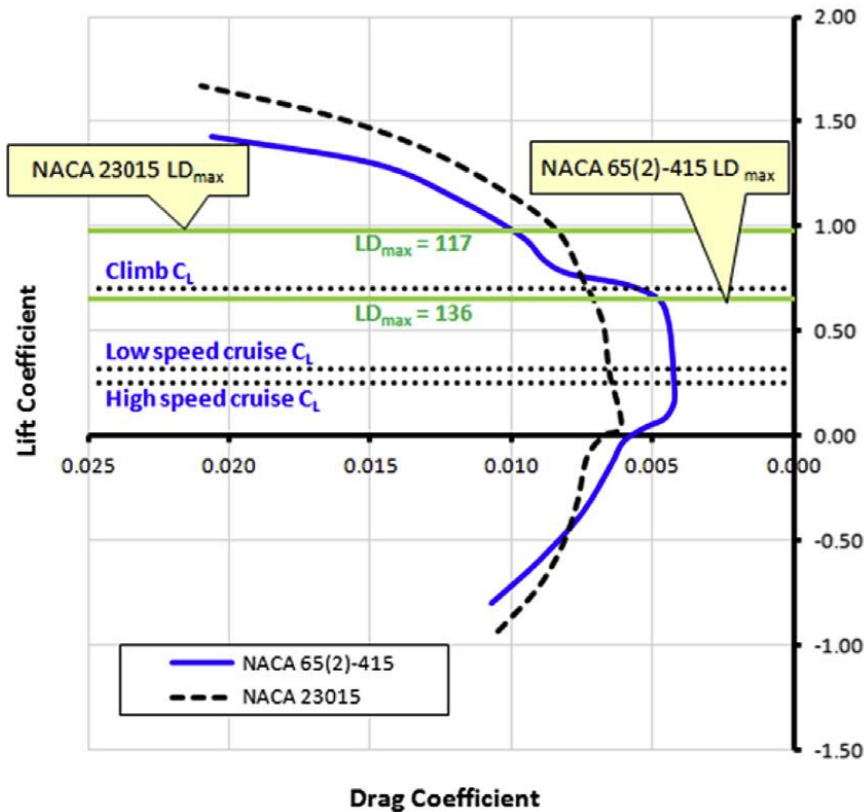


Airfoil selection

- Airfoil selection example.
- The aerodynamic characteristics of two airfoils plotted to compare their characteristics to the target performance.
- What airfoil will you choose?

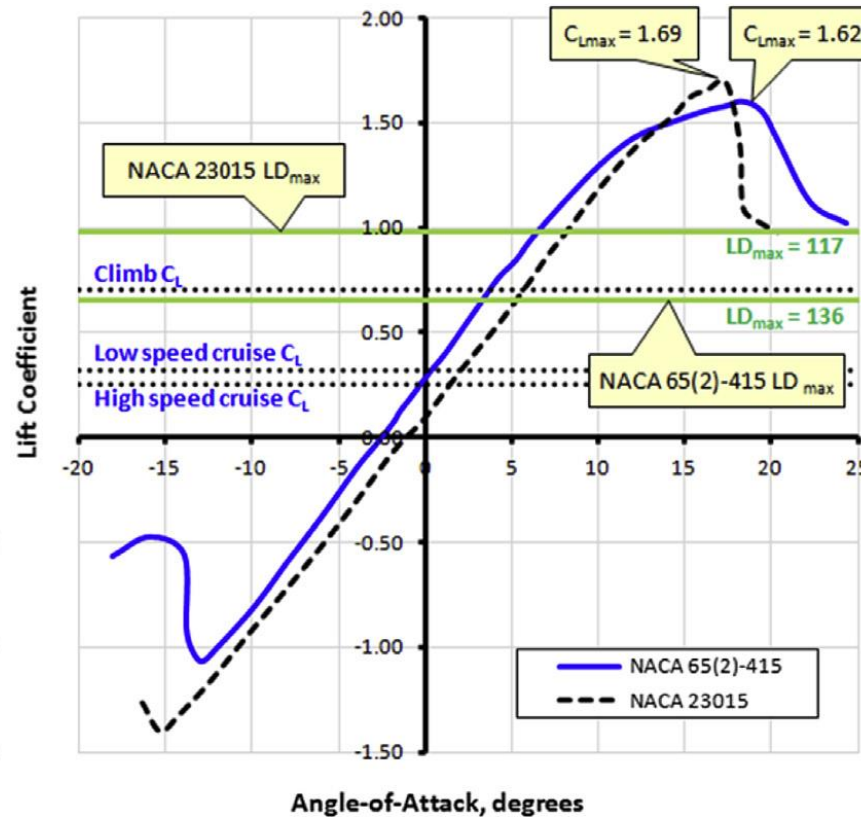
Drag Polars

Source: NACA R-824, $Re = 6 \times 10^6$



Lift Coefficient versus Angle-of-Attack

Source: NACA R-824, $Re = 6 \times 10^6$



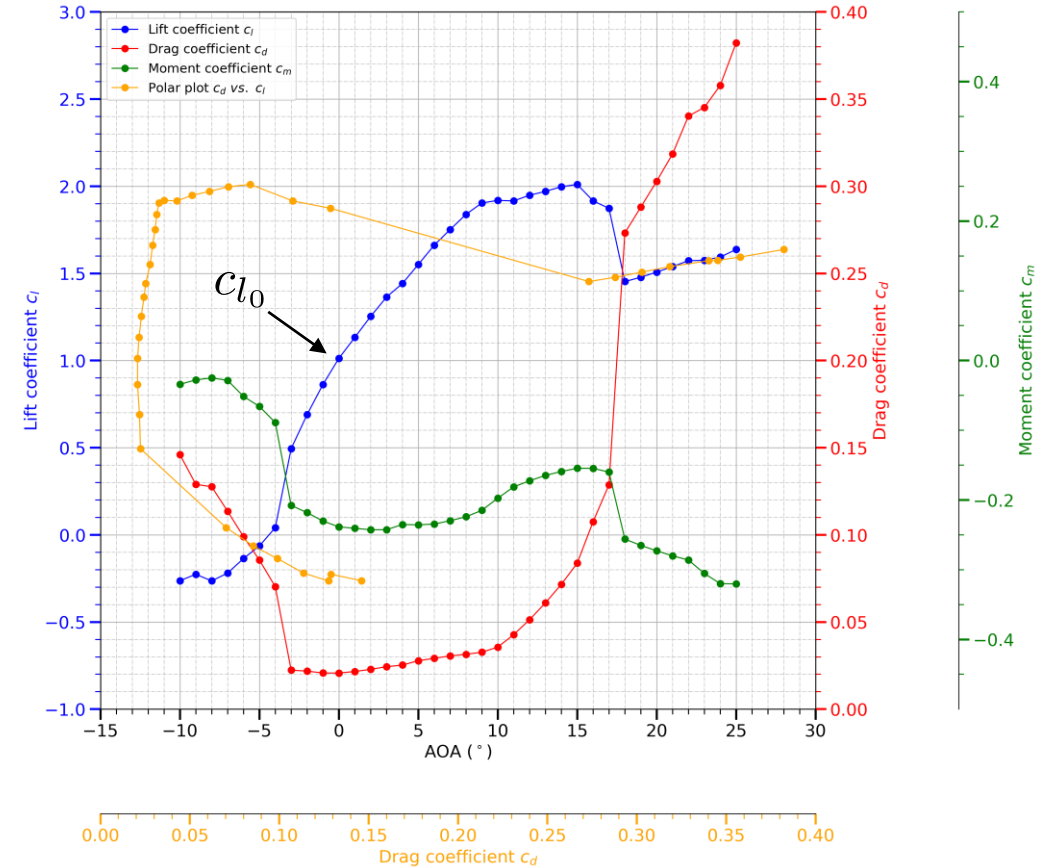
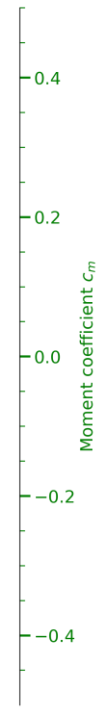
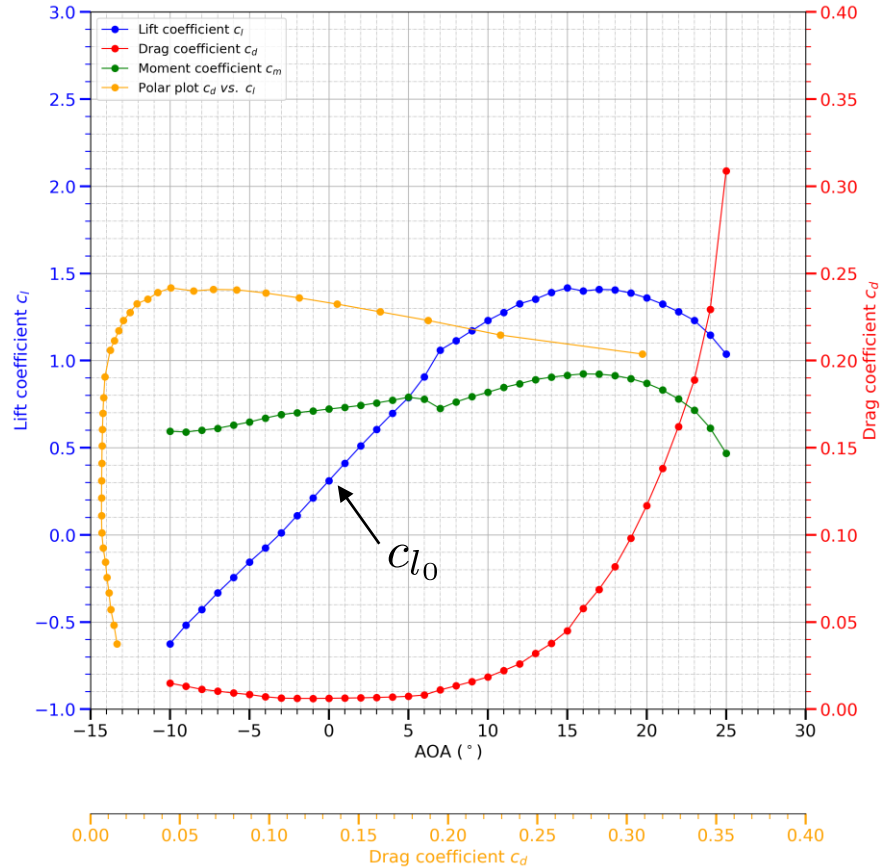
Target performance:

$$0.25 < c_{l_{cruise}} < 0.32$$

$$c_{l_{climb}} \approx 0.7$$

Airfoil selection

- Different airfoils can have very different aerodynamic characteristics.
- The final selection is driven by the design requirements (aerodynamic, performance, economical, environmental, among many).



Airfoil selection

A design case study

Airfoil selection – A design case study

Natural laminar flow airfoil – The SHM-1 Airfoil

- This NLF airfoil is used in the HondaJet.
 - The Honda HA-420 HondaJet is a light business jet produced by the Honda Aircraft Company.
- The airfoil was designed using potential methods, validated and refined using CFD, tested in low-speed and transonic wind tunnels, and flight tested.
- The airfoil was designed to exactly match HondaJet requirements.
 - Low profile drag at cruise and climb conditions.
 - High $C_{l_{max}}$
 - Low nose-down pitching moment at high speeds.
 - Docile stall characteristics.
 - Insensitivity to leading edge contamination.
 - High drag-divergence Mach number.
 - Optimal airfoil thickness for fuel volume to satisfy the range requirement.



Copyright on the images is held by the contributors. Apart from Fair Use, permission must be sought for any other purpose.

References:

- M. Fujino, Y. Yoshizaki, Y. Kawamura. Natural-Laminar-Flow Airfoil Development for a Lightweight Business Jet. Journal of Aircraft, Volume 40, Number 4, July 2003.
M. Fujino. Development of the Honda Jet. 24th Congress of International Council of the Aeronautical Sciences, 29 August-3 September 2004, Yokohama, Japan

Airfoil selection – A design case study

Natural laminar flow airfoil – The SHM-1 Airfoil

- Design methodology and computational aerodynamics software used:
 - **Eppler airfoil design and analysis code [1,2]** – It combines a conformal-mapping method for the design of airfoils with prescribed velocity-distribution characteristics (inverse methods), a panel method for the analysis of the potential flow about given airfoils, and an integral boundary-layer method.
 - Used to design the upper and lower surface separately using conformal mapping method with prescribed velocity distributions.

Images taken from references [3,4]

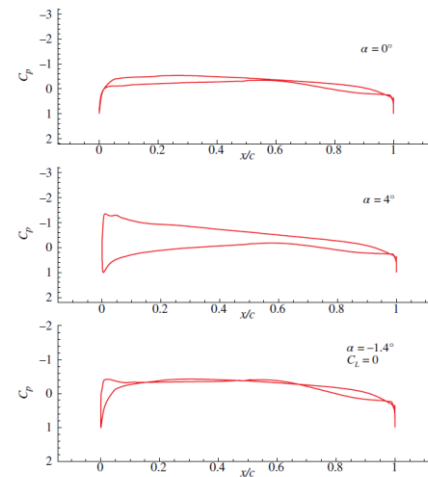
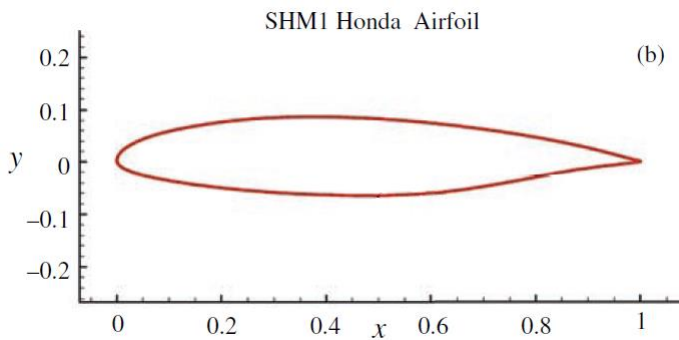


Figure 5.10(b) C_p distributions for the SHM-1 airfoil for the indicated angles of attack

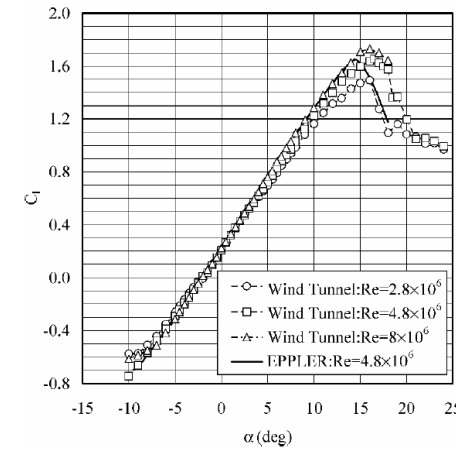


Fig. 10 Comparison of theoretical and experimental (low-speed wind tunnel) lift curves.

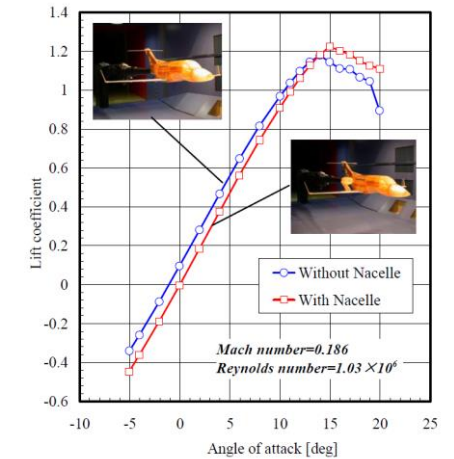


Fig. 7. Comparison of lift curve with and without nacelle configuration.

References:

- [1] R. Eppler. Airfoil Program System PROFIL97 User's Guide. Ver.11.6.97, June 1997.
- [2] R. Eppler. Airfoil Design and Data. Springer-Verlag, Berlin, 1990.
- [3] M. Fujino, Y. Yoshizaki, Y. Kawamura. Natural-Laminar-Flow Airfoil Development for a Lightweight Business Jet. Journal of Aircraft, Volume 40, Number 4, July 2003.
- [4] M. Fujino. Development of the Honda Jet. 24th Congress of International Council of the Aeronautical Sciences, 29 August-3 September 2004, Yokohama, Japan

Airfoil selection – A design case study

Natural laminar flow airfoil – The SHM-1 Airfoil

- Design methodology and computational aerodynamics software used:
 - MSES [1,2]** – It is an evolution of XFOIL with multielement airfoil capabilities. The MSES code contains an Euler method that solves a streamline-based Euler discretization and a two-equation integral boundary-layer formulation simultaneously using a full Newton method.
 - Used to evaluate the high-speed characteristics of the airfoil, including shock formation and drag divergence.
 - MCARF** – It is a two-dimensional, subsonic, panel method; viscous effects are accounted for by altering the geometry of the airfoil to include the displacement thickness obtained from the integral boundary-layer method.
 - Used to evaluate geometry modifications to the airfoil and also for transition-location studies.

Images taken from references [3,4]

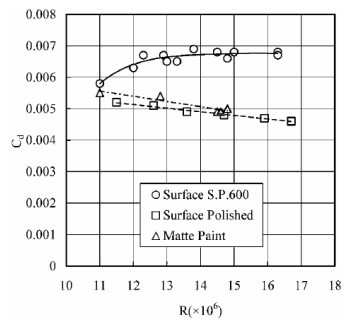


Fig. 16 Effect of surface roughness on drag.

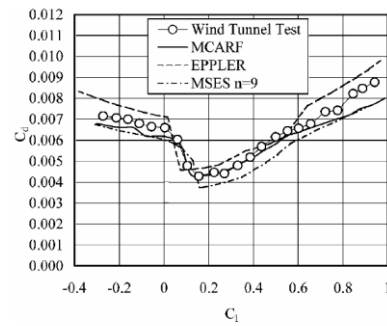


Fig. 13 Comparison of theoretical and experimental (low-speed wind tunnel) drag polars for $Re = 10.3 \times 10^6$ and $M = 0.27$.

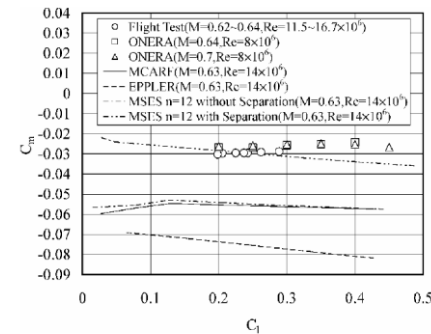


Fig. 14 Comparison of theoretical and experimental (flight and transonic wind tunnel) pitching moment coefficients.

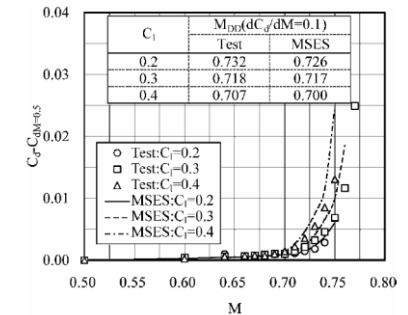


Fig. 17 Comparison of theoretical and experimental (transonic wind tunnel) drag-divergence Mach numbers for $Re = 8.0 \times 10^6$ with transition fixed.

References:

- H. Morgan. High-Lift Flaps for Natural Laminar Flow Airfoils. Laminar Flow Aircraft Certification, NASA CP-2413, 1986, pp. 31–65.
- M. Drela. A User's Guide to MSES 2.95. MIT Computational Aerospace Sciences Lab., Massachusetts Inst. of Technology, Cambridge, MA, Sept. 1996.
- M. Fujino, Y. Yoshizaki, Y. Kawamura. Natural-Laminar-Flow Airfoil Development for a Lightweight Business Jet. Journal of Aircraft, Volume 40, Number 4, July 2003.
- M. Fujino. Development of the Honda Jet. 24th Congress of International Council of the Aeronautical Sciences, 29 August-3 September 2004, Yokohama, Japan

Airfoil selection – A design case study

Natural laminar flow airfoil – The SHM-1 Airfoil

- Resulting airfoil [1,2]:
 - Favorable pressure gradient to about 42% of the chord in the upper surface.
 - Followed by a concave pressure recovery, which represents a compromise between $C_{l_{max}}$, C_m , and M_{DD} .
 - Favorable pressure gradient to about 63% of the chord in the lower surface to reduce drag (with steeper pressure recovery).
 - The leading-edge geometry was carefully designed to cause transition near the leading edge at high angles of attack to minimize the loss in $C_{l_{max}}$ due to roughness.
 - The upper-surface trailing-edge geometry was designed to produce a steep pressure gradient and, thereby, induce a small separation.
 - By the incorporation of this new trailing-edge design, the magnitude of the pitching moment at high speeds is greatly reduced.

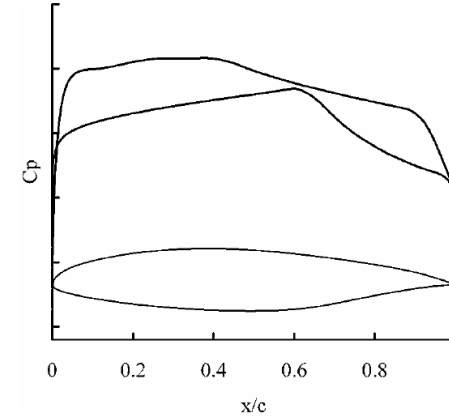


Fig. 1 SHM-1 airfoil shape and pressure distribution.

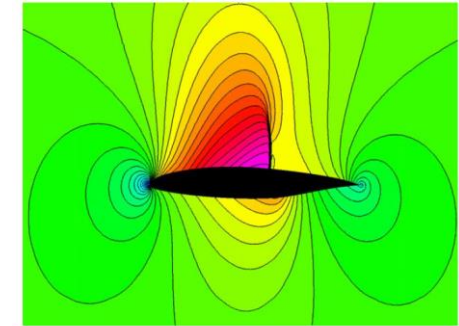
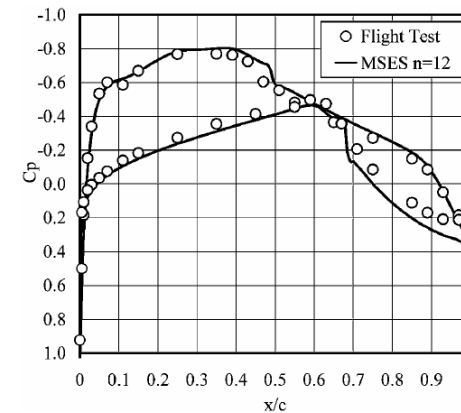
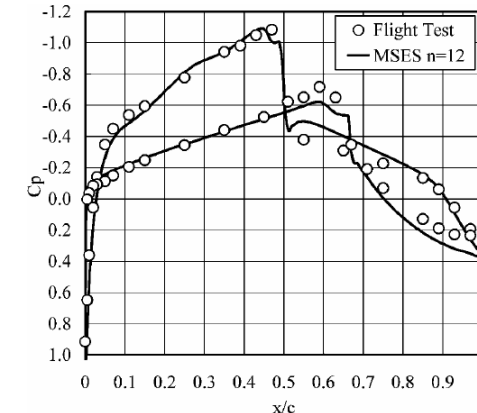


Fig. 8. SHM-1 airfoil shape and pressure contour.



a) $\alpha = 0.27$ deg, $Re = 13.6 \times 10^6$, and $M = 0.62$



b) $\alpha = -0.38$ deg, $Re = 16.2 \times 10^6$, and $M = 0.72$

Fig. 7 Comparison of theoretical and experimental (flight) pressure distributions.

References:

- [1] M. Fujino, Y. Yoshizaki, Y. Kawamura. Natural-Laminar-Flow Airfoil Development for a Lightweight Business Jet. Journal of Aircraft, Volume 40, Number 4, July 2003.
- [2] M. Fujino. Development of the Honda Jet. 24th Congress of International Council of the Aeronautical Sciences, 29 August-3 September 2004, Yokohama, Japan

Airfoil selection – A design case study

Natural laminar flow airfoil – The SHM-1 Airfoil

- Representative performance characteristics of the SHM-1 airfoil [1,2]:
 - $C_{l_{max}} = 1.66$ for $Re = 4.8 \times 10^6$ and $M = 0.134$ (low-speed wind tunnel).
 - Loss in $C_{l_{max}}$ due to leading-edge contamination is 5.6% for $Re = 4.8 \times 10^6$ and $M = 0.134$ (low-speed wind tunnel).
 - $C_d = 0.0051$ at $C_l = 0.26$ for $Re = 13.2 \times 10^6$ and $M = 0.66$ (flight test).
 - $C_d = 0.0049$ at $C_l = 0.35$ for $Re = 10.3 \times 10^6$ and $M = 0.27$ (low-speed wind tunnel).
 - $C_m = -0.030$ at $C_l = 0.20$ for $Re = 16.7 \times 10^6$ and $M = 0.64$ (flight test).
 - $C_m = -0.025$ at $C_l = 0.40$ for $Re = 8.0 \times 10^6$ and $M = 0.7$ (transonic wind tunnel).
 - $M_{DD} > 0.718$ at $C_l = 0.30$ (transonic wind tunnel).
 - $M_{DD} > 0.707$ at $C_l = 0.40$ (transonic wind tunnel).
 - The cross-sectional area of the airfoil is about 9% larger than that of the NACA 64₂-215 airfoil and about 16% larger than that of the NASA HSNLF(1)-0213 airfoil; thus, it is possible to carry the required fuel in the wing without increasing the wing size.
 - Therefore, the wing area is minimized by using the SHM-1 airfoil.

References:

- [1] M. Fujino, Y. Yoshizaki, Y. Kawamura. Natural-Laminar-Flow Airfoil Development for a Lightweight Business Jet. Journal of Aircraft, Volume 40, Number 4, July 2003.
[2] M. Fujino. Development of the Honda Jet. 24th Congress of International Council of the Aeronautical Sciences, 29 August-3 September 2004, Yokohama, Japan

References

References

- Abbott, I., Von Doenhoff, A., Stivers, L. S., Summary of airfoil data. NACA Report 824. 1945.
- Selig, M. S., Donovan, J., Fraser, D., Airfoils at low speed. 1989.
- Selig, M. S., Guglielmo, J. J., Broeren, A. P., Giguere, P., Summary of Low-Speed Airfoil Data. Vol. 1, 1995.
- Selig, M. S., Lyon, C. A., Giguere, P., Ninham, C. N., Guglielmo, J. J., Summary of Low-Speed Airfoil Data. Vol. 2, 1996.
- Lyon, C. A., Broeren, A. P., Giguere, P., Gopalarathnam, A., Selig, M. S., Summary of Low-Speed Airfoil Data. Vol. 3, 1998.
- Selig, M. S., McGranahan, B. D., Summary of Low-Speed Airfoil Data. Vol. 4, 2004.
- Williamson, G. A., McGranahan, B. D, Broughton, B. A., Deters, R. W., Brandt, J. B., Selig, M. S., Summary of Low-Speed Airfoil Data. Vol. 5, 2012.
- Williamson, G.A., Experimental Wind Tunnel Study of Airfoils with Large Flap Deflections at Low Reynolds Numbers, Master's Thesis, Department of Aerospace Engineering, University of Illinois at Urbana-Champaign, 2012.
- Ananda Krishnan, G. K., Aerodynamic performance of low-to-moderate aspect ratio wings at low Reynolds numbers. Master's Thesis, Department of Aerospace Engineering, University of Illinois at Urbana-Champaign, 2012.
- Selig, M. S., Low Reynolds Number Airfoil Design, VKI Lecture Series - Low Reynolds Number Aerodynamics on Aircraft Including Applications in Emerging UAV Technology, von Karman Institute for Fluid Dynamics (VKI) Lecture Series, RTO/AVT-VKI-104, November 2003.

References

- McGranahan, B. D., Selig, M. S., Surface Oil Flow Measurements on Several Airfoils at Low Reynolds Numbers, AIAA 42nd Applied Aerodynamics Conference, AIAA Paper 2003-4067, Orlando, FL, June 2003.
- Selig, M.S., Guglielmo, J.J., High-Lift Low Reynolds Number Airfoil Design, Journal of Aircraft, Vol. 34, No. 1, 1997.
- Hood, M. J., The Effects of Some Surface Irregularities on Wing Drag. NACA TN-695, 1939.
- Wadcock. A. J., Investigation of Low-Speed Turbulent Separated Flow Around Airfoils. NASA Contractor Report 177450.
- Hicks, R. M., Vanderplaats, G. N., Application of numerical optimization to the design of low-speed airfoils. NASA TM X-3213. 1975.
- McCroskey, W. J., A critical assessment of wind tunnel results for the NACA 0012 airfoil. NASA Technical Memorandum 100019, 1987.
- Ladson, C. L., Hill, A. S., Johnson, W. G., Pressure Distributions from High Reynolds Number Transonic Tests of an NACA 0012 Airfoil in the Langley 0.3-Meter Transonic Cryogenic Tunnel. NASA TM 100526, 1987.
- Ladson, C., Effects of independent variation of Mach and Reynolds numbers on the low-speed aerodynamic characteristics of the NACA 0012 airfoil section. NASA Technical memorandum 4074, 1988.
- Gregory, N., O'Reilly, C. L., Low-Speed Aerodynamic Characteristics of NACA 0012 Aerofoil Sections, including the Effects of Upper-Surface Roughness Simulation Hoar Frost. Aeronautical Research Council R&M 3726, 1970.
- Riegels, F. W., Aerofoil sections. 1961.